



University of  
Massachusetts  
Amherst

## DETECTION OF MYCOTOXINS USING SURFACE- ENHANCED RAMAN SPECTROSCOPY

Item Type	Dissertation (Open Access)
Authors	Martinez Rojas, Lourdes B.
DOI	<a href="https://doi.org/10.7275/25843481">10.7275/25843481</a>
Download date	2026-03-08 00:50:14
Link to Item	<a href="https://hdl.handle.net/20.500.14394/18735">https://hdl.handle.net/20.500.14394/18735</a>

**DETECTION OF MYCOTOXINS USING  
SURFACE-ENHANCED RAMAN SPECTROSCOPY**

**A Dissertation Presented**

**By**

**LOURDES MARTINEZ ROJAS**

**Submitted to the Graduate School of the  
University of Massachusetts Amherst in partial fulfillment  
of the requirements for the degree of**

**DOCTOR OF PHILOSOPHY**

**February 2022**

**Department of Food Science**

**© Copyright by Lourdes Martinez 2022  
All Rights Reserved**

**DETECTION OF MYCOTOXINS USING  
SURFACE-ENHANCED RAMAN SPECTROSCOPY**

**A Dissertation Presented**

**By**

**LOURDES MARTINEZ ROJAS**

**Approved as to style and content by:**

---

**Lili He, Chair**

---

**John G. Gibbons, Member**

---

**Matthew D. Moore, Member**

---

**Ricardo B. Metz, Outside Member**

---

**Lynne A. McLandsborough, Department Head  
Food Science**

## **DEDICATION**

To my beloved family, my parents Beatriz and Antonio, and my siblings Lorena and Marcos. Without their unconditional love and constant support none of my achievements would be possible.

## ACKNOWLEDGEMENTS

I would like to start by thanking my academic advisor, Dr. Lili He, whose direction, advice, and constant support allowed me to enjoy this process. There are so many reasons I can list to describe how Dr. He helped me during these years, but I think all of them can be summed up in one sentence: Dr. He helps us to grow academically, to become better researchers, but most importantly, she cares about us and our personal growth; she helps us to become better people. Therefore, I am very thankful for having had her as a role model while I was facing one of the important milestones in my career. Along with her I want to thank all the people that were part of Dr. He's lab during these years. Since I started, I always found people willing to help, lift my spirit in difficult times, and share good talks. I met wonderful professionals and made good friends, Janam, Andy, and Ana. Additionally, I am thankful to the Food Science Department faculty and staff for always being helpful and supportive. Thanks to my dissertation committee, Dr. Mathew Moore, Dr. John Gibbons, and Dr. Richard Metz for their time, kind comments, and advice.

Next, I would like to thank all my dear friends, the ones I met here, in the US, and my friends and colleagues from Paraguay. I am amazed at the love and pride they have always demonstrated. Thanks to my childhood friend, Mariam, for her support in the hardest times and for celebrating more than me during the good moments. Thanks to my friend Katherine, who came into my life when I needed it the most and became one of my best friends, hopefully for life. Thanks to my boyfriend Joe for his unconditional love and for standing by my side no matter how difficult the situation.

Last but not least, I would like to thank my family. Thanks to my siblings, Marcos and Lore - without them I wouldn't have had the courage to spread my wings and fly away from home. Also, without them I wouldn't have my beautiful niece and nephew, Magy and Marquitos - they bring me so much joy and encourage me to be a better person every day. And thank you to my beloved parents, my dad, Antonio, to whom I owe my education. He is my role model for hard work and honesty. And finally, thanks to my best friend and mom, Beatriz, whose unconditional love and support has molded me into the person I have become today. I love you so much!

**ABSTRACT**

**DETECTION OF MYCOTOXINS USING**

**SURFACE-ENHANCED RAMAN SPECTROSCOPY**

FEBRUARY 2022

LOURDES MARTINEZ ROJAS

B.S., NATIONAL UNIVERSITY OF ASUNCION, PARAGUAY

Ph.D., UNIVERSITY OF MASSACHUSETTS AMHERST

Directed by: Professor Lili He

Mycotoxins are toxic metabolites produced by fungus that can be parasites or saprophytes of crops or livestock forage. Consumer demand for plant-based foods and interest in animal-based foods originating from animals fed plant-based feed has been on the rise. Therefore, monitoring mycotoxins occurring in the food supply is more critical than ever. The goal of this project is to improve surface-enhanced Raman spectroscopy's (SERS) ability to identify and detect mycotoxins using label-free SERS substrates. Two simple approaches were designed to enhance the detection of mycotoxins produced by the *Aspergillus* and *Penicillium* genera, ochratoxin A and aflatoxin B1. Ochratoxin A was successfully detected in wine samples spiked with the mycotoxin in a range of 0.01 to 1 ppm using a facile solvent-mediated extraction that showed the key role that the food matrix can play on the SERS substrate performance. The detection of aflatoxin B1' SERS signals using bare gold nanoparticles was enhanced with the addition of human serum

albumin (HSA) as a mediating molecule. A combination of the HSA-mediated protocol and a liquid-liquid extraction (LLE) method allows the detection of up to 2 ppb of AFB1 in compound feedstuff samples. Additionally, a simple SERS protocol applied to *Aspergillus flavus* grown in liquid and solid medium showed the technique's capacity to classify between aflatoxigenic and non-aflatoxigenic species. Raman spectroscopy, SERS, Infrared Spectroscopy (IR) and surface-enhanced infrared absorption spectroscopy (SEIRAS) showed differences yet potential complementarity in their ability to identify mycotoxins produced by the *Fusarium* genus, deoxynivalenol and fumonisin B1.

## TABLE OF CONTENT

	Page
<b>ACKNOWLEDGEMENTS</b> .....	v
<b>ABSTRACT</b> .....	vii
<b>LIST OF TABLES</b> .....	xi
<b>LIST OF FIGURES</b> .....	xii
<b>CHAPTER</b>	
<b>1. DETECTION OF MYCOTOXINS IN FOOD USING SURFACE-ENHANCED RAMAN SPECTROSCOPY</b> .....	<b>1</b>
<b>1.1 Abstract</b> .....	<b>1</b>
<b>1.2 Introduction</b> .....	<b>2</b>
<b>1.3 Current analytical methods and limitations</b> .....	<b>5</b>
<b>1.4 Surfaced-enhanced Raman spectroscopy</b> .....	<b>7</b>
<b>1.5 Applications of SERS on the study of mycotoxins</b> .....	<b>10</b>
1.5.1 Label-free colloids substrates .....	<b>14</b>
1.5.2 Label-free solid surface-based substrates .....	<b>19</b>
1.5.3 Functionalized nanoparticles .....	<b>23</b>
1.5.3.1 Techniques based on antibodies .....	<b>23</b>
1.5.3.2 Techniques based on aptamers .....	<b>26</b>
1.5.3.3 Techniques based on molecularly imprinted polymers (MIPs) .....	<b>29</b>
<b>1.6 Current limitations and future perspective</b> .....	<b>30</b>
1.6.1 Simplified sample pretreatment .....	<b>30</b>
1.6.2 In-situ mapping .....	<b>32</b>
1.6.3 SERS combined with other techniques .....	<b>33</b>
1.6.4 Multi-toxin analysis .....	<b>35</b>
1.6.5 “Detection” to “behavior analysis” .....	<b>38</b>
1.6.6 Application of deep/machine learning .....	<b>39</b>
<b>1.7 Conclusion</b> .....	<b>40</b>
<b>2. A FACILE SOLVENT EXTRACTION METHOD FACILITATING SURFACE-ENHANCED RAMAN SPECTROSCOPIC DETECTION OF OCHRATOXIN A IN WINE AND WHEAT</b> .....	<b>41</b>
<b>2.1 Abstract</b> .....	<b>41</b>
<b>2.2 Introduction</b> .....	<b>42</b>
<b>2.3 Sample preparation and procedure</b> .....	<b>43</b>
<b>2.4 Results and discussion</b> .....	<b>48</b>

2.5 Conclusion .....	58
<b>3. ENHANCEMENT OF SURFACE-ENHANCED RAMAN SPECTROSCOPIC DETECTION OF AFLATOXIN B1 USING GOLD NANOPARTICLE CORE PROTEIN SATELLITE SUBSTRATE .....</b>	<b>59</b>
3.1 Abstract .....	59
3.2 Introduction .....	60
3.3 Materials and methods .....	62
3.3.1 Chemicals .....	62
3.3.2 Optimization of HSA-assisted assay .....	62
3.3.3 AFB1 detection .....	63
3.3.4 SERS measurement and data analysis .....	63
3.4 Result and discussion .....	64
3.4.1 Characterization of AFB1 SERS spectra using AuNPs 50 nm .....	64
3.4.2 Optimization of HSA-assisted assays. HSA concentration .....	67
3.4.3 Optimization of HSA-assisted assays. Time and temperature of incubation .....	69
3.4.4 Optimization of HSA-assisted assays. Order of reactions .....	75
3.4.5 Optimization of HSA-assisted assays. Selectivity .....	77
3.4.6 Quantitative detection of AFB1 using of HSA-assisted assay and SERS .....	79
3.5 Conclusion .....	83
<b>4. DIFFERENTIATION OF AFLATOXIN-PRODUCING AND NON-PRODUCING STRAINS OF ASPERGILLUS USING SERS .....</b>	<b>84</b>
4.1 Abstract .....	84
4.2 Introduction .....	85
4.3 Materials and methods .....	86
4.4 Results and discussion .....	87
4.5 Conclusion .....	92
<b>5. STUDY OF FUSARIUM SPP. MYCOTOXINS USING RAMAN AND INFRARED SPECTROSCOPY .....</b>	<b>93</b>
5.1 Abstract .....	93
5.2 Introduction .....	94
5.3 Materials and methods .....	96
5.4 Results and discussion .....	96
5.5 Conclusion .....	102
<b>6. CONCLUDING REMARKS .....</b>	<b>103</b>
<b>BIBLIOGRAPHY.....</b>	<b>105</b>

## LIST OF TABLES

<b>Table</b>		<b>Page</b>
<b>1</b>	Summary of producing organism, occurrence, and effects in mammals by the main five groups of mycotoxins .....	<b>4</b>
<b>2</b>	SERS methods applied to detect mycotoxin in food samples .....	<b>12</b>
<b>3</b>	Summary of the Raman shifts and vibrational modes of AFB1 from experimental SERS spectra using gold nanoparticles as substrate .....	<b>66</b>

## LIST OF FIGURES

<b>Figure</b>		<b>Page</b>
<b>1</b>	Schematic diagram of metallic nanostructures' benefit through the generation of electromagnetic fields near the analyte to enhance conventional Raman signals .....	<b>9</b>
<b>2</b>	A simple SERS-based detection process using label-free colloidal nanoparticles .....	<b>2</b>
<b>3</b>	Effect of chloroform as solvent extraction for OTA detection in food samples using SERS. Reproduced with permission from ref 113. Copyright © 2020 Elsevier B.V. ....	<b>3</b>
<b>4</b>	a) Schematic illustration of OTA extraction with SLM using the PALME setup; b) SERS-based detection of OTA after extraction and acidification; a) and b) (i) acceptor phase (AW, pH 10) OTA with a negative charge; a) and b) (ii) donor phase (AA, pH 3) OTA in a neutral form (pKa value of 4 (for carboxyl group of phenylalanine) and 7.1 (for hydroxyl group of phenol)); c) SEM image of Ag-capped silicon nanopillars used as SERS ... substrate; d) multiwell system with incorporated SERS chip. Reproduced with permission from ref 100. Copyright © 2020 Elsevier Ltd.	<b>22</b>
<b>5</b>	Schematic diagram of basic principles of functionalized nanoparticles. a). Direct detection. Identification of mycotoxin signal captured by a capturing agent attached to a metallic surface. b) Indirect detection. Mycotoxin is detected tracking the changes in the intensity of capturing agent peak (or peaks) signal. c) and d) Detection using a reporter molecule. c) Sandwich-like assay. The presence of mycotoxin is detected by an increase in the reporter's signal. d) Competitive assay. The presence of mycotoxin is detected by a decrease in the reporter's signal .....	<b>25</b>
<b>6</b>	Exonuclease-assisted recycling aptameric sensing chip method to detect AFB1. Reproduced with permission from ref 132. Copyright © 2017 Elsevier B.V. ....	<b>28</b>
<b>7</b>	SERS mapping-based multitoxin detection system. a) Detection pixels of a microarray well for the scanning of Raman signals. b) SERS mapping images acquired for seven different concentrations of OTA, FB, and AFB1. The scale bar on the right displays the color coding for different	

	Raman intensities. Reproduced with permission from ref 151. Copyright © 2018 WILEY-VCH Verlag GmbH & Co. KGaA, Weinheim. ....	33
8	Antibody-based lateral flow immunosensor for multiple detection of mycotoxin in Maize. Reproduced with permission from ref 93. Copyright © 2020 Elsevier B.V. ....	37
9	Illustrative diagram of liquid-liquid extraction (LLE) tested .....	47
10	a) SERS spectra of pure OTA in methanol and Ochratoxin A molecular structure. b) and b1) SERS spectra and microscope image of contaminated wine treated with extraction method 1. c) and c1) SERS spectra and microscope image of contaminated wine treated with extraction method 2. d) and d1) SERS spectra and microscope image of contaminated wine treated with extraction method 3 .....	50
11	Scanning Electron Microscope (JEOL JCM-5000 NeoScope) image of contaminated wine sample treated with extraction method 2 dried drop on gold slide .....	52
12	a) Mapping image of OTA contaminated wine sample treated with extraction method 2. b) Mapping image of OTA positive control that were treated with extraction method 2 .....	54
13	a) SERS spectra of OTA contaminated wine samples after Method 2 – Liquid-liquid extraction at different concentrations of OTA. b) Correspondent PLS analysis curve showing a linear relationship between OTA concentration and SERS signals at 1003 and 1030 Raman shift .....	56
14	a) SERS spectra of OTA contaminated wheat samples after Method 2 – Liquid-liquid extraction at different concentrations of OTA. b) Correspondent PLS analysis curve showing a linear relationship between OTA concentration and SERS signals at 1003 Raman shift .....	57
15	a) Molecular structure of AFB1, and b) SERS spectra of AFB1 using AuNPs 50 nm as SERS substrate. Seven major AFB1 peaks are highlighted .....	65
16	a) SERS spectra of: (i) AFB1 without protein (ii) AFB1 with 0.001 $\mu\text{M}$ of HSA (iii) AFB1 with 0.005 $\mu\text{M}$ of HSA (iv) AFB1 with 0.01 $\mu\text{M}$ of HSA (v) HSA without AFB1. b) SERS intensity variation for three major AFB1	

	peaks, 687, 1556 and 1272 $\text{cm}^{-1}$ , using 0.001, 0.005 and 0.01 $\mu\text{M}$ as final concentrations of HSA .....	<b>68</b>
<b>17</b>	SERS intensity variation of three major AFB1 peaks, 687, 1556 and 1272 $\text{cm}^{-1}$ a) after 15, 30 and 60 min of AFB1-HSA incubation b) after 15, 30 and 60 min of (AFB1-HSA) + AuNPs incubation .....	<b>71</b>
<b>18</b>	The structure of Human serum albumin (HSA) representing domains, subdomains and Sudlow's binding sites I and II. Ref 204 .....	<b>72</b>
<b>19</b>	Variation of SERS signal intensity of peaks 687, 1272 and 1556 $\text{cm}^{-1}$ when AFB1-HSA is made under 37 °C or at room temperature (25 °C) ....	<b>74</b>
<b>20</b>	SERS spectra of AFB1 detected using SERS by Method 1: addition of nanoparticles to a solution containing AFB1-HSA complexes, and Method 2: addition of the analyte to a solution of HSA-coated AuNPs .....	<b>76</b>
<b>21</b>	SERS spectra of AFB1 and AFB1+OTA at room temperature and AFB1+OTA at 37 °C using HSA-assisted assay .....	<b>78</b>
<b>22</b>	a) SERS spectra of AFB1, in a range of 2 to 10 ppb, using HSA-assisted assay. b) Correspondent PLS analysis curve showing a linear relationship between AFB1 concentration and SERS signals at five Raman shifts .....	<b>80</b>
<b>23</b>	(a) SERS spectra of certified compound feedstuff, in a range of highly contaminated, > 12.9 ppb, to 1 AFB1-free, < 1 ppb (b) Correspondent PLS analysis curve showing a linear relationship between AFB1 concentration and SERS signals in feed samples.....	<b>82</b>
<b>24</b>	SERS spectra of <i>Aspergillus flavus</i> and <i>Aspergillus oryzae</i> grown in PDA medium.....	<b>89</b>
<b>25</b>	3D-plot of PCA analysis of SERS spectra of <i>Aspergillus flavus</i> and <i>Aspergillus oryzae</i> grown in PDA medium.....	<b>90</b>
<b>26</b>	3D-plot of PCA analysis of SERS spectra of <i>Aspergillus flavus</i> and <i>Aspergillus oryzae</i> grown in rice-based medium.....	<b>91</b>
<b>27</b>	Molecular structure of DON and FB1.....	<b>98</b>
<b>28</b>	Raman and SERS spectra of (a) DON and (b) FB1.....	<b>99</b>

<b>29</b>	ATR-FTIR and SEIRAS spectra of (a) DON and (b) FUM.....	<b>101</b>
-----------	---	------------

# CHAPTER 1

## DETECTION OF MYCOTOXINS IN FOOD USING SURFACE-ENHANCED RAMAN SPECTROSCOPY

### 1.1 Abstract

Mycotoxins are toxic metabolites produced by fungi that contaminate many important crops worldwide. Humans are commonly exposed to mycotoxins through the consumption of contaminated food products. Mycotoxin contamination is unpredictable and unavoidable, it occurs at any point in the food production system under favorable conditions and they cannot be destroyed by common heat treatments due to their high thermal stability. Early and fast detection plays an essential role in this unique challenge to monitor the presence of these compounds in the food chain. SERS is an advanced spectroscopic technique that integrate Raman spectroscopic molecular fingerprinting and enhanced sensitivity based on nanotechnology to meet the requirement of sensitivity and selectivity but that can also be performed in a cost-effective and straightforward manner. This review focuses on the SERS methodologies applied so far for qualitative and quantitative analysis of mycotoxins based on a variety of SERS substrates, as well as our perspectives on current limitations and future trends of applying this technique as for mycotoxin analyses.

## 1.2 Introduction

Phytopathogenic fungi can invade crops in the field or during storage and can produce a large and growing family of low-molecular-weight molecules called mycotoxins that can accumulate in food or feed in toxicologically relevant concentrations. There are over 400 compounds recognized as mycotoxins so far, with this number increasing over the years due to the capability of more specialized analytical tools and the increasing number of fungi being isolated. In terms of public health and agroeconomics the most important groups of mycotoxins are: aflatoxins, fumonisins, ochratoxins, and trichothecenes of type A represented by HT-2 toxin and T-2 toxin, and type B represented by deoxynivalenol (DON), zearalenone (ZEN), all produced by members of the genera *Aspergillus*, *Fusarium*, and *Penicillium*.<sup>1</sup>

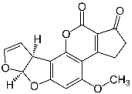
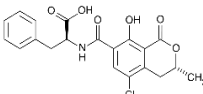
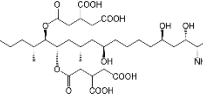
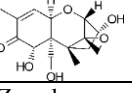
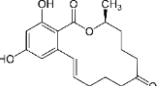
Mycotoxins are prevalent in cereals such as wheat, maize, barley, and rice, and soybean grains which are the most affected crops, as well as nuts, oilseeds, fruits, vegetables, cocoa and coffee beans, herbs, and spices.<sup>2-5</sup> These toxic metabolites are stable compounds that are hard to destroy during most food processing operations, leading to contaminated food products such as fermentation-derived beverages, coffee, dried fruits, and others.<sup>6-9</sup> Consumption of mycotoxin contaminated food can result in a variety of toxicological effects in an organism including toxic hepatitis, hemorrhage, edema, immunosuppression, hepatic carcinoma, equine leukoencephalomalacia, esophageal cancer, and kidney failure linked to aflatoxin B1 (AFB1), fumonisin B1 (FB1), and ochratoxin A (OTA).<sup>10,11</sup> AFB1 has been classified as a Class I human carcinogen, while

FB1 and OTA are classified as Class 2B, probable human carcinogens, by the International Agency for Research on Cancer (IARC).<sup>12</sup> Mycotoxins of the trichothecene type effects include vertigo, vomiting and diarrhea, weight loss, nervous disorders, cardiovascular alterations, immunodepression, hemostatic derangements, skin toxicity, decreased reproductive capacity, and bone marrow damage.<sup>13</sup> Table 1 shows a summary of the occurrence and the major effects on mammals by the main groups of mycotoxins.

The ubiquitous presence of phytopathogenic fungi and their capacity to produce multiple types of toxic metabolites result in considerable exposure to humans and animals. A three-year worldwide survey, from 2009 to 2011, indicates that 48% of 7049 feedstuff samples (corn, soybean/soybean meal, wheat, dried distillers' grains with solubles, and finished feed samples) were contaminated by two or more mycotoxins. The toxicity of mycotoxin combinations cannot always be predicted based on their individual toxicities. Multi-exposure may lead to additive, synergistic, or antagonistic toxic effects, but data on combined toxicokinetics are still limited.<sup>14-17</sup>

Consumption of contaminated feed by farm livestock animals also plays an important role in the introduction of these toxins in our food chain and results in large financial losses due to the reduction of animal performance or direct losses due to disease.<sup>18,19</sup> Considering the effects mentioned, various national and international institutions including the US Food and Drug Administration (FDA), World Health Organization (WHO), Food Agriculture Organization (FAO), and the European Food Safety Authority (EFSA) released strict regulatory guidelines for the major mycotoxin classes in food and feed.

**Table 1.** Summary of producing organism, occurrence, and effects in mammals by the main five groups of mycotoxins.

Mycotoxins / Molecule structure	Producing organism	Commodities affected	Effects in mammals	Ref.
<b>Aflatoxins</b> 	<i>Aspergillus flavus</i> and <i>Aspergillus parasiticus</i>	Maize, wheat, rice, peanut, sorghum, pistachio, almond, ground nuts, tree nuts, figs, cottonseed, spices, milk, milk products, meat	Carcinogenic, acute hepatitis, impaired immune system	10,12,20–24
<b>Ochratoxins</b> 	<i>Penicillium verrucosum</i> and various species of <i>Aspergillus spp.</i> : <i>A. alliaceus</i> , <i>A. auricomus</i> , <i>A. carbonarius</i> , <i>A. glaucus</i> , <i>A. melleus</i> , <i>A. niger</i>	Cereals, dried vine fruit, wine, grapes, coffee, cocoa, cheese	Carcinogenic, nephrotoxic, hepatotoxic, teratogenic	10,12,25,26
<b>Fumonisin</b> 	<i>Fusarium spp.</i> , mostly <i>F. verticilloides</i> and <i>F. moniliforme</i> .	Maize, maize products, sorghum, asparagus	Carcinogenic, hepatotoxic, causative agent in leukoencephalomalacia in horses	11,12,27–30
<b>Deoxynivalenol</b> 	<i>Fusarium graminearum</i> and <i>Fusarium culmorum</i>	Cereals, cereal products	Immuno-depressants, gastrointestinal hemorrhaging	13,31,32,269
<b>Zearalenone</b> 	<i>Fusarium spp.</i>	Cereals, cereal products, maize, wheat, barley	Estrogenic and reproductive disorder	13,33,34

### **1.3 Current analytical methods and limitations**

For regulatory compliance, effective analytical methods to detect and quantify these mycotoxins are essential. The analysis of mycotoxins usually requires toxin extraction from the matrix, a cleanup procedure to remove interfering elements, and detection and quantification using appropriate analytical instrumentation. The most common methods used for mycotoxin analysis are chromatographic systems coupled with highly sensitive detection systems such as liquid chromatography (LC) or high-performance liquid chromatography (HPLC) coupled with fluorescence (FL), ultraviolet (UV), or mass spectrometry (MS) detectors.<sup>2,35-37</sup> The high resolution of these techniques usually requires extensive sample cleanup and purification, usually translating to high costs and laborious protocols.

More rapid and simple alternatives are immunological-based methods, which employ specific antibodies to capture target analytes and reporter molecules to generate the detectable signals. Enzyme-linked immunosorbent assay (ELISA) is the most widely used in research and industry. Other techniques such as lateral flow detection (LFD), fluorescence polarization immunoassay (FPIA), radioimmunoassay (RIA), and immuno-affinity column assay (ICA) implement the same immunological-based fundamentals to develop simple, rapid, and convenient systems for mycotoxin analysis.<sup>38-52</sup> Despite their simplicity major drawbacks for these types of tests are the possibility of cross-reactivity and a high matrix dependence that reduces accuracy. Additionally, there are high costs associated with development and commercial use.<sup>39,53</sup>

Other technologies were developed for the analysis of mycotoxins in the research field but with limited commercial applications as they require further verification and validation by the recognized organizations. Molecular and genomic methods such as fluorescent in situ hybridization (FISH), DNA barcoding, or polymerase chain reaction (PCR), are highly effective in identifying the presence of mycotoxigenic fungi but do not quantify the amount of mycotoxin produced. Approaches such as the electronic nose or hyperspectral imaging (HIS) are rapid and non-destructive methods that can detect the presence of mycotoxins through changes in physicochemical properties occurring in food contaminated with mycotoxigenic fungi, but they generally lack the accuracy needed for commercial applications.<sup>54</sup>

The use of antibodies and other types of biosensors such as aptamers and molecularly imprinted polymers (MIPs) have been adapted to other numerous detection systems: electrochemical, optical, piezoelectric, or innovative devices like microarrays and microfluidics searching to improve the miniaturization and portability for field applications and to offer more straightforward, user-friendly detection systems.<sup>55-57</sup>

The new generation of analytical techniques for mycotoxin analysis is seeking to use these types of miniature systems but so far have not succeeded in integrating the steps of extraction, purification, and detection directly into the system, a desirable requirement to avoid the tedious and time-consuming treatments to separate toxins from the rest of the components, especially in complex matrices like food.

## 1.4 Surfaced-enhanced Raman spectroscopy

Raman scattering is the inelastic scattering of photons that can occur when interacts with matter which contains information on the vibrational modes of the compounds specific for each type of molecule. SERS is an advanced Raman technique that integrates nano-scale rough metal surfaces to enhance the signals (Figure 1) and detect trace amounts of molecules or even one single molecule, making it one of the few techniques capable of reaching this analytical limit.<sup>58-60</sup> The enhanced Raman signals come mainly from the electromagnetic fields originating from the interaction of light with metal surfaces. Regions with a highly enhanced local electromagnetic fields are called “hot-spots” and occur when neighboring nanostructures interact with each other over distances in the order of nanometers.<sup>61</sup> In addition to the electromagnetic mechanism there is a chemical mechanism that depends on the nature of each molecule and involves the formation of new molecular states on molecules chemisorbed on a SERS-active surface.<sup>62-64</sup> Thus, SERS directly detects the target analyte in a way that is molecularly specific allowing identification without the need for extensive separation in some cases, resulting in a rapid and non-destructive technique that is becoming increasingly popular in a wide variety of fields including food quality and safety,<sup>65-69</sup> pharmacy,<sup>70</sup> biomedicine,<sup>59,71</sup> environment,<sup>71-73</sup> forensics science,<sup>74,75</sup> and art and archeology.<sup>76,77</sup>

SERS requires the same instrumentation of conventional Raman spectroscopy: excitation source, filters, spectrograph, and detector which are large in size and not suitable for on-site rapid analysis. The high performance of SERS allows compromising the

traditional spectrometers specifications to reduce cost and increase portability allowing the development of compact, portable Raman spectrometers for field analysis<sup>78,79</sup>, an attribute that other high-performance methods such as HPLC, MS or gas chromatography (GC), have not yet obtained.

SERS experiments can be designed to obtain qualitative and quantitative information, expanding its applicability from a simple qualitative screening to ultra-low detection. A pre-processing of the raw Raman spectra is usually necessary to correct disturbances due to spikes scattering or fluorescence effects. The desired information can be obtained using a univariate approach or a multivariate approach. The univariate approach extracts relevant information from an area, or the intensity of peaks related to the analyte of interest. Multivariate data analysis extracts all the information in complex matrices using algorithms such as Principal Component Analysis (PCA) or regression techniques as Classical Least Square (CLS) and Partial Least Square (PLS).<sup>80</sup> PCA is one of the most useful statistical analyses used to analyze Raman spectra; it helps to determine spectral similarities and differences which is useful for qualitative purposes.<sup>81-83</sup> Other statistical models such as partial least squares regression (PLSR), multiple linear regression (MLR), principal components regressions (PCR), and others, are needed to quantitatively interpret and validate SERS.<sup>81,82</sup>

The parameters to obtain an optimum SERS response are different for each type of analyte and matrix, therefore it is necessary to optimize the technique according to the target compound, the matrix, and the scope of the study.

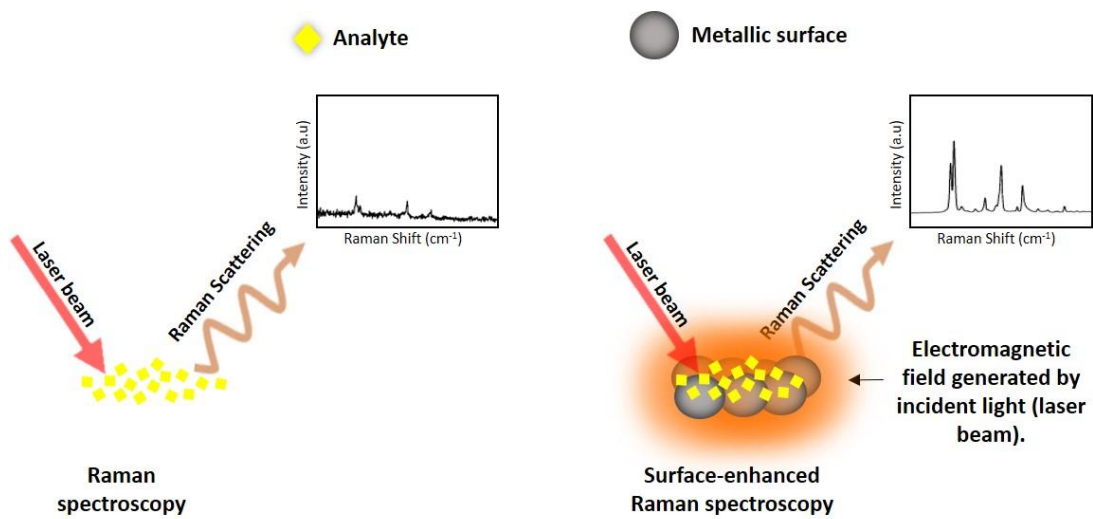


**Figure 1.** Schematic diagram of metallic nanostructures' benefit through the generation of electromagnetic fields near the analyte to enhance conventional Raman signals.

## 1.5 Applications of SERS on the study of mycotoxins

The first use of SERS for mycotoxin detection started at the beginning of this decade and has been gradually increasing. In the last two years, the number of publications doubled from the previous five years, and this year has already seen more publications than previous years. This increasing interest seems to correspond with the availability of appropriate nanostructures for substrates because of the progress in nanotechnology.<sup>84-86</sup> The first step in establishing a new analytical method usually starts with the testing of standards solutions but the minimal sample preparation that the SERS technique requires facilitates rapid testing in real sample matrices as is shown in Table 2. Nevertheless, essential information is obtained from standard solution studies.<sup>83,87,88</sup> In this work, all the studies that applied SERS to the detection of mycotoxins are described through a classification system according to the type of substrate employed.

The type of substrate used is of utmost importance to determine SERS acceptability as an analyte detection technique.<sup>86</sup> The overall Raman signal enhancement, the sensitivity, selectivity, and reproducibility will be determined by the substrate while the practicality and cost will depend mostly on the chosen substrate synthesis method and the further modifications that might be needed. A desirable SERS substrate should be reproducible, and signal enhancement must be homogenous across the surface or from batch-to-batch measurements. For commercial applications, the SERS substrate needs to have good stability to ensure an acceptable shelf-life.

SERS substrates can be divided into two groups: colloidal substrates and solid surface-based substrates. Both groups rely on the physical properties of metallic nanostructures to enhance Raman signals in their proximity, but solid surface-based substrates provide better control over the location of hot spots and therefore enhance the reproducibility. Metallic nanostructures without any surface modification are called “bare or label-free nanoparticles” and although single-molecule detection can be achieved using these types of substrates they cannot isolate the target in complex samples such as food matrices. This is a significant drawback for detecting trace levels of a target analyte in complex matrices where they might be masked by the signals of other food components. In order to overcome this non-specific nature, metallic nanostructures can be modified or functionalized with common target capture mediators such as antibodies, aptamers, or MIPs.<sup>86,89,90</sup>

**Table 2.** SERS methods applied to detect mycotoxin in food samples.

Mycotoxin	Sample	Extraction	SERS substrates	LOD	US* (µg/kg)	EU* (µg/kg)	Ref.
Aflatoxin B1	Maize	Methanol 70% followed by filtration	AgNPs	13–36 µg/kg	20	2-5	1
	Maize	Methanol 20%, sonication, and centrifugation	3D-Nanocauliflower (AuNPs@PDMS@AAO)	1.8 ng/mL			1
	Maize meal	Methanol 50% followed by filtration	AFB1-aptamer Ag@Au CSNPs	0.003 ng/mL			2
	Maize meal	Dilution, centrifugation, and another dilution	Antigen Ni@Au NPs and AFB1-Ab AuNPs	0.05 fg/mL			3
	Maize	Methanol 70% followed by centrifugation and 10-fold dilution of the supernatant	AFB1-Ab Au@AgNPs	0.96 pg/mL			4
	Corn, rice, and wheat	Methanol 70% followed by centrifugation and addition of PBS (10mM, pH 7.4)	OTA-Ab AuNPs	0.061-0.066 µg/kg		5	
	Peanuts	Methanol 60%, ultrasonication, and centrifugation	AuNBPs-AAO	0.5 µg/L		2-8	6
	Wheat, corn, protein feed powder	QuEChERS	AuNPs	0.85 µg/kg		2-20	7
	Cocoa beans powder	Methanol 70%, centrifugation, and filtration	AgNPs	4.15 pg/mL		-	8
Ochratoxin A	Maize	Methanol 70% followed by centrifugation and 10-fold dilution of the supernatant	OTA-Ab Au@AgNPs	15.7 pg/mL	-	5	4
	Wine	Distillation of dilute samples	OTA-aptamer Au-Ag Janus NPs	1.28pM		2	9
	Wine	Direct	OTA-aptamer Au@Ag	5pM			00
	Wine	Supported liquid membrane (SLM) extraction	Ag-capped silicon nanopillar	115 µg/kg			01
	Coffee, wheat	Methanol 70%, centrifugation, and filtration	OTA-aptamer AuNTs	25 nM		3-10	02
	Cocoa beans powder	Methanol 70%, centrifugation, and filtration	AgNPs	2.63 pg/mL		-	8
	Maize	Methanol 70% followed by filtration	Ag Dendrites	5-25 mg/kg			2

Fumonisin B1	Maize	Methanol 70% followed by centrifugation and 10-fold dilution of the supernatant	FUM-Ab Au@AgNPs	0.96 ng/mL	2000-4000	200-4000	4		
	Maize	Methanol 80%, centrifugation, and filtration	FUM-aptamer AuNRs	3 pg/mL			03		
Deoxynivalenol	Maize	Methanol 20%, sonication, and centrifugation	3D-Nanocauliflower (AuNPs@PDMS @AAO)	24.8 ng/mL	-	750-1250	1		
	Maize	Methanol 70% followed by centrifugation and 10-fold dilution of the supernatant	DON-Ab Au@AgNPs	0.11 ng/mL			4		
	Pig feed	Methanol 50%, sonication, centrifugation	AgNCs@polydopamine	0.82 fM			5000	900	04
Zearalenone	Maize	Methanol 20%, sonication, and centrifugation	3D-Nanocauliflower (AuNPs@PDMS @AAO)	47.7 ng/mL	-	100-350	1		
	Maize	Methanol 70% followed by centrifugation and 10-fold dilution of the supernatant	ZEA-Ab Au@AgNPs	0.26 ng/mL			4		
	Corn, rice, and wheat	Methanol 70% followed by centrifugation and addition of PBS (10mM, pH 7.4)	ZEA-Ab AuNPs	0.53–0.57 µg/kg			-	75-100	5
	Feed	Dispersive liquid–liquid extraction	ZEA-Ab 4,4'-dipyridyl-AuNPs	1 pg/mL			-	100-3000	05
Patulin	Apple juice	Solvent-mediated extraction	AuNBPs	6 µg/L	50	50	06		
	Blueberry and grapefruit, orange juice	Solvent-mediated extraction	MIPs-AuNPs	5.37x10 <sup>-12</sup> M			07		
Alternariol	Pear	Solvent-mediated extraction	Pyridine-AgNPs	1.30 µg/L	-	-	08		
T-2	Maize	Methanol 70% followed by centrifugation and 10-fold dilution of the supernatant	ZEA-Ab Au@AgNPs	8.6 pg/mL	-	100	4		

\*US Food and Drug Administration advisory levels for mycotoxins<sup>109</sup>

\*European Commission advisory levels for mycotoxins<sup>110</sup>

### 1.5.1 Label-free colloids substrates

The simplest SERS experiments use colloid substrates, mixing a known amount of the analyte with a colloidal suspension of metallic nanoparticles (Figure 2), such as silver (Ag) or gold (Au) colloids ranging in diameter from 10 to 200 nm. Ag and Au nanoparticles are arguably the most used substrates due to their physical properties, stability, low cost, and simple preparation.<sup>86</sup> Ag in the form of nanospheres, usually referred to as Ag nanoparticles (AgNPs), was used to explore the detection of citrinin (CTN), aflatoxins, DON and in the form of dendrites to detect FB1.<sup>81,82,87,88</sup> Lee and coworkers<sup>81,82</sup> detected aflatoxins and fumonisins in maize samples using a simple procedure consisting in a solvent-mediated extraction following a mixing with nanoparticle solutions. Maize samples were divided into groups according to their levels of contamination, being 20-200  $\mu\text{g}/\text{kg}$  and 5000-25000  $\mu\text{g}/\text{kg}$  the groups with the lowest detectable amount of mycotoxin for aflatoxins and fumonisins, respectively. The authors presented their concern about the inaccuracy of the technique for detection at lower concentrations, but nevertheless, SERS showed its potential as a technique to screen mycotoxin contamination directly from food samples. AFB1 was also detected using Au nanoparticles (AuNPs) with a limit of detection (LOD) of 0.85  $\mu\text{g}/\text{kg}$  in wheat, corn, and protein feed powders.<sup>97</sup> The first SERS spectrum of DON was obtained and characterized by combining experimental results using AgNPs with density functional theory (DFT) analysis.<sup>88</sup> Similarly, a detailed description of CTN spectra was obtained using AgNPs on the surface of hydrophobic Teflon films. Unlike hydrophilic platforms, like glass, where molecules dispersed in a solution are free to diffuse

over the surface, hydrophobic surfaces can concentrate molecules into a smaller region due to an effect known as the hydrophobic condensation effect, forcing them to enter the “hot spot” areas and thereby enhancing the intensity of SERS signals.<sup>111</sup> Using a different platform is just one of the many ways to improve the Raman enhancement factor, reproducibility, and stability of the colloidal substrates. For example, when AgNPs were synthesized under an alkaline condition, the computed analytical enhancement factor (EF) improved ( $1.45 \times 10^8$  compared to  $4.54 \times 10^7$  for a neutral pH 7), allowing the detection of OTA and AFB1 in spiked cocoa bean samples at very low LODs, 0.00263  $\mu\text{g}/\text{kg}$ , and 0.00415  $\mu\text{g}/\text{kg}$ , respectively.<sup>98</sup> There is also an indication that extraction solvents can play a role in improving the distribution of nanoparticles. A study showed the improvement of OTA’s Raman signal from wine and wheat samples when using only chloroform instead of a combination of salt/chloroform or using ethyl acetate as an extraction solvent. The interaction between the solvent and the food components led to the formation of small structures similar to crystals that served as platforms for nanoparticles therefore avoiding the formation of regions with high nanoparticle aggregation (coffee rings) and reducing the variability (Figure 3).<sup>112</sup> The magnitude of electromagnetic enhancement is strongly dependent on the shape, size, and arrangement of the metallic nanostructures, or SERS substrates. It was seen that other shapes of nanoparticles, such as nano-rod, nano-triangles, nano-cubes, nano-stars, and core-shells can generate higher Raman enhancement than spherical nanoparticles, due to stronger plasmonic oscillation generated by the sharp edges<sup>64,89</sup>. The nanoparticles’ performance can also be improved by the addition of a

coating agent to maintain the stability of the suspensions or enhance the adsorption of the analytes on the substrate surfaces. Silver nanocubes coated with polydopamine (AgNCs@PDA) were used as a SERS substrate to detect DON in pig feed with a low LOD in a femtomolar range, 0.82 fM. An ultrathin shell of PDA (1.6 nm) increased the EF in one order of magnitude compared to bare AgNCs and improved the stability of the substrate maintaining 88.24% of the original Raman intensity after storage for three months.<sup>104</sup> Alternatively, AgNPs were used to coat silica nanoparticles to detect mycotoxin alternariol (AOH). Using silica nanoparticles (~145 nm) as a template, AgNPs were more uniformly distributed in a colloid suspension as were the “hot spots”. Using this substrate, AOH was detected at 4.3 nM, and this substrate showed high reproducibility with a relative standard deviation of 2.33–5.95%.<sup>113</sup> In general, colloid nanostructures are affordable and easier to synthesize but the weak signal reproducibility is a major challenge due to the lack of control on their assembly and the exact location of the interaction with the analytes.

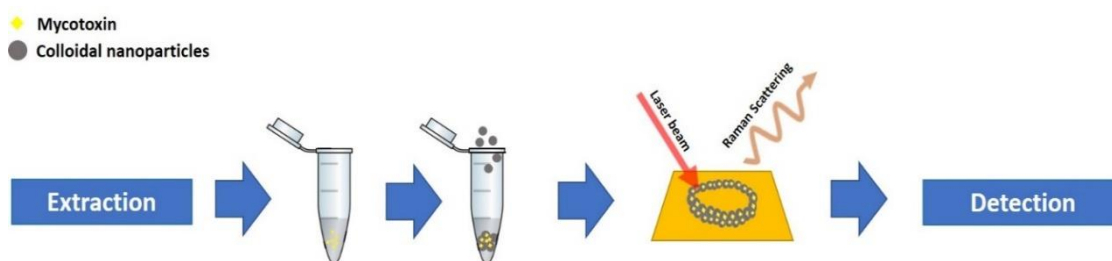


**Figure 2.** A simple SERS-based detection process using label-free colloidal

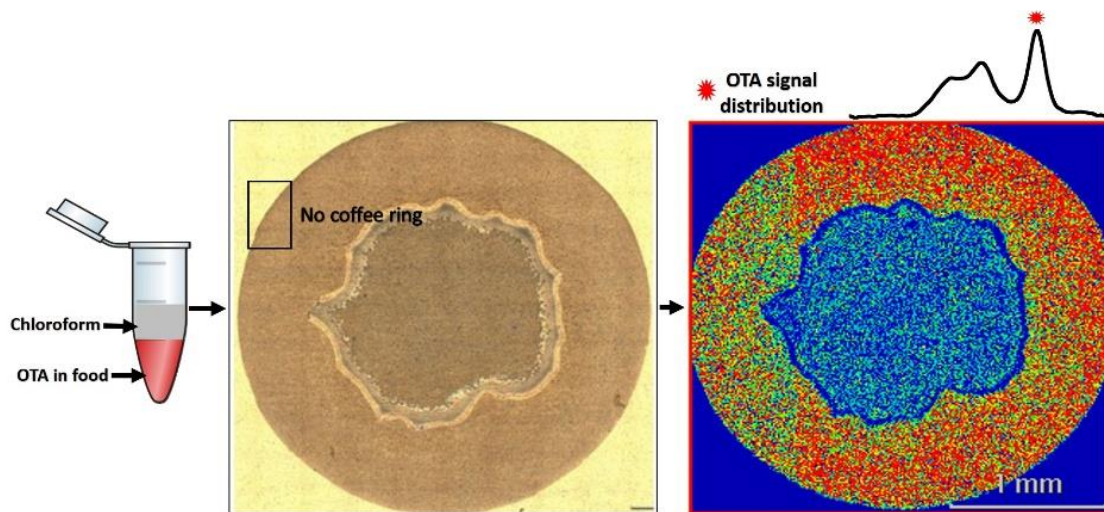


**Figure 3.** Effect of chloroform as solvent extraction for OTA detection in food samples using SERS. Reproduced with permission from ref 113. Copyright © 2020 Elsevier B.V.

### 1.5.2 Label-free solid surface-based substrates

Solid surface-based substrates reduce the high variance common on colloid substrates by the immobilization of them in solid platforms. The main purpose of this approach is to control the proximity of the “hot spots” with the analytes, to optimize the magnitude of the SERS effect, and to obtain a highly reproducible and long-term stable substrate. The immobilization can be made by direct deposition of colloid suspension or by fabrication of the nanostructures directly on solid platforms by template-based synthesis and nanolithography.<sup>67</sup> There are only a small number of studies using this type of substrate to detect mycotoxins. Perhaps this is because they can be costly compared to colloid substrates and they still lack the high selectivity that functionalized nanostructure substrates offer. Nevertheless, two studies using bare solid surfaced-based substrates showed that SERS can differentiate between the four types of aflatoxins (B1, B2, G1, and G2).<sup>83,96</sup> The first study in 2012, employed an oblique angle vapor deposition technique to fabricate a silver nanorods (AgNRs) array.<sup>83</sup> In this technique, a thin layer of the substrate initially deposited on a solid surface is rotated by a stepper motor in an angle greater than 75°, in front of a vapor source that controls the growth of AgNRs by a shadowing effect and surface diffusion. Pure solutions of the four types of aflatoxins were added directly to the surface of these arrays and allowed to dry before spectrum acquisitions<sup>114</sup>. Combined with DFT calculations, it was one of the first studies to provide a detailed characterization of these mycotoxin spectra. Similarly, the ability of SERS to discriminate between these molecules with minor differences was shown using Au nanobipyramids (AuNBPs)

uniformly distributed into the nanoholes of anodic aluminum oxide (AAO) template. The fabrication was simple; a colloid suspension of the nanoparticles was dropped on the surface of the template directly to allow the distribution into the nanoholes by diffusion. Although the promising selectivity of this method was based only on the differences of pure solutions, the LOD obtained for the main type, AFB1, from peanut extracts was low, 0.5 µg/kg, and the standard deviation of 8.39% showed reproducibility.<sup>96</sup> AFB1 was also quantified up to 5 ng/mL in piked peanut extracts using a pre-etched Ag nanocluster as the SERS substrate. For this method, Chen and colleagues<sup>115</sup> used mesoporous silica as a template to synthesize the Ag nanoclusters prior to its immobilization on a silicon wafer. Other mycotoxins detected using solid surfaced based substrates are OTA, DON, and FB1.<sup>101,116</sup> In another clear example of SER's minimal sample preparation requirement, OTA was detected (LOD 115 µg/kg) in wine samples after being extracted using a high throughput SLM platform named parallel artificial liquid membrane extraction (PALME) and Ag-capped silicon nanopillars made by plasma as a SERS substrate (Figure 4). The use of chip-sized microscope slides as solid platforms for the Ag-capped silicon nanopillars allowed the construction of a multiwell system, an approach that can be useful when processing a high volume of samples simultaneously.<sup>101</sup>

The spectra of DON and FB1, on their respective European Union (EU) advisory limits for unprocessed cereals 1250 and 4000 µg/kg were discriminated using nano-pillar arrays fabricated by means of two-photon polymerization (2PP) process.<sup>116</sup> The 2PP is a type of the denominated “additive manufacturing techniques” that allows the fabrication of

physical components from virtual three-dimensional (3D) computer models by building the component layer-by-layer.<sup>117</sup>

In general, the main advantages of this type of substrate are more stability and reproducibility, ease of use, and a low sample volume requirement, which makes it ideal for use with a handheld device for on-site detection.

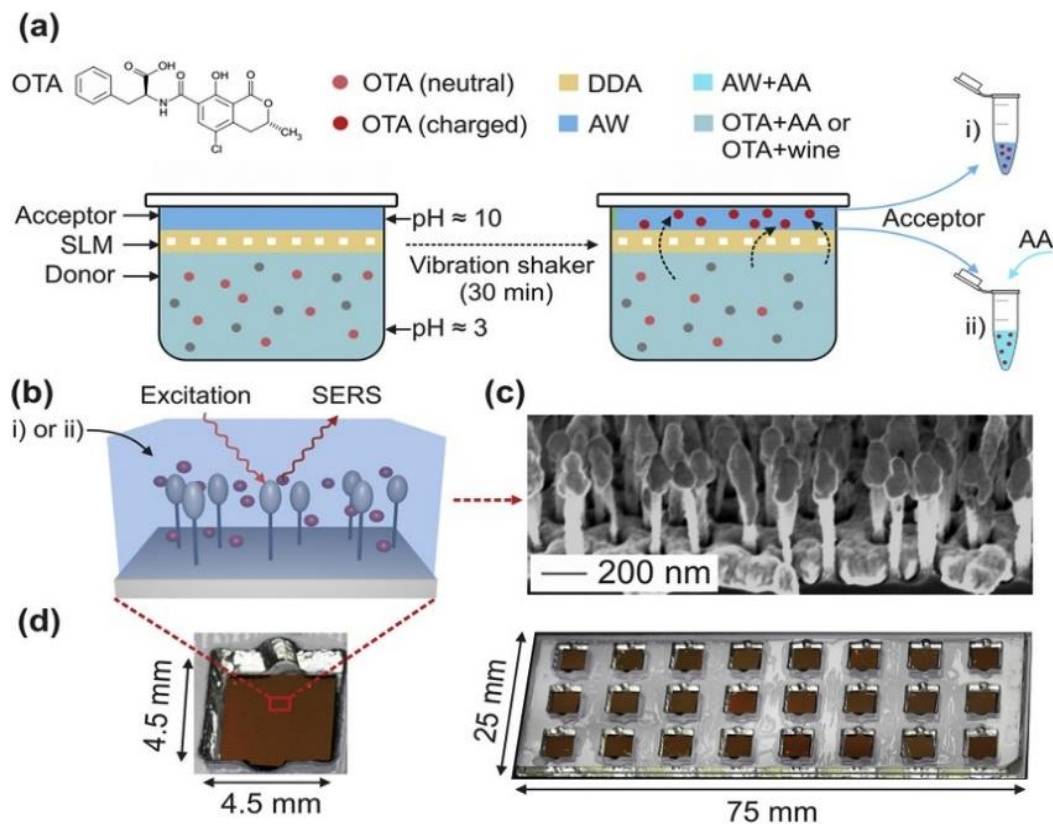


**Figure 4.** a) Schematic illustration of OTA extraction with SLM using the PALME setup; b) SERS-based detection of OTA after extraction and acidification; a) and b) (i) acceptor phase (AW, pH 10) OTA with a negative charge; a) and b) (ii) donor phase (AA, pH 3) OTA in a neutral form (pKa value of 4 (for carboxyl group of phenylalanine) and 7.1 (for hydroxyl group of phenol)); c) SEM image of Ag-capped silicon nanopillars used as SERS substrate; d) multiwell system with incorporated SERS chip. Reproduced with permission from ref 100. Copyright © 2020 Elsevier Ltd.

### **1.5.3 Functionalized nanoparticles**

Most of the methods developed to detect mycotoxins using SERS employ functionalized substrates. One reason is that the sensitivity and selectivity obtained can be comparable to conventional analytical methods.<sup>67</sup> Capturing agents used to functionalize SERS active nanostructures can be single molecules or polymers with a chemical affinity to the target molecules or biosensors specifically designed for the recognition of one target analyte. An illustration of the basic principles used for the detection of mycotoxins with functionalized nanoparticles is provided in Figure 5.

#### **1.5.3.1 Techniques based on antibodies**

Immunoassays are based on the extreme specificity and strong interaction of an antibody with his antigen. The principles of immunoassays are like the ones used in conventional methods such as ELISA, where the presence of a “reporter” is required to monitor minimal changes occurring on the presence of the target analyte. In 2014, ZEN was detected on spiked and naturally contaminated feed samples through a competitive assay using 4,4'-dipyridyl as a reporter and AuNPs as SERS substrates. The LOD reached the picogram range, 1 pg/mL, for ZEN standard solutions. On feed samples, the extreme sensibility of the method required the sample dilution before any Raman signals could be observed<sup>105</sup>. In the following years, three works using antibody-functionalized nanoparticles were developed to detect aflatoxins.<sup>93,118,119</sup> Two of these included nanoparticles with strong electromagnetic properties to combine the steps of antigen capture and cleanup, using a magnet. Fang and coworkers<sup>93</sup> employed Ni@Au

nanoparticles as a magnetic SERS substrate. The surface of these nanoparticles was modified with AFB1 coating antigens that in the absence of the mycotoxin binds to the AFB1 antibodies attached to the surface of AuNPs. Using this approach, the presence of AFB1 was detected with a LOD of 0.05 fg/mL on pure solutions and up to 1 fg/mL in maize samples. Similarly, Ko and coworkers<sup>118</sup> conjugated AFB1 antibodies to magnetic beads and to silica-encapsulated hollow gold nanoparticles (SEHGNs) to create a sandwich-like (Ab-AFB1-Ab) immunoassay, achieving a LOD of 0.1 ng/mL in tap water. Finally, a different approach was taken with the development of an on-site SERS-based lateral flow immunosensor for the monitoring of aflatoxin M1 (AFM1) levels in urine.

The actual presence of aflatoxins in food and feed is not always accurately reflected regardless of the type of analytical method used due to sampling and analysis errors.<sup>120,121</sup> AFM1, a AFB1 metabolite, concentration in serum (in form of albumin-AFM1 complexes) or in urine (as free AFM1) is related to AFB1 intake,<sup>122-124</sup> making it suitable to track the real AFB1 exposure. AuNPs conjugated with AFM1-bovine serum albumin were immobilized on a nitrocellulose membrane served as a lateral flow strip. Reporter molecule, 5,5-dithiobis-2-nitrobenzoic acid, and anti-AFM1 monoclonal antibodies were conjugated with Au@Ag nanoparticles to capture free AFLM1. Once the strip is in contact with the samples the degree of AFM1-BSA/anti-AFM1Ab complexes formation will depend on free AFM1 concentration, being translated to an increasing or decreasing of the reporter's Raman signal. This immunosensor was able to detect up to 1.7 pg/mL of AFM1 in the urine.<sup>94</sup>

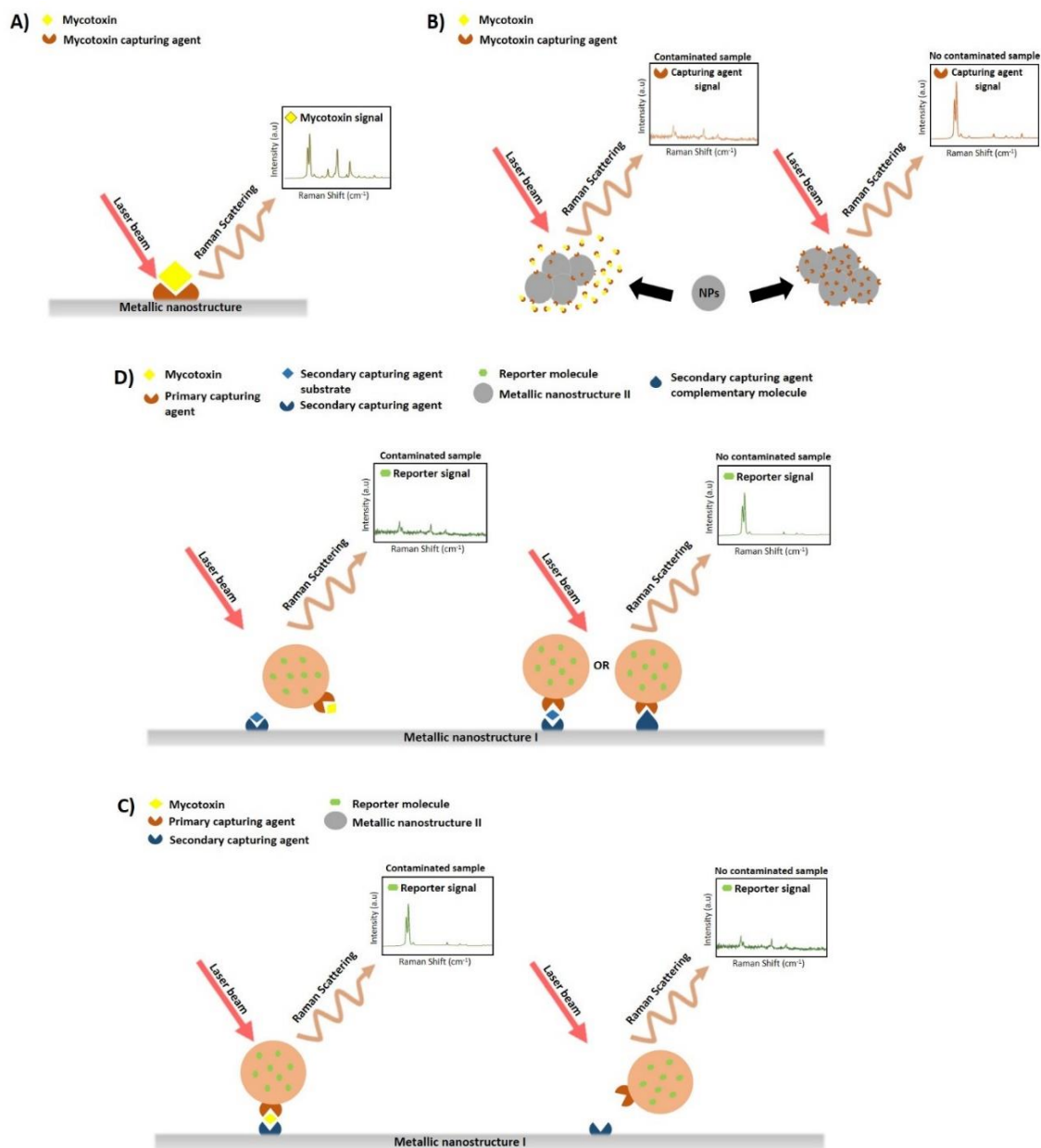


**Figure 5.** Schematic diagram of basic principles of functionalized nanoparticles. A). Direct detection. Identification of mycotoxin signal captured by a capturing agent attached to a metallic surface. B) Indirect detection. Mycotoxin is detected tracking the changes in the intensity of capturing agent peak (or peaks) signal. C) and D) Detection using a reporter molecule. C) Sandwich-like assay. The presence of mycotoxin is detected by an increase in the reporter's signal. D) Competitive assay. The presence of mycotoxin is detected by a decrease in the reporter's signal.

### 1.5.3.2 Techniques based on aptamers

Aptamers are small oligonucleotides ligands, DNA, RNA, or peptides engineered to bind a specific target with high affinity. These molecules are thermally more stable than antibodies due to their simplest structure. There is no risk of denaturation under high temperatures, maintaining their structures over repeated cycles of denaturation/renaturation.<sup>125</sup> Aptamers can be easily modified to introduce signal moieties or facilitate the linkage to a solid support, which makes them of extreme interest for functionalizing SERS substrates. Almost all the studies applying aptamer-based SERS detection for mycotoxins were developed for OTA, a few of them for aflatoxins and one study for FB1.<sup>66,99,100,103,126–129</sup> These studies took two main directions, the first one consisted of the adsorption of aptamer molecules on Au surfaces by thiol-alkane linkage to analyze the spectral variation after adding the analyte.<sup>66,102</sup> The processes in these experiments were simple and they reached a satisfactory LODs although the applicability in real food samples was not tested. The main problem with this approach is that structural changes occurring in the aptamer when capturing its analyte might not be translated to easily observable spectral variations and therefore it will require extensive statistical analysis becoming time-consuming. The second direction consists of indirect detection, monitoring the Raman signal intensity of reporter molecules, which are well known to have strong and well-characterized Raman activity. The simplest of these experiments used mycotoxin aptamers labeled with a reporter molecule that can be adsorbed on the surface of nanoparticles<sup>126</sup> or other supporting surfaces<sup>99</sup> when there are no mycotoxins in the

sample, giving strong SERS signals from the reporter. But the presence of the analyte prevents the adsorption from occurring and this is translated to a reduction in the intensity of the reporter's Raman signals. Other more sophisticated methods employed a complementary strand aptamer to improve the affinity of the labeled-mycotoxin aptamers to the surface of the nanoparticles.<sup>100,103,127,128,130</sup> One of the main benefits of using highly affine complementary aptamers is the guarantee that the reduction in the signal intensity is due to the presence of the mycotoxin and not a consequence of weak interaction between the aptamer and the nanoparticles. The LOD obtained using these methods can reach the range of picograms, even on real food samples.<sup>103</sup> Li and coworkers<sup>131</sup> adopted a different strategy to detect AFB1 by integrating four types of DNA: a AFB1 DNA-aptamer, a complementary DNA strand, a hairpin DNA and a capture DNA. The presence of the toxin will initiate a cycle that ends with the detection of the labeled-AuNP on the surface of the Au-coated glass (Figure 6). The LOD achieved using this approach was 0.4 fg/mL and the applicability was proved by quantifying the level of AFB1 in peanut samples.

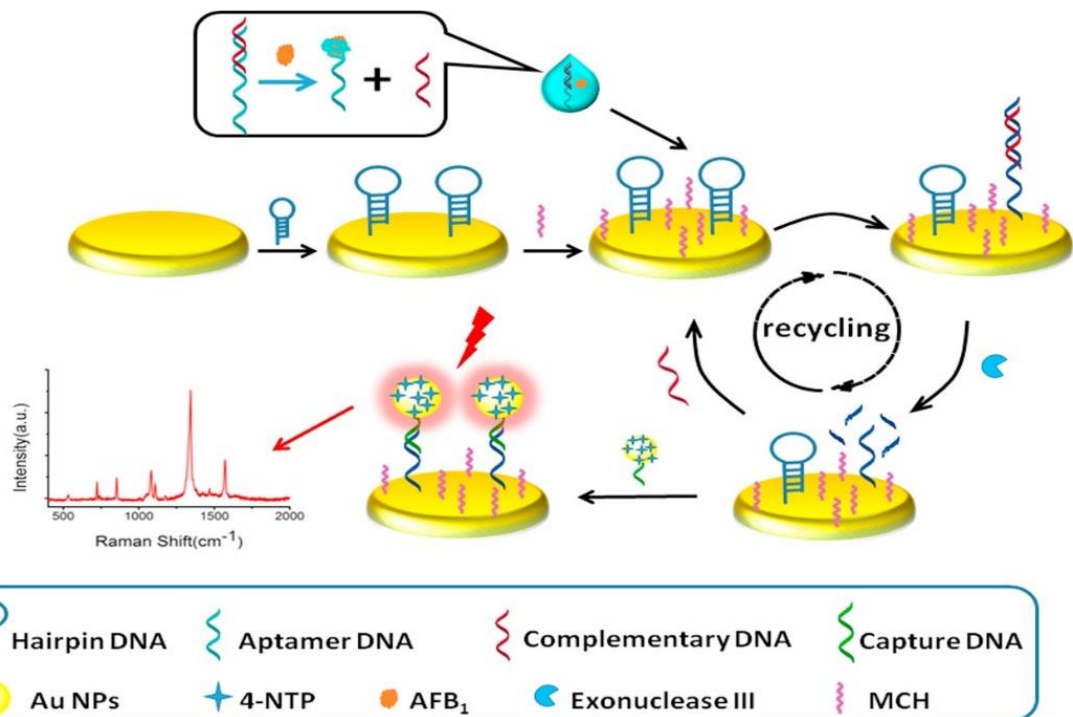


**Figure 6.** Exonuclease-assisted recycling aptameric sensing chip method to detect AFB<sub>1</sub>. Reproduced with permission from ref 132. Copyright © 2017 Elsevier B.V.

### 1.5.3.3 Techniques based on molecularly imprinted polymers (MIPs)

These stable polymers can mimic the function of biological receptors using a template (target analyte) during their synthesis. The specificity of these polymers is compared to one between an antibody and its antigen. Additionally, MIPs can be applied to recognize and capture low-molecular-weight analytes.<sup>132,133</sup> MIPs can be synthesized directly on the surfaced of nanoparticles in the presence of the template, a monomer, a cross-linker, and an initiator molecule and as a result, MIPs@NPs will be obtained. Using these substrates, mycotoxins such as PAT, a very small molecule, was detected with high performance using SERS.<sup>107</sup> MIPs has been developed for the recognition of other mycotoxins, DON, OTA, ZEN, FB1, and trichothecene T-2 indicating a possible application in SERS.<sup>134-139</sup>

High sensitivity and selectivity are not difficult to accomplish using functionalized nanoparticles and the practicality and accuracy can always be improved due to the flexibility of these systems. For example, magnetic nanoparticles can be used to facilitate the separation process using a magnet;<sup>93,118,127,129,130</sup> a wide variety of surfaces can be used as platforms to immobilize nanoparticles or biosensors allowing the fabrication of devices for on-site detection;<sup>94,119</sup> more than one reporter can be used to improve the accuracy of the quantification;<sup>100</sup> and a wide number of nanostructures or a combination of them can be employed to magnify the SERS effects.<sup>93,99,127,129</sup> The selection of the type of substrate will depend mainly on the scope of the study. If the main purpose is the applicability, it is necessary to develop a rapid, sensitive, selective, reproducible method and will require important monetary resources. On the other hand, if the purpose is to explore SERS'

potential to study mycotoxins as fundamental research, the use of non-complex, less expensive substrates might satisfy the requirements, but it will need extensive data processing and analysis.

## **1.6 Current limitations and future perspective**

The increasing popularity that SERS has gained over recent years accompanied by the exponential progress in nanoscience is helping to solve one of the most common limitations attributed to SERS, the low reproducibility. The possibility to adapt biosensors has been crucial to improving the selectivity of the technique. However, there are still some drawbacks that need to be addressed, like the high-level expertise that the data analysis requires along with a deep understanding of statistical concepts to process and interpret results or the limited application due to the difficulty to implement a quantitative methodology correctly validated. There are many alternative routes to take to elevate this technique to the group of future analytical methods for mycotoxin detection.

### **1.6.1 Simplified sample pretreatment**

One of SERS's main characteristics is its simple sample pre-treatment that is easily ascertainable as the samples do not need extensive cleanup steps subsequent to the extraction when compared to most of the AOAC Official Methods of Analysis.<sup>2</sup> SERS is compatible with the liquid-liquid extraction (LLE) method, one of the most traditional mycotoxin extraction methods, which is simple and affordable and it can be adapted to different scales.<sup>36</sup> Generally, LLE extraction utilizes solubility properties to separate the analyte from most of the matrix components, followed by a filtration or centrifugation step

to eliminate the remaining solid suspensions. The choice of solvents also depends on the compatibility of the solvent and substrate, particularly for antibody/aptamer functionalized substrates that require compatible buffering conditions to maintain the activity of the antibodies or aptamers. In addition to the conventional LLE extraction method, a supported-liquid membrane (SLM) method and a QuEChERS (quick, easy, cheap, effective, rugged, safe) system were employed to extract OTA from wine samples<sup>101</sup> and AFB1 from wheat, corn, and protein feed powders,<sup>97</sup> respectively. These simplified sample pretreatments can integrate sampling, extraction, and concentration while reducing sample handling and using a lower volume of solvents<sup>36,140</sup>. Another approach is solid-phase extraction (SPE) which uses the principle of chromatographic techniques employing disposable cartridges packed with an analyte-bonding material to recognize and separate the target analyte from the rest of the sample. Several SPE methods were developed for the extraction of mycotoxins OTA, AFB1, fumonisins, AOH, and PAT from different food samples, however, one of the main disadvantages of this method is that it requires specific conditions for each type of analyte, making it unlikely to find a universal type of cartridge for mycotoxins.<sup>36</sup> QuEChERS methods on the other hand have been validated to extract fourteen mycotoxins from different commodities for a UHPLC-MS/MS analysis<sup>141</sup> or up to seventeen mycotoxins for detection using an LC-Quadruple Orbitrap MS.<sup>142</sup> This technique includes a micro-scale extraction with acetonitrile coupled to a dispersive solid-phase extraction (d-SPE) to remove most of the remaining matrix interferences.<sup>143</sup> Additionally, these methods can be done using magnetic systems<sup>144–149</sup> indicating the

potential to combine them with some of the previously mentioned SERS systems. Developing an all-in-one device for mycotoxins extraction and SERS detection is the ultimate goal for a commercial product.

### **1.6.2 In-situ mapping**

Spectral data can be collected from discrete sections of an area or volume and integrated to generate artificial color images based on the intensity of a designated peak. This approach, named mapping technique, provides a better relative standard deviation than a simple average of a few randomly chosen points. Choo and coworkers<sup>150</sup> developed a microarray platform to detect three mycotoxins, OTA, FB, and AFB1. Using an antibodies-based system, this group showed that SERS mapping facilitates the interpretation of the results without affecting the sensitivity (Figure 7). This method also allows the use of a larger quantity of samples, usually meaning more representative sampling. A large amount of liquid sample or diluted solid sample can be concentrated by filtration and the detection will be made using the same filter or membrane as the solid support.<sup>135</sup> Mapping analysis' most exciting feature is probably the possibility of directly analyzing the surface of vegetables, fruits, or other food products<sup>151,152</sup> thus providing valuable information on the distribution and behavior of mycotoxins in matrices. The main limitation of this method is the need for a Raman microscope and sample staging moving in automation which increases the time and cost for sample analysis.<sup>153</sup>

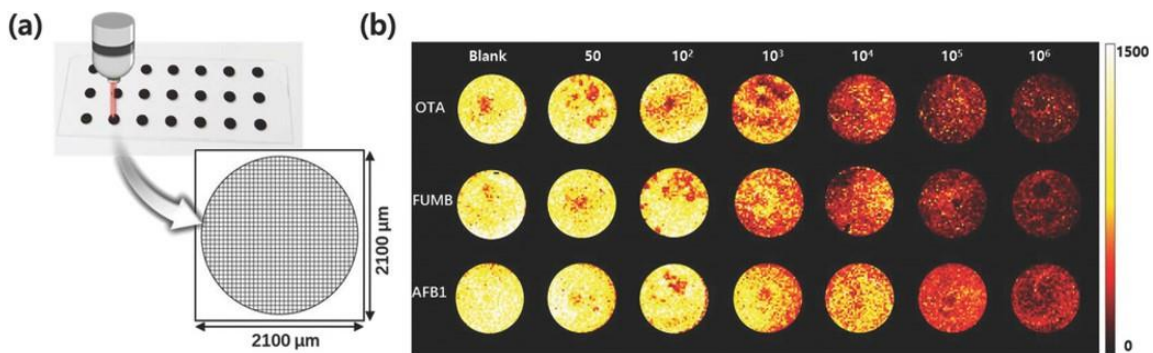


**Figure 7.** SERS mapping-based multitoxin detection system. a) Detection pixels of a microarray well for the scanning of Raman signals. b) SERS mapping images acquired for seven different concentrations of OTA, FB, and AFB1. The scale bar on the right displays the color coding for different Raman intensities. Reproduced with permission from ref 151. Copyright © 2018 WILEY-VCH Verlag GmbH & Co. KGaA, Weinheim.

### 1.6.3 SERS combined with other techniques

SERS can be combined with other techniques to complement their advantages and to overcome their individual limitations. Basically, SERS detection capability will be enhanced if it is combined with separation, colorimetric, labeling techniques, or microfluidic devices. If SERS is combined with other spectroscopic techniques, MS, nuclear magnetic resonance (NMR), infrared spectroscopy (IR), or X-ray spectroscopy (XR), the characterization capability will benefit greatly.<sup>154</sup> This approach was proven before on the mycotoxin field combining SERS with thin-layer chromatography (TLC) for on-site detection of AFB1 from peanut samples, that additionally, due to TLC high separation abilities allowed the differentiation of the three remaining types of aflatoxins, B2, G1, and G2.<sup>155</sup> Another example is the combination with fluorescence resonance energy transfer effect (FRET) for simultaneous detection of three mycotoxins (OTA, ZEN and FB1). Using this method the spectra of the three different analytes showed clear differences facilitating the discrimination although it required a complicated procedure.<sup>156</sup> The use of microfluidic devices for the development of miniature detection systems is one of the most promising approaches. The continuous flow condition generated in a microfluidic system guarantees reproducible results even using low laser intensity as it is seen in a study that attached OTA-aptamers on the surface of a microfluidic channel for the development of an on-site detection device.<sup>157</sup> This integration is being studied and successfully applied to the detection of many other food contaminants showing numerous benefits like a fine control over the size and shape of the nanostructures, allowing highly

reproducible quantitative results.<sup>158</sup> The application of these devices in food matrixes is still in its early stage and a fast expansion in the research field is expected. Integration with a smart mobile device will open the possibility of the SERS approach of reaching wider users and applications. In fact, the development of a smartphone-based SERS spectroscopy method was reported last year. The device showed easy operation and a rapid response time when analyzing typical SERS model molecules, rhodamine 6G and crystal violet<sup>159</sup>, with the potential to extend to other analytes.

#### **1.6.4 Multi-toxin analysis**

In addition to the basic requirements, the possibility of studying multiple analytes simultaneously adds extra value to any analytical technique but this becomes particularly necessary if the target is a market in which the co-existence of several analytes of interest in one sample, is well known.<sup>1,14,17</sup> This concern has been considered and a few studies have already investigated SERS' capability to detect multiple mycotoxins simultaneously. The first one in 2015, employed an indirect aptameric-based method for simultaneous detection of OTA and AFB1 in maize meals with satisfactory LODs, 0.006 ng/mL and 0.03 ng/mL, respectively.<sup>92</sup> Later, another group developed a method to detect three mycotoxins, OTA, DON, and ZEN on the same sample based on the positive effects provided by nanoparticles with irregular shapes, and uniformly distributed on the surface of a solid platform. The SERS substrate was cauliflower-shaped AuNPs in an AAO template. This substrate showed high stability, relative standard deviation (RSD) of 4.5%, and the method detected mycotoxins at concentrations lower than the FDA advisory levels.

Another explored approach was the use of antibodies for the simultaneous detection of AFB1, OTA, and ZEA in foodstuffs,<sup>95</sup> and AFB1, OTA, DON, ZEN, FB1, and T2 in maize samples. In the second example, Zhang and colleagues<sup>94</sup> developed a triple test line lateral flow strip system that can be used on-site to detect six mycotoxins, reaching a picogram level. This method (Figure 8) is an indication of SERS' significant potential to be miniaturized in an on-site multi-mycotoxin detection device. The goal is to develop a rapid method for multi-toxin detection combined with a universal simplified sample pre-treatment that is applicable to various types of food matrixes.

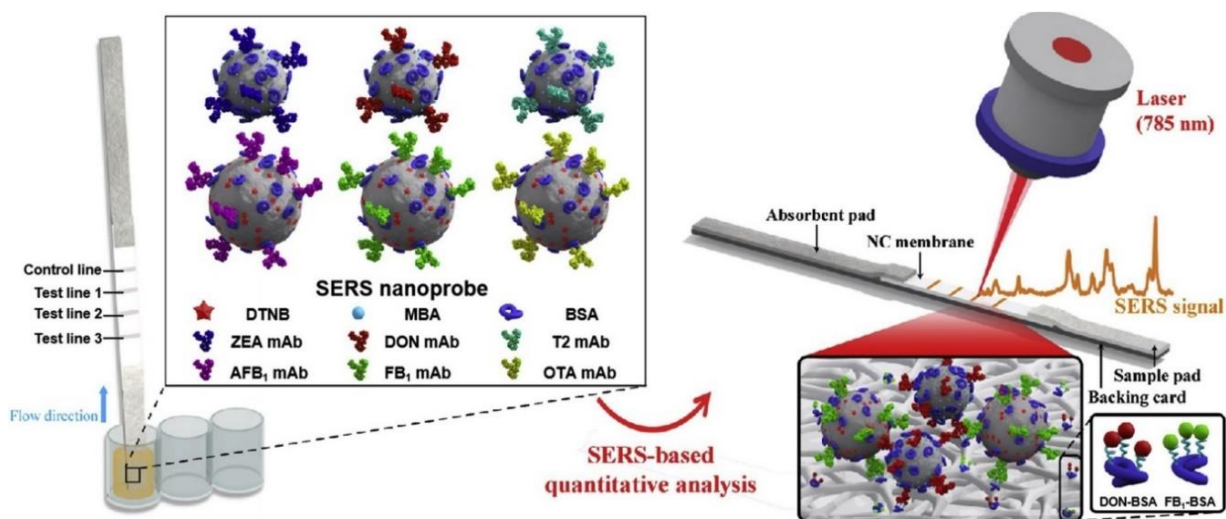


**Figure 8.** Antibody-based lateral flow immunosensor for multiple detection of mycotoxin in Maize. Reproduced with permission from ref 93. Copyright © 2020 Elsevier B.V.

### 1.6.5 “Detection” to “behavior analysis”

Mycotoxin products formed after thermal treatments during food processing may have different toxicological properties than the parent mycotoxin, which makes it imperative to understand the fate of these molecules under degradation treatments. A recent study discussed the limited availability of analytical methods to study the fate of mycotoxins during thermal food processing. Most studies rely on targeted analysis that uses a set of expected compounds that might differ from the formed products. Alternately, untargeted analysis allows the elucidation of the complete spectrum of degradation products, known and unknown, in an unbiased way.<sup>160</sup> By monitoring and interpreting the changes in the SERS spectra of mycotoxins during and after processing we may obtain valuable information on the stability and degradation of the toxins. Computational methods such as DFT help to provide a theoretical description of the chemical enhancement and to predict a Raman spectrum for metallic surface-adsorbed molecules. DFT-simulated spectra can be compared with experimental data to provide valuable insight into the interaction of the target molecule with SERS substrates.<sup>63,64,84</sup> SERS already demonstrated the ability to describe mycotoxin spectra at a molecular level in combination with DFT analysis.<sup>83,87,88,115</sup> Also, its capability to monitor in real-time the kinetics of catalytic degradation of dyes molecules<sup>161–163</sup> shows the potential to expand its applicability beyond detection analysis. Furthermore, SERS might help unravel the behavior of molecules during interaction with biosensors or nanostructures and provide information to improve bonding, stability, etc. and therefore develop better protocols.

### 1.6.6 Application of deep/machine learning

Future trends for both, SERS techniques and mycotoxin studies are not limited to their adaptation into the smart device's universe. The concept of deep learning and artificial intelligence methods for Raman and mycotoxin analysis is not new in either of these fields. Machine learning can be defined as a system capable of acquiring knowledge by extracting features from raw data and then using this knowledge to make decisions to tackle real-world problems.<sup>164</sup> Electronic nose and electronic tongue have been already applied for rapid detection of toxigenic fungi and mycotoxins.<sup>165</sup> OTA/CTN-producing strains of *Penicillium verrucosum* on bread were successfully detected using an electronic nose.<sup>166</sup> Likewise, identification of food adulteration<sup>167-172</sup> or food contaminants such as pesticides<sup>173-175</sup> has been made by applying different approaches of Raman/SERS-machine learning concepts. SERS characteristics like the ability to generate a large number of spectral profiles in a short time make it suitable for use with artificial intelligence. It is conceivable to think about the possibility of quickly constructing a database of Raman spectral profiles of mycotoxigenic fungi and mycotoxins, with special attention to emerging mycotoxins, and implementing a machine learning method for the early detection of contaminated crops. Although it is important to generate information about the physicochemical properties of these molecules and to understand their toxicological effects, the food industry already has the information needed to understand that the new technologies should focus on the elimination of these toxic substances from the food chain.

## **1.7 Conclusion**

This review is the first to survey studies that applied SERS for the study and detection of mycotoxins. Contrary to the well-established conventional methods, SERS proved to be extremely flexible and adaptable to a large number of substrates, biosensors, and platforms for sensitive and selective mycotoxin detection and characterization. With the continuous miniaturization of Raman spectrometer devices and the development of the cost-effective and compatible SERS substrates, SERS holds the potential to reach the goal of the next generation of analytical techniques for mycotoxin research including a direction toward simple, fast, and field-deployable detection of multiple classes of mycotoxins, and toward advanced characterization and analysis for fundamental research.

**CHAPTER 2**

**A FACILE SOLVENT EXTRACTION METHOD FACILITATING  
SURFACE-ENHANCED RAMAN SPECTROSCOPIC DETECTION OF  
OCHRATOXIN A IN WINE AND WHEAT**

**2.1 Abstract**

The capability of a solvent-mediated liquid-liquid extraction (LLE) method to improve the detection of ochratoxin A (OTA) in food matrixes using surface-enhanced Raman spectroscopy (SERS) is described. SERS detection of mycotoxins with nanoparticle aggregation is a simple method but with low reproducibility due to the heterogeneous distribution of the nanoparticle aggregates. We evaluated three different LLE protocols to analyze their performance in combination with SERS. A facile extraction method based on sample acidification and addition of chloroform as a separation solvent showed to not only extract OTA from wine and wheat but also facilitate the uniform distribution of the nanoparticles leading to an improvement of the detection signals and the reproducibility. This method enables rapid and simple analysis of mycotoxin Ochratoxin A in food systems.

## 2.2 Introduction

Ochratoxin A is one of the most widely spread mycotoxins metabolized by some toxigenic species of *Aspergillus* and *Penicillium* that contaminate a large variety of agricultural commodities such as grains, nuts, spices, coffee beans, and grapes, and imposes a hazard on both human beings and animals. Based on animal studies, the toxin has been shown to affect mostly the kidney but it can also have teratogenic, immunosuppressive, and carcinogenic properties.<sup>176,177</sup> Despite the implementation of good agricultural, storage, and processing practices, OTA might be still present in food products even when the mold is not visible.<sup>2</sup> Hence, a rapid screening method that can be employed out of a lab setting is desired to facilitate the control of OTA contamination in agricultural commodities.

Surface-enhanced Raman spectroscopy (SERS) has been explored as a rapid screening method with the potential of on-site measurement with a portable device. It is an advanced Raman spectroscopic technique that enhances the molecular fingerprint of analytes in the presence of nanoscale roughened metal particles and/or surfaces.<sup>68,178</sup> In terms of mycotoxin detection, several SERS methods have been developed using nanoparticles; AuNPs or Au and Ag core/shell nanorods coated with aptamers or MIPs.<sup>66,107,127,129</sup> Compared to the classical chromatographic methods, such as HPLC, TLC coupled with FL detection or MS/MS<sup>179-183</sup> SERS is more cost-effective and simpler.

Compared to the lateral flow immunoassays (LF-IA)<sup>184,185</sup> SERS has demonstrated better sensitivity and quantitative capability. Despite that various functionalized SERS

substrates have been reported to be useful for mycotoxin applications, these substrates are not commercially available nor can be synthesized easily, thus limiting this technique for practical applications. Alternatively, unfunctionalized Ag or Au nanoparticles can be purchased commercially or synthesized easily as SERS substrate, however, but this is still limited mainly because of the difficulty to control the aggregation of the nanoparticles thus leading to signal inconsistency.<sup>73,92,186</sup> In addition, sample pretreatment before SERS measurement is critical for real food sample analysis, which has not been extensively studied.

In this study, we investigated three LLE methods of OTA from a wine sample and their impacts on SERS analysis utilizing inexpensive colloidal silver nanoparticles that can be purchased commercially or synthesized easily. We demonstrated a facile but effective approach to not only extract OTA from complex food matrices such as wine and wheat but also facilitate a formation of uniform SERS substrate which solved the signal variation issues from the use of silver nanoparticles. With the demonstration of sensitive detection in real complex food matrices, this approach shows great potential to be used as a screening method for OTA in wine and wheat.

### **2.3 Sample preparation and procedure**

OTA, silver nitrate, chloroform and phosphoric acid were purchased from Sigma-Aldrich (St. Louis, USA). Sodium citrate dihydrate, methanol, ethyl acetate, chloroform was purchased from Fisher Scientific (Hampton, USA). A stock solution of OTA was prepared dissolving 1 mg of OTA in 5 ml of methanol and stored at -4 °C. Silver

nanoparticles were synthesized via reduction of silver nitrate using sodium citrate. All aqueous solutions were prepared with ultrapure water from Thermo Scientific Barnstead Smart2Pure Water Purification System. Red wine and wheat samples were purchased from a local market and spiked with a known amount of OTA solution. Triplicate samples were taken to perform the following OTA extraction methods (see Figure 9 for clarity).

Method 1: Acidification with a solution of  $\text{H}_3\text{PO}_4$  and NaCl followed by extraction with chloroform.<sup>187</sup> 500  $\mu\text{L}$  of the sample was thoroughly mixed with 1000  $\mu\text{L}$  of an aqueous solution containing 3.4% of phosphoric acid (85%) and 11.8% of NaCl. 500  $\mu\text{L}$  of chloroform were added and intensively mixed during 1 min using a vortex followed by centrifugation at 2500 X g for 15 min. A compact thin layer was formed between the two phases. The clear organic phase at the bottom was separated and the extraction was repeated with another 500  $\mu\text{L}$  of chloroform. The combined extracts were evaporated to dryness in a vacuum evaporator at 30 °C. The residue was redissolved in 100  $\mu\text{L}$  of an aqueous solution containing 15% of methanol (v/v).

Method 2: Acidification with  $\text{H}_3\text{PO}_4$  followed by extraction with chloroform.<sup>188</sup> This method was based on the one described previously with some modifications as follows: 200  $\mu\text{L}$  of the sample was acidified to pH 2 using  $\text{H}_3\text{PO}_4$  85% and intensively mixed during 1 min using a vortex. Then 200  $\mu\text{L}$  of chloroform was added and the organic phase was separated by centrifugation (3200 X g, 15 min). The aqueous phase was extracted one more time with 200  $\mu\text{L}$  of chloroform. Organic extracts were reunified and evaporated in

a vacuum evaporator at 30 °C. The residue was redissolved in 100  $\mu$ L of an aqueous solution containing 15% of methanol (v/v).

Method 3: Extraction using ethyl acetate as the extraction solvent.<sup>189</sup> 300  $\mu$ L of ethyl acetate was added to 200  $\mu$ L of a non-acidified contaminated wine sample and the mixture was mixed for 5 min using a rotating shaker. After that, samples were incubated at room temperature for 15 min to allow the phases separation. The organic phase at the top was separated in a new tube and evaporated in a vacuum evaporator at 30 °C. The residue was redissolved in 100  $\mu$ L of an aqueous solution containing 15% of methanol (v/v).

All extracts were mixed in a 1:1 ratio followed by a quick 3 min incubation, after those three drops of 10  $\mu$ L of the mixture was dropped in a gold slide and dried at room temperature. A total of 30 spectra per drop were collected using a Thermo Scientific DXR Raman Spectro-microscope under the following conditions: 780 nm laser source, 20x objective resulting in laser spot of 2mm diameter, 10 mW laser power, and 1 s exposure time. SERS mapping was performed using DXRxi Raman Imaging Microscope with the following parameters: 20x objective, 780 nm excitation wavelength, 5 mW laser power, 50  $\mu$ m slit aperture and 0.01 s collection time for an area of 2.8 mm x 2.8 mm.

To quantify OTA in real samples, wine and wheat samples were spiked with five different concentrations of OTA: 0.01, 0.05, 0.1, 0.5 and 1 ppm. The wine samples were subjected to the method 2 for extraction and measurement directly. For wheat samples, the pretreatment of the sample was performed as follows; 1 g of ground contaminated wheat samples were suspended in pH 2 aqueous solution and rigorously mixed during 30 min.

The liquid phase was separated from the pellet by centrifugation (10000 rpm, 15 min) and transfer to a clean glass vial after where the protocol for extraction method 2 was applied. All the experiments were performed by triplicate and repeated on different days independently. TQ Analyst 9.8.208 software was used to construct a partial least squared (PLS) regression model to analyze the results. PLS is a multivariate analysis that reflects the intrinsic feature of one or more pure component spectra in a sample in which many sources contribute to the observed signal.<sup>190</sup> The PLS model was built using direct SERS spectra of each sample set, correlating OTA concentration with the intensity of peaks assigned to OTA characteristic spectra.

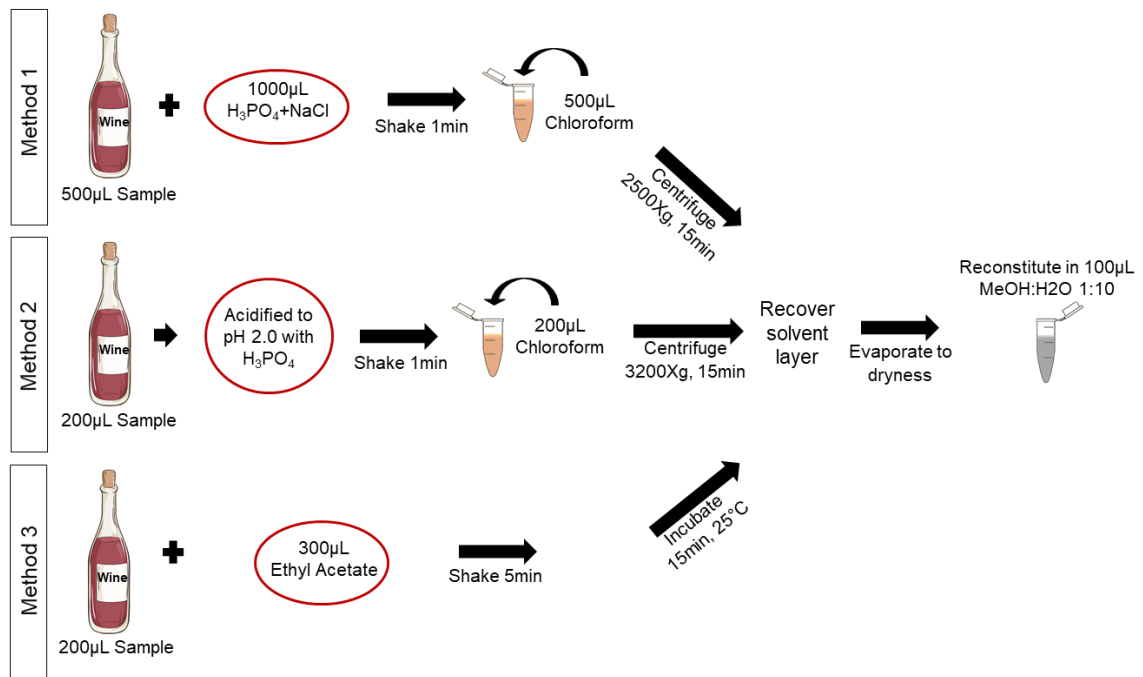


**Figure 9.** Illustrative diagram of LLE methods tested.

## 2.4 Results and discussion

Figure 10A shows the OTA molecular structure, which consists of a dihydroisocoumarin moiety linked with phenylalanine through an amide bond. Three of the major peaks founded in the SERS spectra of an aqueous solution of OTA are highlighted in Fig. 10B. Peaks at  $1003\text{ cm}^{-1}$  and  $1030\text{ cm}^{-1}$  are generally attributed to the ring breathing mode and C-H in plane bending mode of phenylalanine respectively<sup>191</sup>, and due to the strong signals of  $1003\text{ cm}^{-1}$  on OTA spectra, this peak has been already used to quantified the mycotoxin concentration in wines using SERS<sup>101</sup>. An important characteristic of OTA chemical structure is the presence of an amide bond, a group that has been previously associated with peaks in a range between  $1600\text{-}1610\text{ cm}^{-1}$ .<sup>192,193</sup> These three peaks were present with intensity variations in all OTA control spectrums regardless of the solvent utilized, which might indicate good OTA stability under the presence of organic solvents. But nevertheless, other differences observed between these spectrums showed that solvents (ethyl acetate or chloroform) or reagents (salts or acids) have an important influence on the final OTA spectra. Figure 10 also shows the spectra obtained from contaminated wine samples that were treated with different OTA extraction methods. The  $1003\text{ cm}^{-1}$  peak was present only using extraction method 2 (Fig. 10C) while it completely disappeared in the other two spectra of wine treated with methods 1 and 3. Although there was a small peak in the wine background at the same position, the background peak was significantly lower. The  $1030\text{ cm}^{-1}$  peak was also detectable only in the spectra of samples that were treated using method 2 but overlap with a peak at  $1045\text{ cm}^{-1}$  was observed. Interestingly, the last

peak of interest at  $1604\text{ cm}^{-1}$  showed strong signals, with some small shifting in the spectra obtained from the methods 1 and 3 (Fig. 10B and 10D) but not the method 2. This shift seems to be more related to the combination of the solvent (chloroform) with the acidic environment than to the influence of the matrix because this attenuation was already observed on the spectra of the corresponded OTA control.

Microscope images of prepared SERS samples on gold slides revealed different drying patterns for each method of extraction (Fig 10 B1, C1, and D1). With methods 1 and 3 the usual coffee ring structure was observed with a strong nanoparticle aggregation, for the first method possibly due to the presence of sodium chloride at high concentration.<sup>194</sup> With method 2, this coffee ring structure disappeared and instead, a donut-like structure was observed.

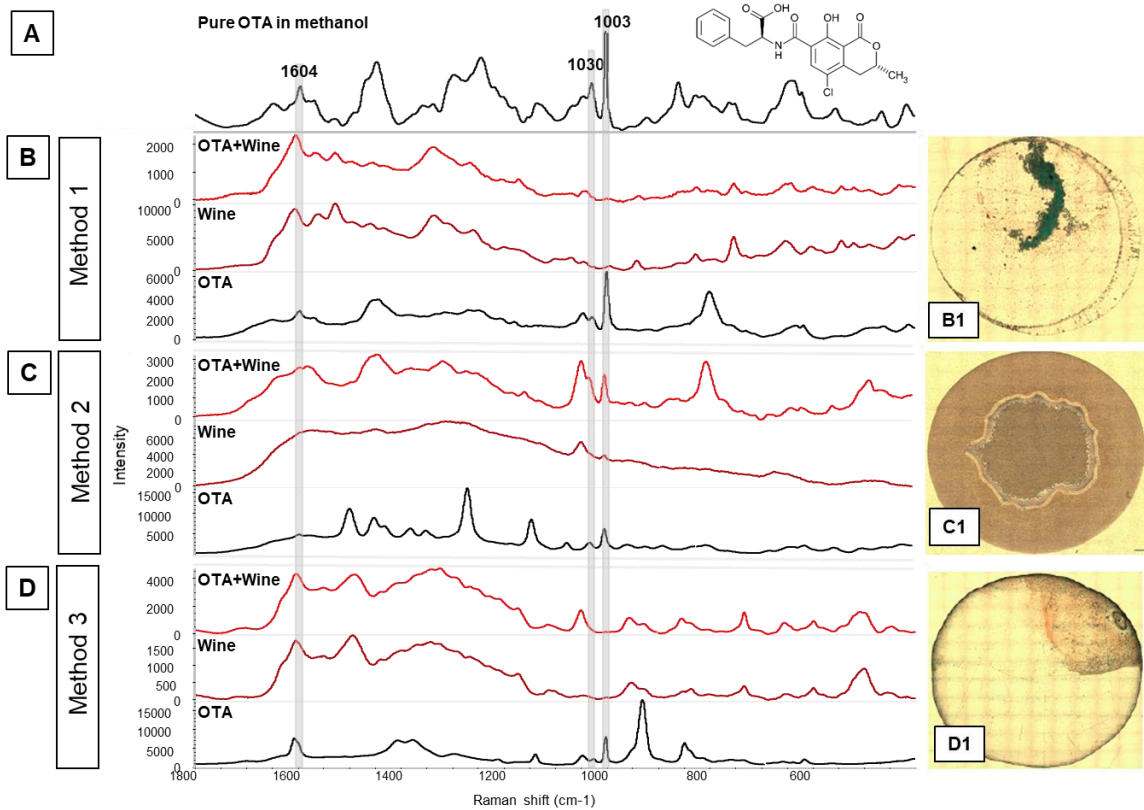


**Figure 10.** (A) SERS spectra of pure OTA in methanol and Ochratoxin A molecular structure. (B and B1) SERS spectra and microscope image of contaminated wine treated with extraction method 1. (C and C1) SERS spectra and microscope image of contaminated wine treated with extraction method 2. (D and D1) SERS spectra and microscope image of contaminated wine treated with extraction method 3.

To further investigate this phenomenon, we measured the samples from method 2 using scanning electron microscopy and Raman mapping. As shown was observed in Fig. 11, AgNPs (white bright spots) seem to be spread around bigger crystal-like structures which were homogeneously distributed and forming one thick ring. Compared to the coffee ring structure where nanoparticles are extensively aggregated on the ring, the nanoparticles in this structure had a much lower degree of aggregation. Although nanoparticles aggregation to form the coffee ring is desired for enhancing SERS sensitivity, the aggregation process is difficult to control and often leads to non-reproducible results, making the implementation of quantitative analysis more difficult.<sup>63</sup> This donut structure demonstrated a much more homogenous distribution of the nanoparticles that facilitate quantitative analysis.

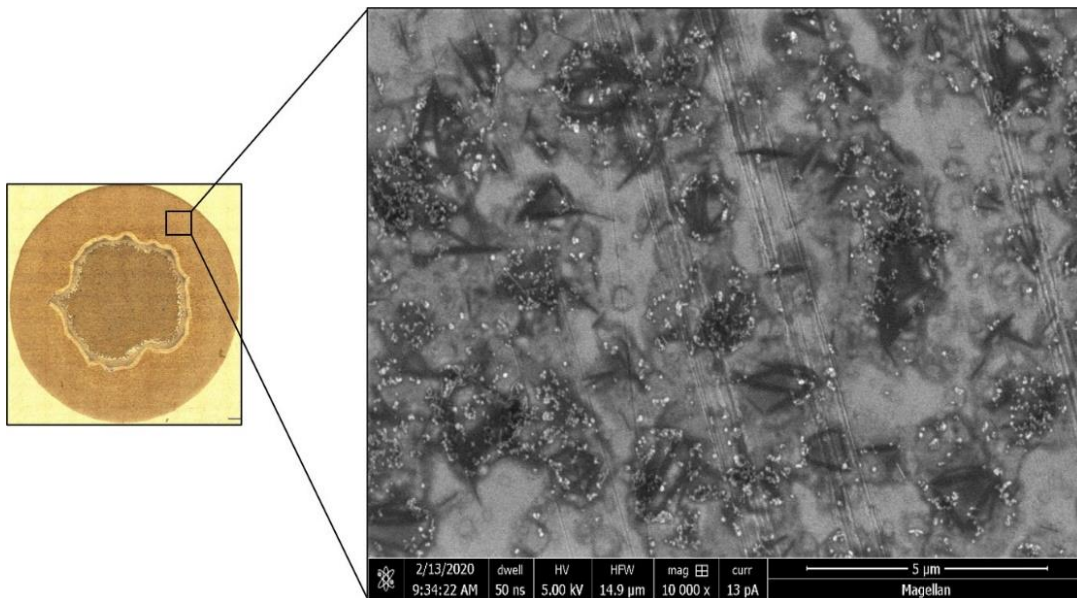


**Figure 11.** Scanning Electron Microscope (JEOL JCM-5000 NeoScope) image of contaminated wine sample treated with extraction method 2 dried drop on gold slide.

The Raman mapping (Fig. 12A) of the OTA spiked wine sample treated with the extraction method 2 shows the OTA 1003  $\text{cm}^{-1}$  signal was distributed fairly even around the entire outer ring. As a comparison, Fig. 12B shows a sample of pure OTA in methanol that was treated with the same procedure, and this peak signal was mostly concentrated towards one edge of the ring with uneven distribution. In addition, the OTA signal intensity was found significantly improved when the matrix was involved. These results indicate the matrix effect facilitated the formation of the donut-like structure, which may be resulted from the complex (the crystal-like structure shown in SEM) formed by the interaction between the OTA, matrix, and nanoparticles. The formation of such a complex may not only reduce the driving force of the nanoparticles towards the coffee ring when drying, but also enhance the OTA and nanoparticle interaction so that the signals were enhanced. Based on the characteristic peaks at 1446, 1318, 1027, and 802  $\text{cm}^{-1}$  in the SERS spectra of method 2 sample, that were assigned to protein-related structures,<sup>195-198</sup> we speculate that the nature of these crystal-like structures might involve proteins. Bin et al reported an enhanced SERS activity based on the formation of a satellite-like complex involving AgNP, bovine serum albumin (BSA), and triclosan (TCS).<sup>199</sup> We will further investigate this structure in the future.

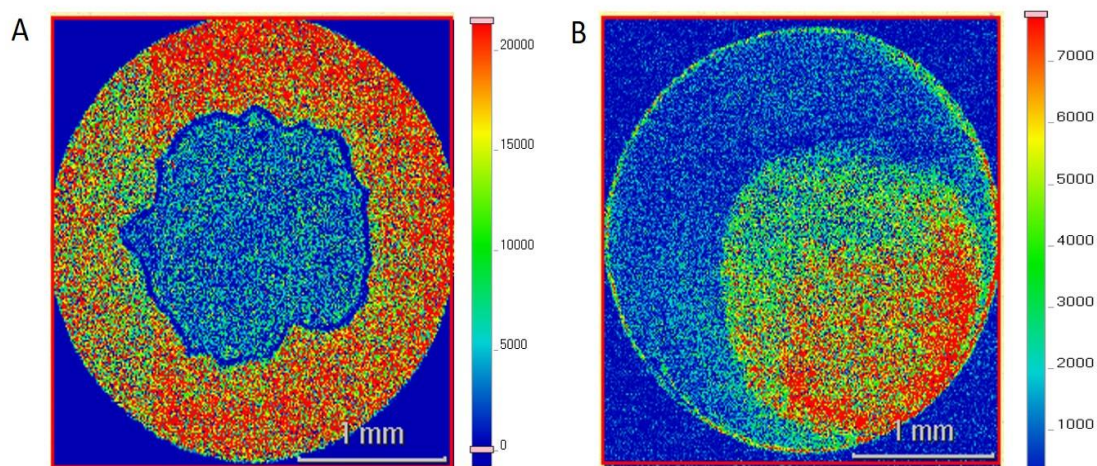


**Figure 12.** (A) Mapping image of OTA contaminated wine sample treated with extraction method 2. (B) Mapping image of OTA positive control that were treated with extraction method 2.

SERS signals for the increasing concentration of OTA in wine and a typical calibration curve are presented in Fig. 13. PLS regression analysis showed a good linear dependency between Raman intensity of the representative OTA peaks  $1030\text{ cm}^{-1}$  and  $1003\text{ cm}^{-1}$  and OTA concentration with a correlation factor of  $R = 0.9938$  in the range of  $0.01\text{--}1\text{ ppm}$ . The experiment was repeated independently on three different days, and the coefficient of variation of the R was calculated to be  $1.7\%$ . This result suggests the reliability of the method for quantifying OTA in wine.

Contaminated wheat seeds were also tested to determine the applicability of the technique in different matrix samples (Fig. 14). In addition to the phenylalanine peaks, two peaks at  $1520$  and  $1156\text{ cm}^{-1}$  showed strong signals until  $0.5\text{ ppm}$  of OTA but disappearing below that concentration. PLS regression analysis applied for  $1003\text{ cm}^{-1}$  and  $1030\text{ cm}^{-1}$  peaks showed an  $R = 0.9257$  but this coefficient improved drastically if the analysis was only applied to  $1003\text{ cm}^{-1}$  peak achieving  $R = 0.9883$  for wheat samples contaminated with OTA in a range of  $0.01\text{--}1\text{ ppm}$ . Similarly, this experiment was repeated independently on three different days, the coefficient of variation was calculated to be  $3.9\%$ .

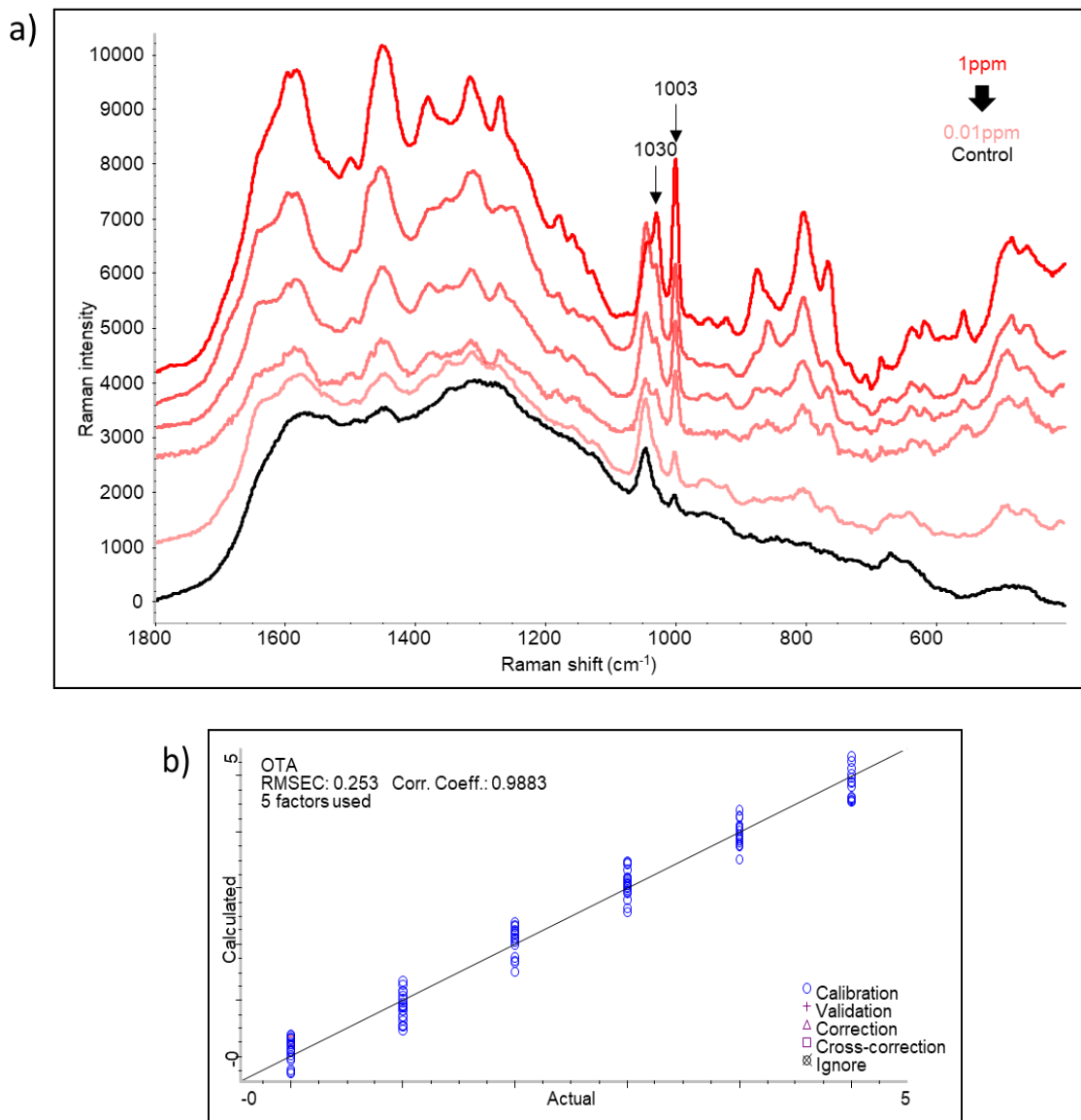


**Figure 13.** (a) SERS spectra of OTA contaminated wine samples after Method 2 – Liquid-liquid extraction at different concentrations of OTA. (b) Correspondent PLS analysis curve showing a linear relationship between OTA concentration and SERS signals at 1003 and 1030 Raman shift.

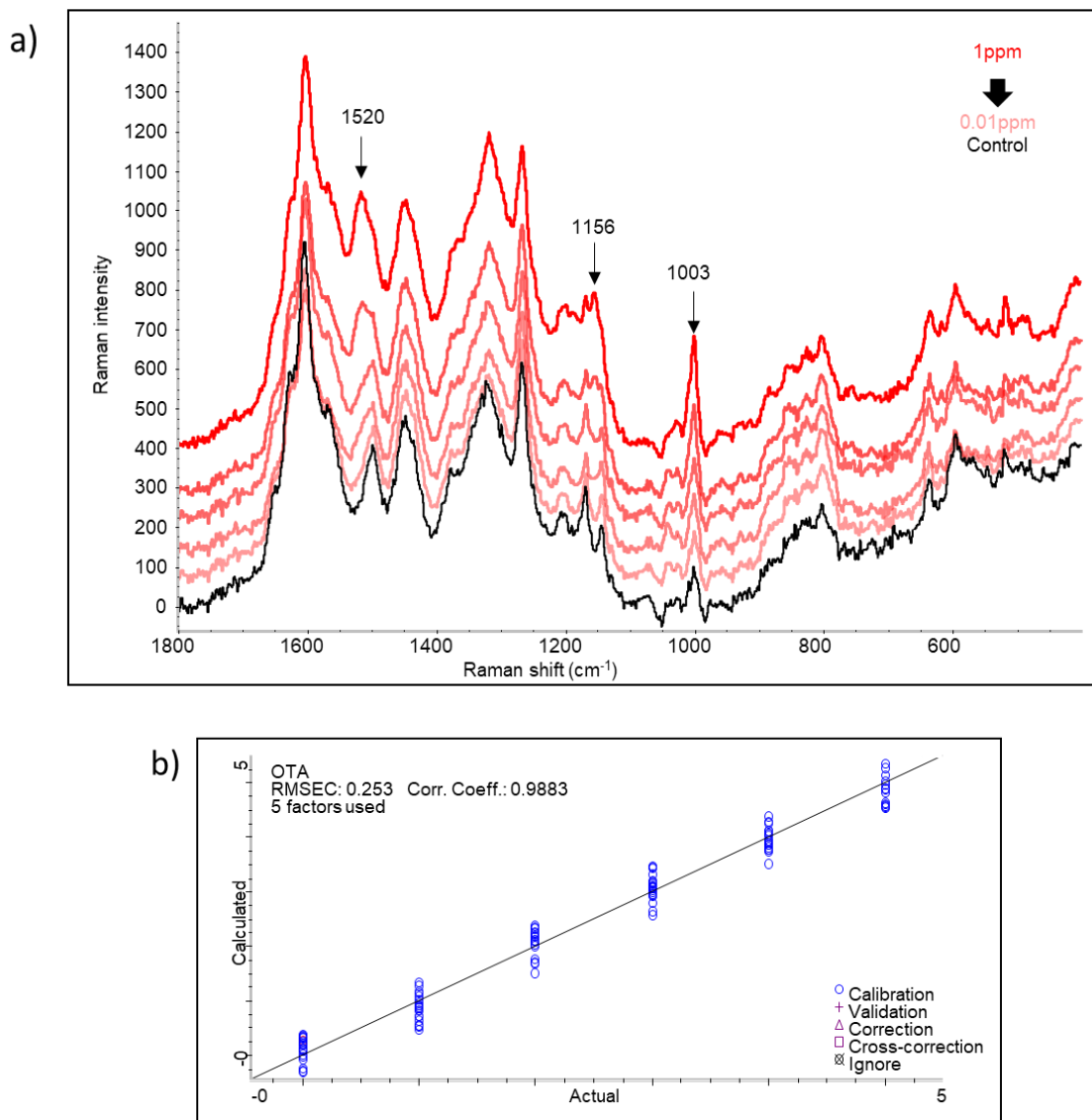


**Figure 14.** (a) SERS spectra of OTA contaminated wheat samples after Method 2 – Liquid-liquid extraction at different concentrations of OTA. (b) Correspondent PLS analysis curve showing a linear relationship between OTA concentration and SERS

## **2.5 Conclusion**

We demonstrated a simple approach to extract OTA from wine and wheat samples for SERS analysis. This extraction method that is based on the acidification of the sample followed by extraction with chloroform facilitates the uniform distribution of nanoparticles that produced consistent and enhanced signals, which demonstrated a positive impact of the matrix to SERS analysis. The simplicity of this technique that avoids the use of complex and tedious extraction/clean-up procedures reducing time and cost is an important breakthrough towards the development of faster and cost-efficient detection methods of mycotoxins on-site. Further study will focus on improving the sensitivity of this method and explore its application to other mycotoxins in food.

## CHAPTER 3

### HUMAN SERUM ALBUMIN ASSISTED DETECTION OF AFLATOXIN B1 USING SURFACE-ENHANCED RAMAN

#### 3.1 Abstract

A human serum albumin (HSA)-assisted assay enhanced mycotoxin aflatoxin B1 (AFB1) SERS signals using gold nanoparticles as SERS substrate. The optimized experimental parameters were established. Time of incubation played an important role in the interaction of AFB1-HSA with the SERS substrate. Optimum time of AFB1 and HSA incubation is 30 min. Optimum time of incubation of AFB1-HSA complexes with gold nanoparticles is 15 min. AFB1-HSA interaction showed a better performance under room temperature compared to 37 °C. The order or reaction between the three components, AFB1, HSA, and AuNPs affected the results. The presence of other HSA ligand such as mycotoxin ochratoxin A (OTA) did not affect the detection of AFB1 if the experiment was performed at room temperature. The applicability of this protocol was tested using certified compound feedstuff. AFB1 was extracted from feed samples by a liquid-liquid extraction method (LLE). Results showed a linear ( $R = 0.8905$ ) relationship of AFB1 concentration and SERS spectra. This approach provides a simple method that can be applied as a rapid and simple analysis of AFB1 in food systems.

### 3.2 Introduction

Aflatoxin B1 (AFB1) is a metabolite of *Aspergillus flavus* and *parasiticus*, prevalent mostly in cereals, nuts and tree-nuts. AFB1 is the most prevalent, potent genotoxic and hepatocarcinogenic identified agent that poses a serious risk for humans and livestock.<sup>122,200</sup> IARC has classified AFB1 as a human carcinogen belonging to Group 1.<sup>12</sup> In the US, AFB1 is the mycotoxin with the lowest limit of tolerance, 20ppb for all types of food destined for human consumption.<sup>201</sup> Due to its importance, an extensive number of methodologies have been developed for the detection of this mycotoxin in food products. Although the official method of the AOAC for chemical confirmation AFB1 is by chemical derivative<sup>37</sup>, modern techniques such as LC-MS, LC-FL are preferred due to their accuracy and reliability. But the limited access to the instrumentation due to the cost requires the development of more simple and affordable detection methods. Immunological-based methods such ELISA dominate the market but generally they cannot achieve the level of accuracy and sensitivity of the chromatographic/spectrometric methods.<sup>202,203</sup> These immunological methods in combination with SERS proved to be highly sensitive when detecting AFB1, reaching limits of detection in the low-femtogram range.<sup>94</sup> SERS is a modification of traditional Raman spectroscopy that enhances the vibrational spectrum of molecules in the proximity to the metal surface due to the large electromagnetic field induced by localized surface plasmon resonance.<sup>204</sup> SERS, has gained attention for being one of the few spectroscopic techniques that is moving towards the use of portable devices

for on-site or point-of-sampling (POC) analysis.<sup>205,206</sup> Chemically synthesized silver or gold nanoparticles and/or surfaces are generally the more popular SERS substrates, they are easy to prepare especially suitable for researchers who cannot fabricate sophisticated substrates and they can be easily adapted to portable systems. But a limited reproducibility and homogeneity which may complicate quantitative determinations is the main disadvantage of this type of substrate.<sup>207-209</sup> Different approaches have been used to address this problem, such as the innovate method previously developed by our group using AgNP core-bovine serum albumin (BSA) protein satellite to improve the detection of triclosan (TCS) in water samples.<sup>199</sup> Human serum albumin (HSA), from the same family of BSA, is the most abundant protein in human blood plasma. It functions on the membrane transport, distribution, and elimination of numerous compounds including mycotoxins and the formation of complexes with many of these compounds including AFB1<sup>210-215</sup> it has been previously studied. Additionally, the use of HSA to coat the gold nanoparticles for biomedical applications<sup>216</sup> demonstrate its compatibility with this type of colloidal SERS substrate. AFB1 and its detection in food have been previously studied using SERS, achieving satisfactory results, but most of the studies employed antibodies, aptamers, or other complex compounds to enhance the selectivity and sensitivity of this technique.<sup>217</sup> In this study we optimized an HSA assisted method of detection for AFB1 using SERS, as the first attempt to achieve a simpler analysis using bare nanoparticles without the need for complex ligands that can be expensive or hard to adapt when moving towards the use of portable SERS devices.

### **3.3 Materials and Methods**

#### **3.3.1 Chemicals**

AFB1, OTA and HSA were purchased from Sigma-Aldrich (St. Louis, USA). Citrate-capped AuNP (50 nm, 0.05 mg/mL) was purchased from nanoComposix (San Diego, USA). All aqueous solutions were prepared with ultrapure water (18.2 M $\Omega$ ·cm) from Thermo Scientific Barnstead Smart2PureWater Purification System.

#### **3.3.2 Optimization of HSA-assisted assays**

Stock solutions of AFB1 (200 ppm) and HSA (1  $\mu$ M) were prepared with methanol and ultrapure water, respectively and diluted to desired concentrations with ultrapure water. To optimize signal amplification, several parameters were tested as following: three different concentrations of the protein were mixed with AFB1 and AuNPs in a ratio of 1:1:2. HSA final concentration were 0.01, 0.005, 0.001  $\mu$ M. HSA (50  $\mu$ L) and AFB1 (50  $\mu$ L, 5 ppm) were incubated under slow agitation at room temperature and at 37  $^{\circ}$ C for 15, 30, and 60 min. After that, a second incubation was made mixing the AFB1+HSA mixture with 100  $\mu$ L of AuNPs for 15, 30, and 60 min, at room temperature and under slow agitation. Finally, 10  $\mu$ L of the sample was placed on the surface of a gold slide and air-dried for SERS measurement. Once the optimum parameters were selected, we tested a second protocol consisting of coating the nanoparticles with HSA, previous to the interaction with the toxin. HSA (50  $\mu$ L) and AuNPs, 50 nm (100  $\mu$ L) were incubated for 15 min under slow agitation. After that, 50  $\mu$ L of AFB1 (5 ppm) was added to the solution

and incubated for 30 min. SERS measurement was performed as previously described. The capability of the method to detect AFB1 on the presence of other HSA ligand was tested using a mixture of AFB1 and mycotoxin OTA in equal concentrations.

### **3.3.3 AFB1 detection**

The minimum detectable concentration of AFB1 using HSA-assisted assay was tested using five different concentrations of the mycotoxin, 2, 4, 6, 8, and 10 ppb. The applicability of our assay was evaluated using AFB1-free (< 1 ppb) and AFB1-highly contaminated (> 12.9 ppb) certified compound feed samples mixed at different ratios. Final concentrations of AFB1 were 2.5, 5.1, 7.7, 10.32 and 12.9 ppb. 0.75g of each mixture was placed in a 15 mL conical tube and 1.5 mL of methanol/water (8:10) was added. Tubes were vigorously shaken for 30 min on a mechanical shaker, after that samples were centrifugated at 3000 rpm for 5 min and 500 uL of the supernatant were placed in a new, clean microcentrifuge tube. Then, 100 uL of chloroform and 600 uL of 3% potassium bromide (KBr) was quickly added to each tube. After 5 min centrifugation at 3000 rpm, the extraction phase, settled at the bottom, was transferred to microcentrifuge tubes and dried in a vacuum evaporator at 30 °C for 30 min. Finally, the pellet was redissolved in 25 µL of methanol/water (8:10) and the HSA-assay protocol was applied as described before.

### **3.3.4 SERS measurement and data analysis**

Thermo Scientific DXR Raman Spectro-microscope equipped with a 780 nm laser source and 20 x objective was used in this study. For each sample, 20 spots were randomly selected, and the SERS spectra was collected using 10 mW laser power and 2 second

acquisition time. All the experiments were repeated 3 times. The mean and standard deviation were analyzed using OMNIC 9.0 software (Thermo Scientific). Partial least square (PLS) analysis was made using TQ Analyst software (Thermo Scientific).

### **3.4 Results and discussion**

#### **3.4.1 Characterization of AFB1 SERS spectra using AuNPs 50 nm as substrate**

AFB1 (Fig. 15a) presents a strong Raman fingerprint when mixed with AuNPs 50 nm (Fig. 15b). Most of the distinct peaks observed in this study are consistent with the ones found in the literature and a summary of the vibrational modes assigned to those Raman shifts are listed in Table 3.

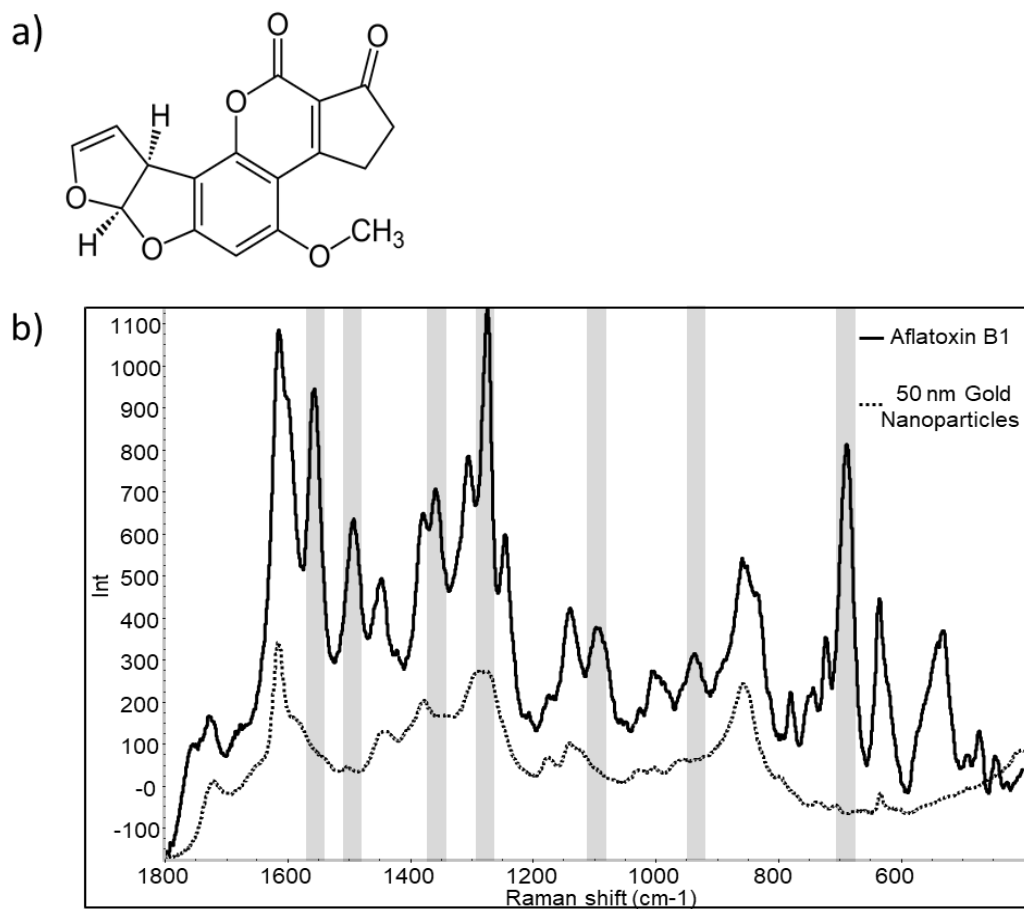


**Figure 15.** a) Molecular structure of AFB1, and b) SERS spectra of AFB1 using AuNPs 50 nm as SERS substrate. Seven major AFB1 peaks are highlighted.

**Table 3.** Summary of the Raman shifts and vibrational modes of AFB1 from experimental SERS spectra using gold nanoparticles as substrate.

Peak position (cm <sup>-1</sup> )	Vibrational modes	Ref.
1556	$\nu(\text{C-C})$ and ring deformation	83
1490	$\nu(\text{C7=C8})$ and ring deformation	
1357	$\delta\text{CH}_3$	
1272	$\beta(\text{C-H})$ and ring deformation	
1090	$\nu(\text{C-C-C})$ and ring deformation	
935	$\nu(\text{C-O})$ and ring breath	
687	C-H in-plane bending	

### 3.4.2 Optimization of HSA-assisted assays. HSA concentration

Previously, in a study using AgNP core –BSA satellite as SERS substrate to improve SERS signals of the antimicrobial agent TCS<sup>199</sup>, the importance of the protein:nanoparticle ratio to optimize the enhancement was demonstrated. Hence, we first tested three different concentrations 0.01, 0.005, and 0.001  $\mu\text{M}$  as final concentrations of HSA, chosen according to the results presented in the previous study. Figure 16a shows the SERS spectra of AFB1 without and in the presence of different concentrations of HSA. The strongest peaks at 687, 1271 and 1556  $\text{cm}^{-1}$  were selected to show the changes in the intensity under the presence of HSA. A slight enhancement on the SERS signals is observed when 0.001  $\mu\text{M}$  of HSA was used but the best signal is obtained when the HSA final concentration is 0.005  $\mu\text{M}$  (Fig. 16b), similar to the results obtained in the previous study. However, after using 0.01  $\mu\text{M}$  of HSA, the value of the AFB1 peak intensities decreased even under the control values. The use of ligand proteins like HSA reduces the distance between the analyte and the surface of the nanoparticles increasing the local electric field around a nanoparticle resulting in a SERS enhancement.<sup>219</sup> However, after passing the threshold of the HSA concentration it is reasonable to think that these molecules can become an interference and produce the opposite effect resulting in a decrease of the analyte signals.

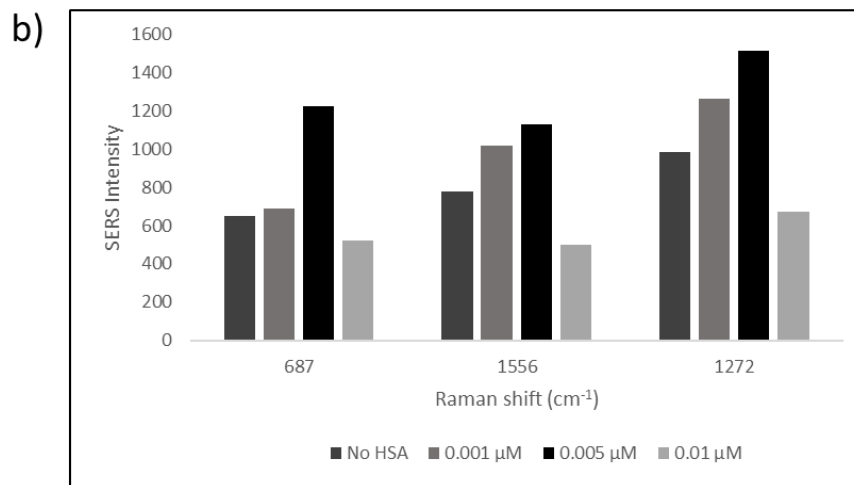
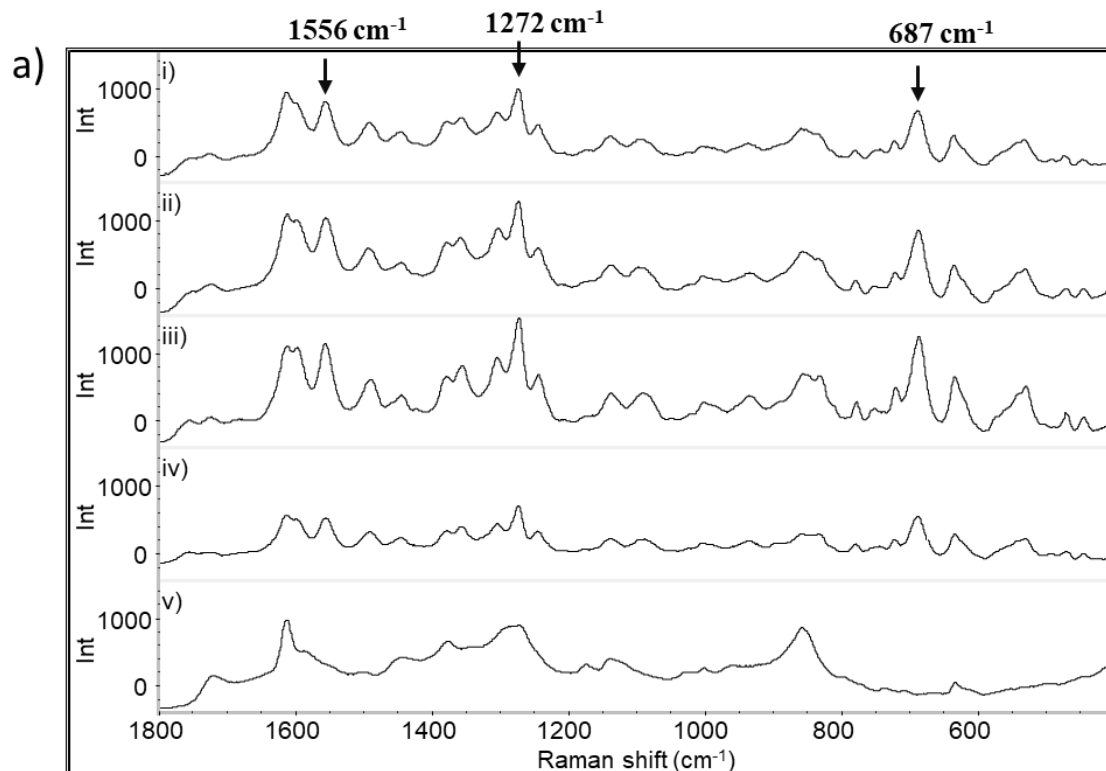


**Figure 16. a)** SERS spectra of: **(i)** AFB1 without protein **(ii)** AFB1 with 0.001 μM of HSA **(iii)** AFB1 with 0.005 μM of HSA **(iv)** AFB1 with 0.01 μM of HSA **(v)** HSA without AFB1. **b)** SERS intensity variation for three major AFB1 peaks, 687, 1556 and 1272 cm<sup>-1</sup>, using 0.001, 0.005 and 0.01 μM as final concentrations of HSA.

### 3.4.2 Optimization of HSA-assisted assays. Time and temperature of incubation

Time and temperature are generally important factors on the formation of chemical complexes. The binding process between AFB1 and HSA seems to be spontaneous at room-temperature<sup>214</sup> but when working at a low concentration of the analyte, a longer time of incubation might be needed to guarantee all the analyte molecules are captured by the protein. Figure 17a shows the average intensity of three major AFB1 peaks when this is incubated with HSA during 15, 30 and 60 min. The following incubation of the formed complexes with nanoparticles was maintained constant, for 15 min. The intensity of the three peaks followed the same trends, the maximum enhancement is observed when 30 min of incubation was applied. This result might indicate that 15 min is not enough to bind the present HSA with all the AFB1 molecules. However, when the incubation time reached 60 min, SERS signals suffered a drop in intensity. The HSA molecule is composed of three homologous domains (I, II and III), each of which is subdivided into a pair of subdomains called “A” and “B” (Fig. 18).<sup>220</sup> Most of the studies associated a site called Sudlow I on the subdomain IIA as the AFB1 binding site, while the stabilization of the HSA-AuNPs interaction is led by amino acids residues, mainly Trp and Tyr, in the Sudlow's site II (subdomain IIIA), the absorption of HSA on gold surfaces can affect the binding of ligands in near domains due to the changes generated on the tertiary structure of the protein.<sup>221</sup> Likewise, increasing the concentration of aflatoxins induced conformational changes in the protein structure proved by a blue shift (5 nm) in the emission spectra of HSA.<sup>214</sup> If the incubation time is long, most of the AFB1 present in the sample will bind to the HSA

molecules, and may be similar to what happens when the toxin concentration increases. This can result in changes in the protein conformation that can affect the interaction with the nanoparticles and therefore reduce the intensity of the analyte signals.

In comparison, SERS signal intensity of AFB1 in the presence of HSA followed a linear trend, decreasing over time, after the incubation with gold nanoparticles were made at 15, 30 and 60 min. Similar to the first test, the peaks at 687 and 1556  $\text{cm}^{-1}$  showed small variations; the most significant difference is observed on the 1272  $\text{cm}^{-1}$  peak. According to a DFT study performed by Wu, 2012 and co-workers<sup>83</sup> the three peaks are related to the primary structure of aflatoxins. That is to say, that these peaks appeared for any of the four types of aflatoxins (B1, B1, G1 and G2) tested in that experiment. However, the peak 1272  $\text{cm}^{-1}$  is also associated with amide III bands coming from protein backbones.<sup>222,223</sup> If in our experiment the source of this peak also comes from the protein, it might be another indication of changes on the protein structure after interaction with the mycotoxin over time. This hypothesis is based on the similarity between HSA controls spectra using different time of incubations, but deeper studies are needed before making any final conclusions.

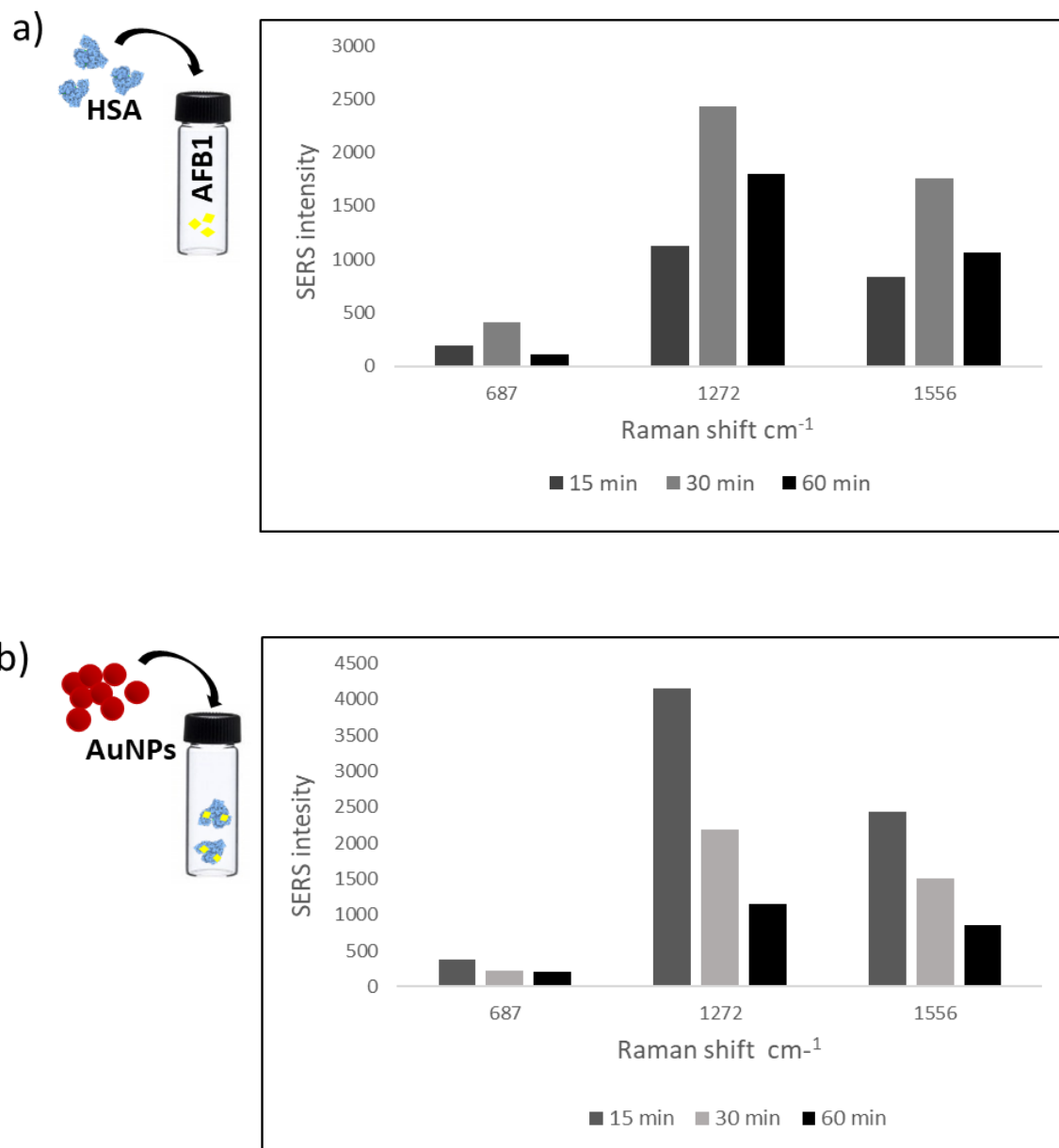


**Figure 17.** SERS intensity variation of three major AFB1 peaks, 687, 1556 and 1272  $\text{cm}^{-1}$  **a)** after 15, 30 and 60 min of AFB1-HSA incubation **b)** after 15, 30 and 60 min of (AFB1-HSA) + AuNPs incubation.

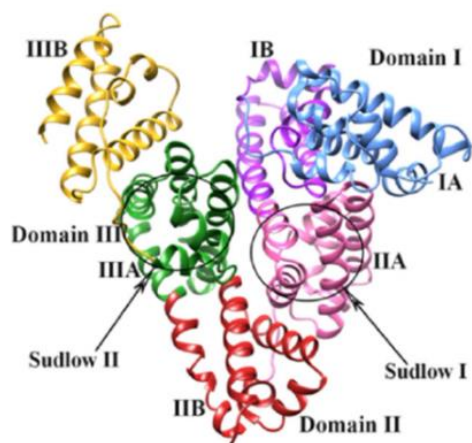


**Figure 18.** The structure of Human serum albumin (HSA) representing domains, subdomains, and binding sites Sudlow I (subdomain IIA) and Sudlow II (subdomain IIIA) related with AFB1 and gold surfaces binding sites, respectively. Ref. 204

The formation of AFB1-HSA complexes occurs in physiological conditions, pH 7.4 and 37 °C but studies suggests a decrease in the stability of the AFB1-HSA complex when increasing the temperature.<sup>211,214</sup> We incubated AFB1 and HSA at 37 °C and at room temperature to compare their SERS spectra. Figure 19 showed the changes in the SERS signal intensity of the peaks chosen as reference (687, 1227, and 1556  $\text{cm}^{-1}$ ). Results agreed with the information found in the literature. An increment in the temperature represents a non-favorable condition for the AFB1-HSA interaction. These results also have a positive connotation for our purpose, eliminating the need for a piece of equipment as an incubator.

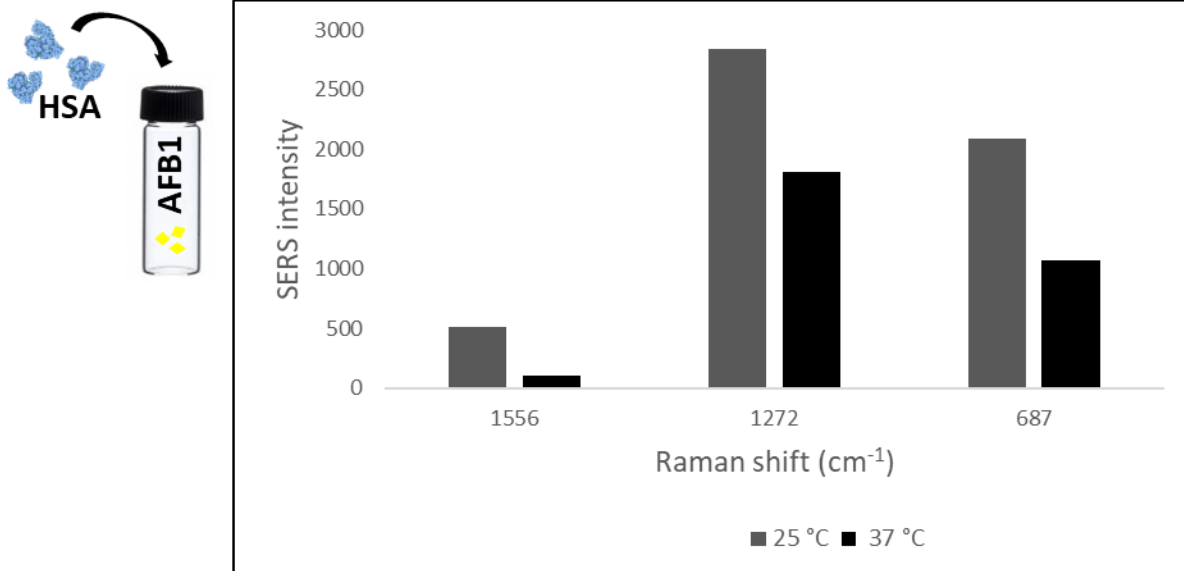


**Figure 19.** Variation of SERS signal intensity of peaks 687, 1272 and 1556  $\text{cm}^{-1}$  when AFB1-HSA is made under 37 °C or at room temperature (25 °C).

### **3.4.3 Optimization of HSA-assisted assays. Order of reactions**

The order of the interaction AFB1-HSA-AuNPs was reversed in an attempt to reduce total experiment time. The experiment consisted of adding the analyte to previously prepared HSA-coated gold nanoparticles that may be prepared ahead and stored, ready for use when necessary. Figure 20 shows the SERS spectra of AFB1 detected using SERS after using the first protocol in which the interaction between AFB1 and HSA is the first step (Method 1) and compared to the second protocol (Method 2) in which the toxin is added to an HSA-capped AuNPs substrate. Results indicated that the order of addition of the compounds has a significant impact on the toxin's SERS signals. The reduction in the intensity observed on Method 2 supports the idea previously suggested about conformational changes occurring in the protein when interacting with gold surfaces, resulting in an alteration of its ability to bind other ligands.

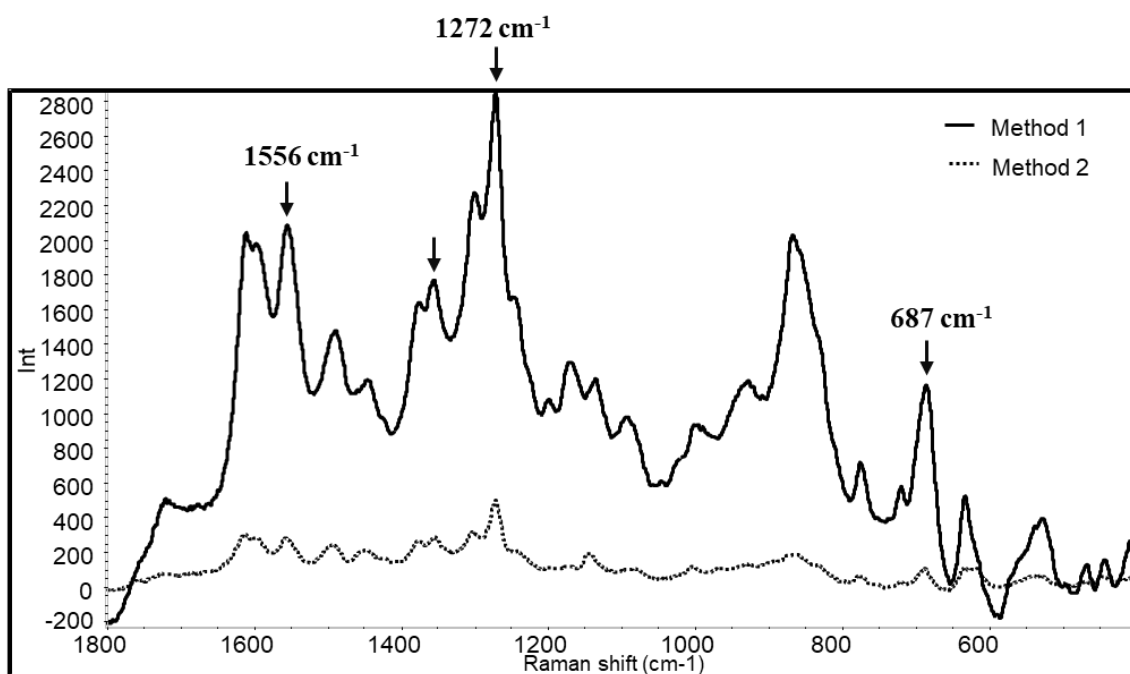


**Figure 20.** SERS spectra of AFB1 detected using SERS by Method 1: addition of nanoparticles to a solution containing AFB1-HSA complexes, and Method 2: addition of the analyte to a solution of HSA-coated AuNPs.

### 3.4.3 Optimization of HSA-assisted assays. Selectivity

Aflatoxin B1 binds to HSA with high affinity ( $K_a \sim 10^4$  L/mol) but other molecules including other mycotoxins such ochratoxin A showed higher affinity ( $K_a \sim 10^7$  L/mol) to the protein<sup>215</sup>. According to the literature, OTA binds to HSA in the two Sudlow sites, competing for one of the sites with AFB1 (site I, IIA). A mixture of AFB1 and OTA at the same concentrations were used in an HSA-assisted assay to test the selectivity of the method for AFB1. Figure 21 shows the result of this experiment. A reduction in the signal intensity is observed when OTA is present on the sample, but OTA's characteristic SERS peaks at 1003 and 1030  $\text{cm}^{-1}$  are not present. Compared to AFB1, the interaction of OTA with HSA was shown to be optimum under 37 °C.<sup>224-226</sup> The observation of the OTA related peaks, on 1003 and 1030  $\text{cm}^{-1}$ , when the experiment is performed under 37 °C supports previous studies. This experiment also demonstrated the crucial factor that temperature plays in the interaction of HSA with its ligands.

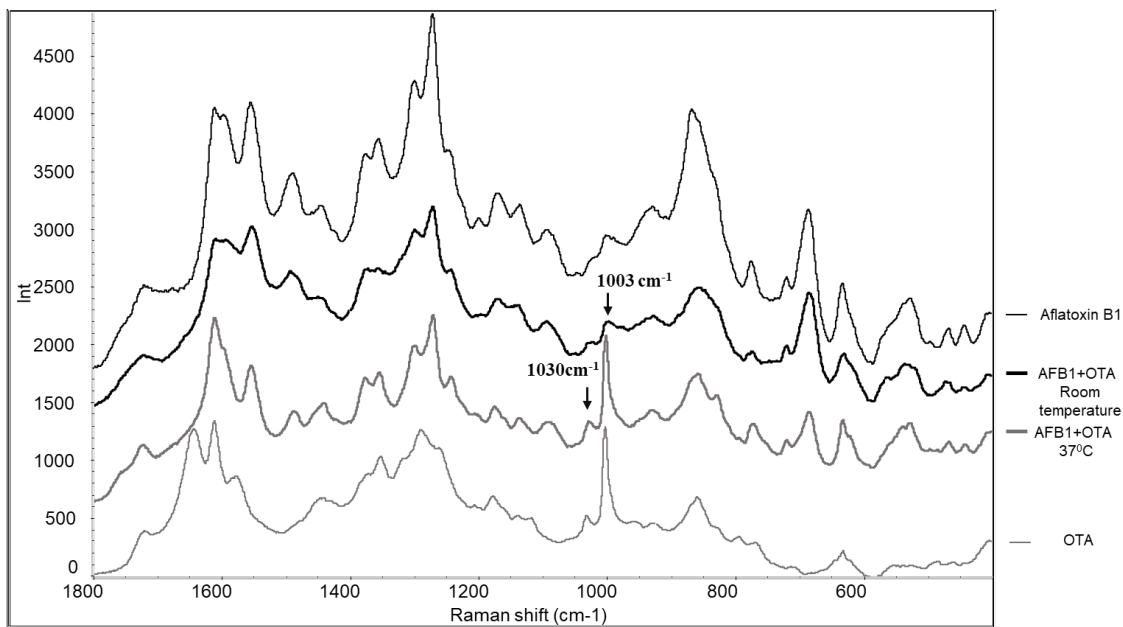


**Figure 21.** SERS spectra of AFB1 and AFB1+OTA at room temperature and AFB1+OTA at 37 °C using HSA-assisted assay.

### 3.4.3 Quantitative SERS analysis of AFB1

We tested the potential of this method for quantitative detection of AFB1 using five different concentrations of the toxins, 2, 4, 6, 8, and 10 ppb. Initially, we employed a final sample that was 1/10 than the total sample for the SERS measurement. In order to increase the accuracy, we added a concentration step consisting of the centrifugation of the samples containing AFB1-HSA-AuNPs (200  $\mu\text{L}$ ) complexes at 8 g for 5 min following by a removal of 180  $\mu\text{L}$  of supernatant and a final resuspension of the precipitate on the remaining 20  $\mu\text{L}$ . PLS analysis performed using the three major characteristics peaks, 687, 1272 and 1556  $\text{cm}^{-1}$  showed an  $R = 0.9341$ , showing that AFB1's SERS signals increases with increased toxin concentration (Fig. 22 a and b).

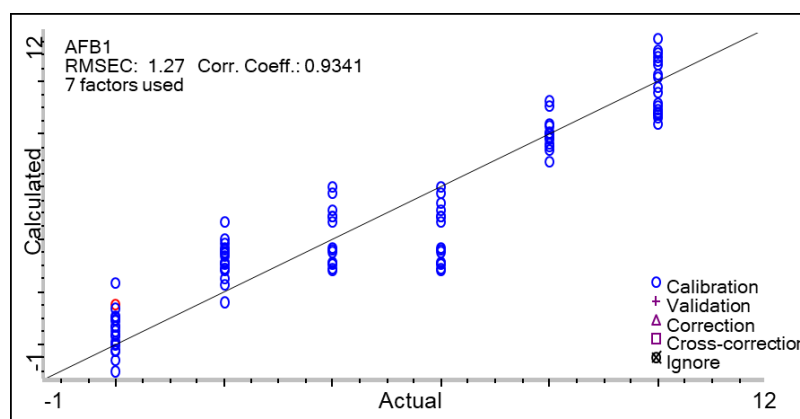
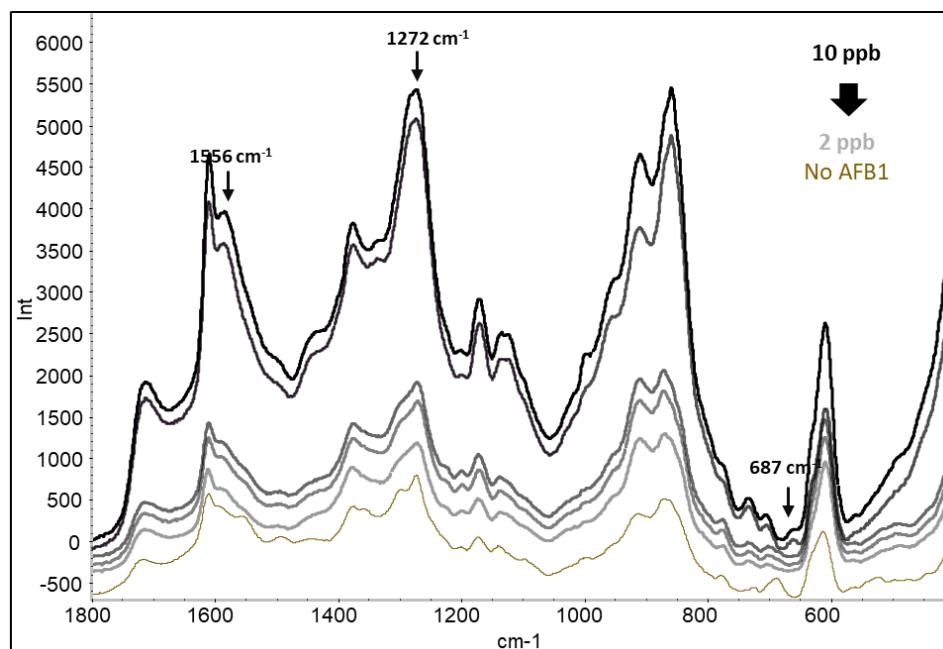


**Figure 22.** (a) SERS spectra of AFB1, in a range of 2 to 10 ppb, using HSA-assisted assay. (b) Correspondent PLS analysis curve showing a linear relationship between AFB1 concentration and SERS signals at five Raman shifts.

The applicability of the protocol was tested using AFB1-free ( $< 1$  ppb) and highly contaminated ( $< 12.9$  ppb) certified compound feedstuff. Both samples were taken as a negative and positive control, respectively. Five mixtures at different ratios were prepared to analyze the performance of the protocol as a quantitative method. Figure 23a shows that the assigned AFB1 peaks were not observable in the raw SERS spectra, however there are differences between the SERS spectra of AFB1-free and the highly contaminated compound feed samples. Peaks at 1003, 1032, 1150, 1364, and 1377  $\text{cm}^{-1}$  showed a visible change in their intensity that appears closely linked to AFB1 concentration as they decreased when AFB1 concentration decreased. These bands are usually observed in biological samples,<sup>227-230</sup> indicating that the presence of the mycotoxin facilitated the aggregation of nanoparticles and therefore the SERS signal of the surrounding molecules including HSA improved. PLS analysis for the whole 1495-720  $\text{cm}^{-1}$  region showed a reduction in the correlation coefficient, 0.8905, compared to the one obtained using the AFB1 pure solution. This is an expected result because of the inevitable interference of the other matrix components. This problem could be solved using more selective extraction and purification procedures, but nevertheless this simple and affordable protocol can differentiate between highly contaminated and non-contaminated compound feedstuff showing potential as a detection method.

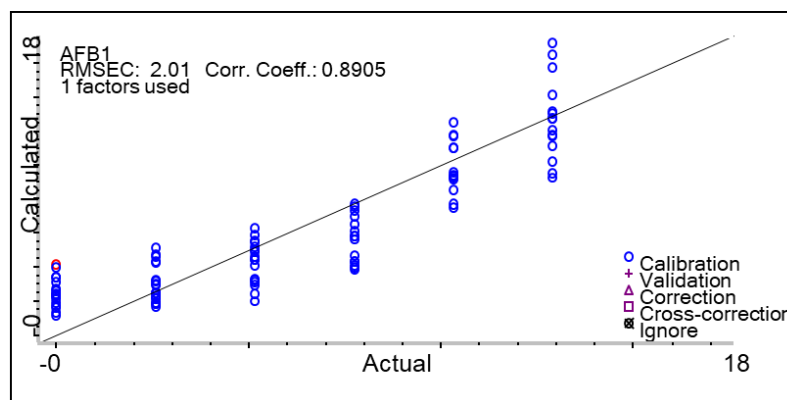
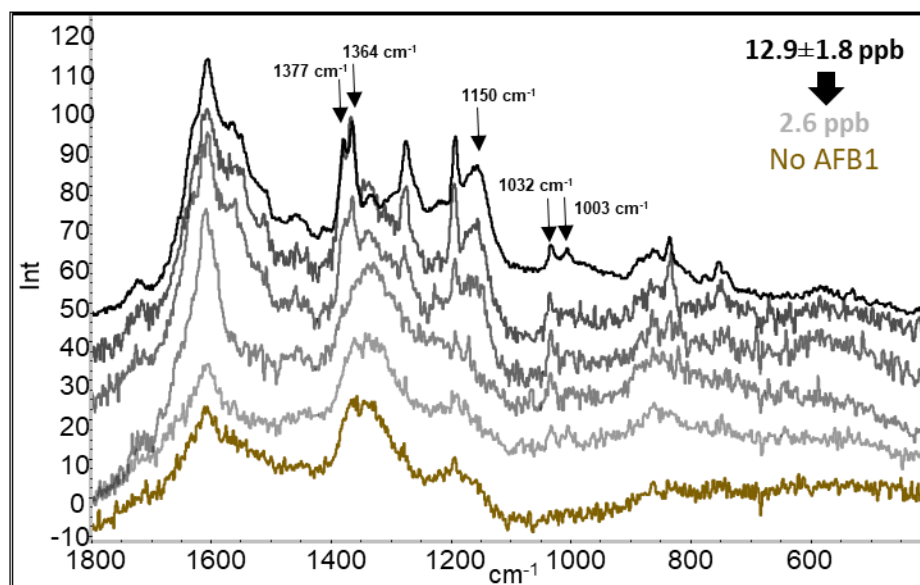


**Figure 23.** (a) SERS spectra of certified compound feedstuff, in a range of highly contaminated, > 12.9 ppb, to 1 AFB1-free, < 1 ppb (b) Correspondent PLS analysis curve showing a linear relationship between AFB1 concentration and SERS signals in feed samples.

## 2.8 Conclusion

In conclusion, we demonstrated that SERS spectra of mycotoxin AFB1 can be enhanced by the addition of the albumin protein HSA as a nano-interface between the analyte and the surface of the nanoparticles. Additionally, our study provides support to previous studies about AFB1-HSA interaction showing an improvement on the toxin spectra when the interaction occurs at room temperature. Results also support studies that suggest possible conformational changes in the protein when the analyte increases in concentration. More detailed studies are needed to fully comprehend this phenomenon. Although the AFB1 concentrations used for the quantification analysis were higher than the limit of quantification achieved for some of the sophisticated techniques, this method demonstrated good performance ( $R = 0.9341$ ) for a range of concentration of the toxin that includes its minimum tolerable amount in the US, 20 ppb, for all food destined for human consumption. Likewise, this method in combination with a simple liquid-liquid extraction protocol differentiated between non-contaminated and contaminated compound feedstuff even below 10 ppb, showing the application potential of this protocol as a rapid and affordable screening method to facilitate mycotoxin monitoring.

**CHAPTER 4**

**DIFFERENTIATION OF AFLATOXIN-PRODUCING AND  
NON-PRODUCING STRAINS OF ASPERGILLUS USING SERS**

**4.1 Abstract**

In this study, *A. flavus* and *A. oryzae* aflatoxin-producing and non-producing strains were successfully differentiated using surface-enhanced Raman spectroscopy (SERS) and principal component analysis (PCA). A simple method consisting of a direct measurement of *Aspergillus* culture filtrates mixed with silver nanoparticles using a portable Raman analyzer was applied. PCA analysis showed two separated clusters corresponding to the SERS spectra of fifteen *A. flavus* strains and seven *A. oryzae* strains. Similar results were obtained when comparing seven *A. flavus* and five *A. oryzae* grown in a rice-based solid medium. This method appeared valuable for rapid screening aflatoxigenic and non-aflatoxigenic *Aspergillus* strains.

## 4.2 Introduction

*Aspergillus flavus* has ubiquitous worldwide distribution and represents the most common species associated with aflatoxin contamination of agricultural crops. This genus has been subdivided into sections including a *Flavi* section, also referred to as the *A. flavus* group. This group is likewise divided into 2 groups of species: the first group includes *A. flavus* and *A. fumigatus*, species that are reported as the leading cause of invasive aspergillosis and the most common cause of superficial infection. The second groups which includes the non-aflatoxin producing species *A. oryzae*, *A. sojae* and *A. tamari*.<sup>231,232</sup> *A. oryzae* is closely related to *A. flavus* in morphology and genetic characteristics but compared to *A. flavus*, *A. oryzae* is a beneficial fungus generally recognized as safe (GRAS) with relevance to the food industry.<sup>232,233</sup> *A. oryzae* is a filamentous fungus used for centuries in the oriental food fermentation industry to saccharify rice, sweet potato, and barley in the production of alcoholic beverages such as sake and shōchū, and also to ferment soybeans for making soy sauce and miso.<sup>234</sup> Therefore, differentiation of aflatoxin productivity and non-productivity in the *Flavi* section has important implications in ensuring the safety of the fermented products.

Traditional methods primarily used to differentiate between aflatoxin-producing and non-producing strains are based on morphological parameters or the use of different media that allow the release of aflatoxins combined with the following evaluation of the aflatoxin production using HPLC.<sup>235–237</sup> These classic methods are laborious and need the expertise of mycologists to avoid misidentification. Additionally, they are time-consuming and

expensive because HPLC requires further purification steps. PCR technology allows for accurate detection of aflatoxin-producing *Aspergillus spp.* on different food products such as maize, pepper, paprika, peanut and wheat<sup>238–241</sup>. However, this method has not been applied in a concerted way, therefore showing the importance of developing alternative routine techniques to rapidly discriminate aflatoxin-producing and non-producing strains.

Spectroscopic techniques can be used to discriminate different types of microorganisms, cells, tissues, diseased, and normal biological samples, based on the identification of functional groups of molecules and the characterization of conformationally distinct structures in the biological molecules. SERS has been successfully used for detecting and identifying various microorganisms such as bacteria and yeasts<sup>242–244</sup> but to our knowledge this is the first attempt to discriminate between different strains of an organism based in the toxigenicity.

In this study, we evaluated the capabilities of SERS to discriminate between aflatoxigenic *A. flavus* strains and non-aflatoxigenic *A. oryzae* strains using a simple SERS procedure and a portable Raman spectrometer.

#### **4.3 Materials and methods**

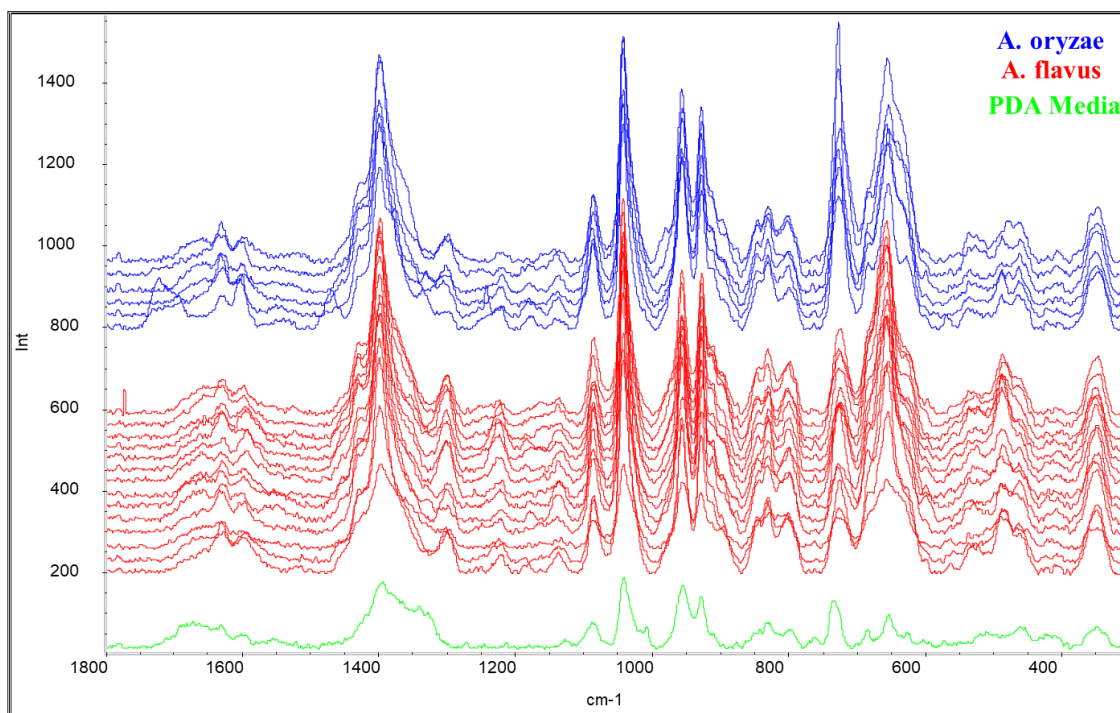
Twenty-two aflatoxigenic and non-aflatoxigenic strains of *Aspergillus flavus* 13 tox, FH 113, 1273, 46450, 4651, 46452, 46814, 46816, NPK 141, NPK 125, NPK FH 164, NPK 1009, SRRC 28, and Guard, and *Aspergillus oryzae* 694, 2079, 2103, 3483 and 5590 were provided by Dr. John Gibbons at The Gibbons Lab from the Food Science Department – University of Massachusetts, Amherst. For the first experiment, all fungal strains were

cultured 50 ml conical tubes containing potato dextrose agar (PDA) liquid medium. Each tube was incubated at 32 °C during 3 days under agitation to allow heterogeneous distribution of cells in the media. After incubation, the content of the tube was filtrated using a 2.2 mm filter and collected in a new, clean conical tube. For the second experiment, seven *A. flavus* and five *A. oryzae* strains were cultivated for 5 days at 37 °C in petri dishes containing liquefied boiled rice mixed with agar. After incubation, grown colonies were collected in a saline solution by scratching mycelium using disposable spatulas. Silver nanoparticles (AgNPs) were synthesized via reduction of silver nitrate using sodium citrate as follows: aqueous solution of silver nitrate was heated under vigorous stirring (700 rpm) at ~350 °C. When boiling, sodium citrate was added to the flask and the solution was left to boil until the color turned greenish brown, which indicates the formation of AgNPs. The flask was kept under continuous stirring without heat until the color became constant indicating that stability was achieved. Aspergillus filtrate and silver nanoparticles were mixed (1:1) in a 5 mL glass vials that were directly placed the liquid sample holder of a EZRaman-I High Sensitivity Portable Raman Analyzers (Enwave Optronics, Inc.) . SERS spectra were obtained using 780 nm laser and settings of a 5 s integration time and 3 s averaging parameter. Spectral data were analyzed with Thermo Scientific OMNIC Series software.

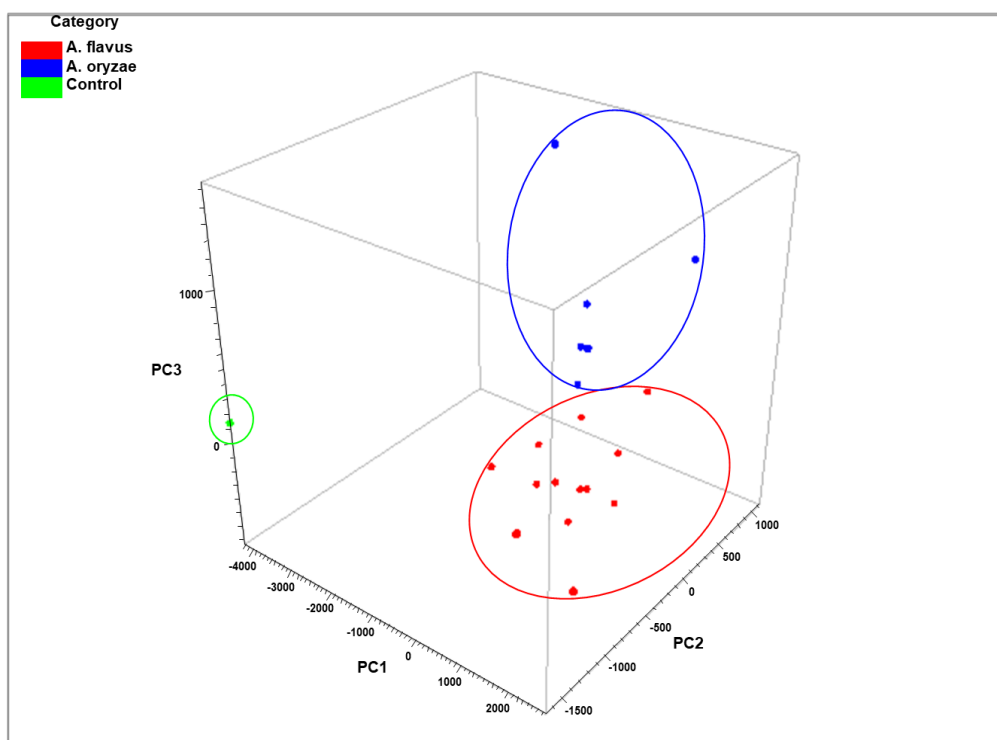
#### **4.4 Results and discussion**

Figure 24 shows that the original spectra corresponding to the strains of the 2 species are homogeneous. Differences between species are not obviously distinguished therefore

multivariate statistical methods are necessary to differentiate the spectra of these 2 species. Principal component analysis (PCA) maximizes the spectral variances through the reduction of the dimensionality of a multi-dimensional dataset while retaining those characteristics that contribute most to its variance. The information content of each spectrum is described by a limited number of variables, known as principal components (PCs). These PCs contain most of the spectral information.<sup>245</sup> Figure 25 shows PCA 3D-plot resulted from conducting the analysis for the range of 100–1700  $\text{cm}^{-1}$  and a maximum of 10 PCs. Two clear groups are observed corresponding to *A. flavus* and *A. oryzae* data points. Similarly, a PCA analysis of the SERS spectra of *Aspergillus* strains grown in a solid rice-based media showed a differentiation of two groups coinciding with the strain's capacity to produce AFB1. This indicates that the source of the spectral variance analyzed by PCA comes directly from differences between the strains, like extracellular metabolites or differences in the cellular structure of the strains independent of the culture medium used.



**Figure 24.** SERS spectra of *Aspergillus flavus* and *Aspergillus oryzae* grown in PDA medium.



**Figure 25.** 3D-plot of PCA analysis of SERS spectra of *Aspergillus flavus* and *Aspergillus oryzae* grown in PDA medium.

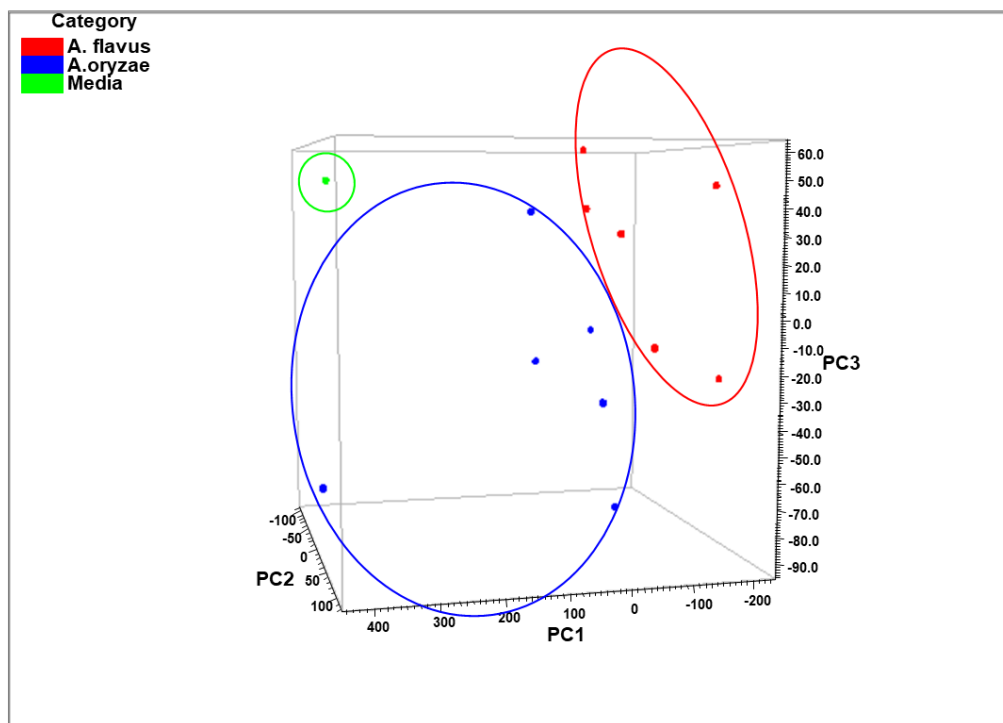


**Figure 26.** 3D-plot of PCA analysis of SERS spectra of *Aspergillus flavus* and *Aspergillus oryzae* grown in rice-based medium.

## 6.5 Conclusion

By combining a simple SERS using silver nanoparticles and a portable Raman spectrometer with multivariate data analysis, PCA, aflatoxigenic and non-aflatoxigenic *Aspergillus* strains were clearly differentiated into two groups. Similar results were obtained when applying the same method to *Aspergillus* strains cultivated in a different medium showing the potential of the technique to be expanded to different matrices. This SERS method could provide a rapid, simple, and affordable way to screen between aflatoxigenic and non-aflatoxigenic strains. This information could contribute to assessing the potential risk of aflatoxin contamination in agricultural feedstuff, a resource that can be useful in local agricultural management practices or to monitor the safety of non-aflatoxin-producing strains used in the production of food commodities.

## CHAPTER 5

### STUDY OF FUSARIUM SPP. MYCOTOXINS USING SERS

#### 5.1 Abstract

Four spectroscopic techniques were evaluated in terms of their ability to detect mycotoxins deoxynivalenol (DON) and fumonisin B1 (FB1). Spectroscopic techniques based on inelastic scattering of photons, Raman, and surface-enhanced Raman (SERS) showed a characteristic fingerprint for mycotoxin DON, at high concentration. The presence of metallic nanoparticles (SERS) improved DON's Raman signals. Infrared spectroscopy (IR), a technique based on light absorption showed that mycotoxins DON and FB1 have unique infrared spectra. However, in the presence of a metallic film, (surface-enhanced infrared absorption spectroscopy (SEIRAS), the infrared spectra of these two mycotoxins were not observed. Future work should focus on the improvement of the metallic substrate. The combination of these techniques is an approach that has not been taken so far in the mycotoxin field, but that could provide useful information about these molecules and/or offer an interesting detection method.

## 5.2 Introduction

Major mycotoxins affecting the food industry are mainly produced by three fungi genera *Aspergillus*, *Penicillium* and *Fusarium*. *Fusarium* species are commonly found in maize, rice, wheat, and oats in temperate and semi-tropical areas. Among the most important mycotoxins produced by species of *Fusarium* are the trichothecenes and the fumonisins. Trichothecenes are potent inhibitors of protein synthesis while fumonisins cause fatal livestock diseases and are considered potentially carcinogenic mycotoxins for humans. The most notorious trichothecenes and fumonisin mycotoxins are DON and FB1, respectively.<sup>246</sup> DON is also known as “vomitoxin” because of its toxic effects on swine and other animals. Humans consuming flour made from scabby wheat or moldy corn containing DON have been reported to suffer nausea and headaches which lasted 2–4 days.<sup>247</sup> In the U.S. the guidance level for DON in finished wheat products for human consumption is 1 ppm.<sup>201</sup> FB1 is implicated in the stimulation or suppression of the immune system, defects in the neural-tube, and nephrotoxicity. FB1 is classified in the group 2B, possible human carcinogen according to IARC, showing a synergistic interaction with AFB1, to initiate and to promote hepatocarcinoma in animal models.<sup>248</sup> The guidance level for this mycotoxin in the U.S varies from 2 to 4 ppm in food destined for human consumption.<sup>201</sup> Innovative approaches have been used to detect both mycotoxins, DON and FB1 using SERS, with successful results. Most of them used substrates that require highly laborious synthesis<sup>82,91,104,249</sup> or employ immunosensors for specific recognition,<sup>92,94,103,250</sup> that are expensive and difficult to apply. The most direct and simple

SERS approach uses label-free metallic nanoparticles usually synthesized by chemical reduction; this type of substrate is still facing challenges to obtain accurate and reliable results.<sup>251</sup>

Infrared spectroscopy (IR) is a technique that relies on molecule's light absorption. In comparison to Raman spectroscopy, that measures relative frequencies at which a sample scatters radiation, IR measures absolute frequencies at which a sample absorbs radiation, thus generating stronger signals more suitable for quantitative measurements of analytes at lower concentrations, using univariate or multivariate methods.<sup>252</sup> Similar to SERS, molecules adsorbed on metal island films or particles exhibit up to 1000 times more intense infrared absorption, this resulted in the development of an IR variation called surface-enhanced infrared absorption spectroscopy or SEIRAS.<sup>253</sup> Several studies used IR spectroscopy to analyze DON and FB1 levels in different food commodities,<sup>254-260</sup> but there are no studies about the use of SEIRAS to detect mycotoxins.

In general, weak bands in the Raman spectra correspond to strong bands in the infrared spectrum and vice versa<sup>261</sup>. Therefore, in this study, we collected and examined the attenuated total reflectance-Fourier transform infrared (ATR-FTIR) spectra of DON and FB1 in an attempt to explain if the inconsistency of the Raman spectra of these two mycotoxins is related to their structure and to evaluate ATR-FTIR and SEIRAS as an alternative detection method.

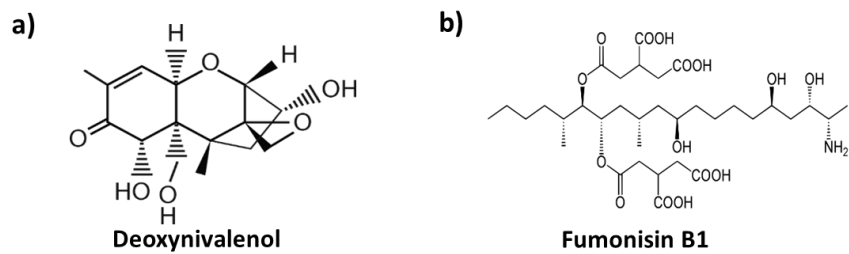
### 5.3 Material and methods

Deoxynivalenol (1 mg) and Fumonisin B1 from *Fusarium moniliforme* (1 mg) were purchased from Sigma Aldrich, St. Louis, MO. Powder samples were directly used to detect Raman and ATR-FTIR spectra. Mycotoxins were dissolved in methanol and a solution of 100 ppm was used to perform SERS and SEIRAS analysis. For SERS, spherical AgNPs (60 nm) were mixed with mycotoxin solutions (1:1) and a 5  $\mu$ L drop was deposited and air-dried in a glass slide wrapped with aluminum foil. For SEIRAS, the substrate employed, silver mirror, was obtained mixing highly concentrated silver nanoparticles with a mediating solvent, hexane:acetonitrile (1:1). The mirror formed in the bottom of the tube was deposited in a glass slide and air-dried, after that, 3  $\mu$ L of mycotoxin solution was dropped on top of the substrate. DXR Raman Spectro-microscope (Thermo Scientific) and IRTracer-100 (Shimadzu) spectrophotometer were used to collect Raman/SERS and ATR-FTIR/SEIRAS, respectively. OMNIC 9.0 software (Thermo Scientific) and Panorama Pro (Kaplan Scientific) were used to analyze the obtained spectra.

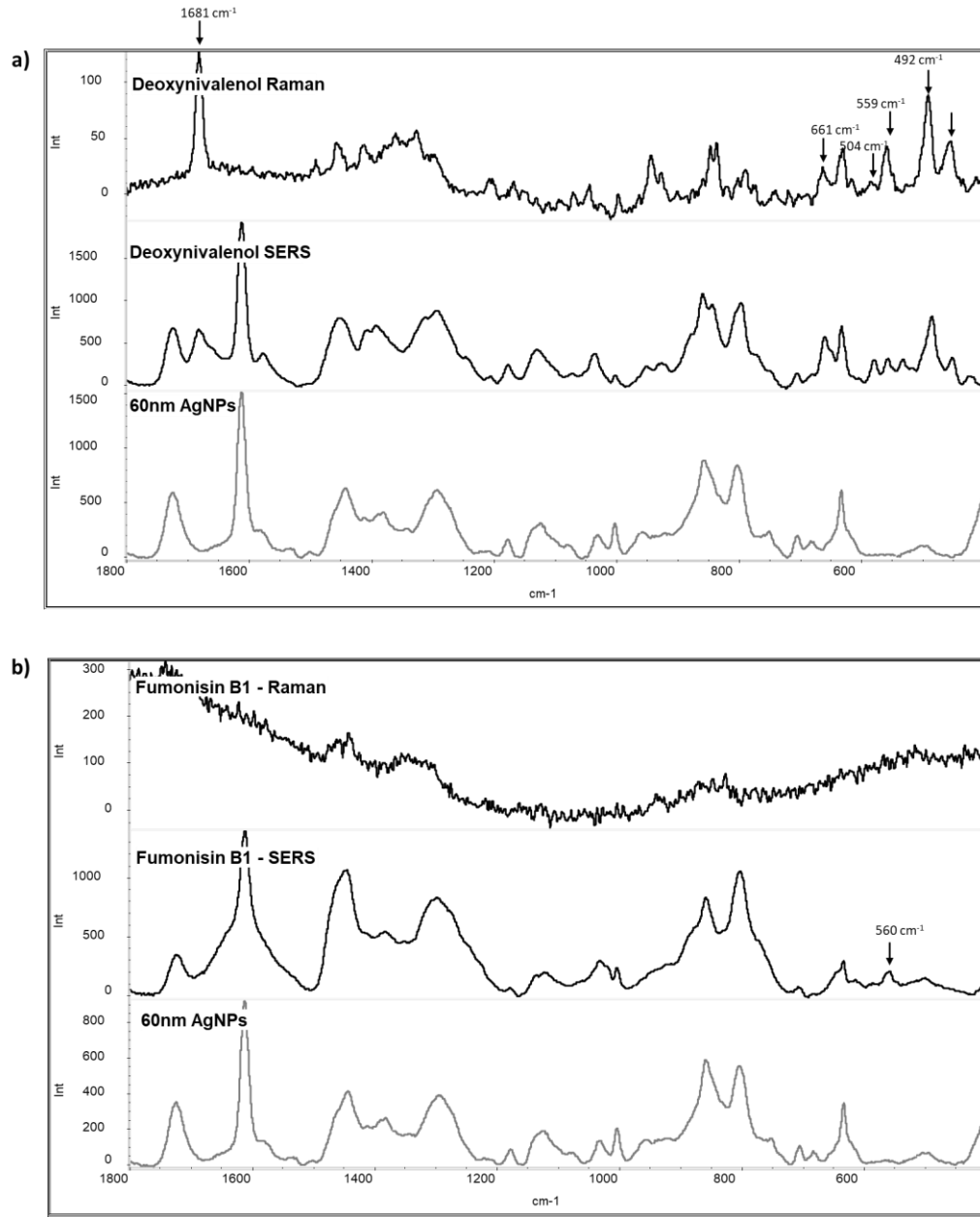
### 5.4 Results and discussion

Figure 28a and b shows DON and FB1 Raman and SERS spectra. A significant increment of DON's Raman characteristic peaks, mainly located at the 435-600  $\text{cm}^{-1}$  region, was observed using SERS. Raman bands located at 1681  $\text{cm}^{-1}$  and in the region of 435-600  $\text{cm}^{-1}$  were previously associated with DON based on DFT calculations<sup>88</sup>. FB1 showed high fluorescence interference on its Raman spectra and a single peak at 560  $\text{cm}^{-1}$  was differentiated using SERS but the weak intensity and the lack of information does not

allow us to support its association with the mycotoxin molecular structure. The improvement of DON's Raman signals was clearly observed at a high concentration of the mycotoxin, however, DON signals are weak and inconsistent at low concentrations (<5 ppm), thus limiting the application of the technique.



**Figure 27.** Molecular structure of DON and FB1.



**Figure 28.** Raman and SERS spectra of (a) DON and (b) FB1.

Figure 29a and b show a comparison between ATR-FTIR and SEIRAS spectra. Results suggested that these mycotoxins can be identified through IR, using their solid form. In both, DON and FB1, ATR-FTIR spectra, the main components of their backbone structure, C-H and C=O stretch are observed, but additionally, the main structure characteristic of DON, an epoxy group, is clearly differentiated in the 955-900  $\text{cm}^{-1}$  region. Similarly, a  $\text{NH}_2$  bend at 1150-1110  $\text{cm}^{-1}$  region represents the amine group of FB1. The motion of atoms in a molecule has a natural frequency of vibration related to their bond strength. Molecules with strong dipole bonds such as C=O, O-H, N=O, and C=N are ideal for the infrared technique, therefore organic solvents such as methanol, strongly absorb in mid-IR which can represent a limitation when testing liquid samples. Raman does not present this limitation. These results attest to why most IR-based mycotoxin detection has been made directly in food samples<sup>254,255,262,263</sup> which although showed to be an efficient method, it requires extensive data analysis and does not guarantee selectivity. In our results, neither DON nor FB1 showed a characteristic peak when the SEIRAS technique was applied. The SEIRAS phenomenon is different from SERS because the electromagnetic enhancement provided by plasmonic fields is far less, therefore SEIRAS has not advanced as rapidly as SERS.<sup>264,265</sup> A better understanding of SEIRAS's driving forces is necessary to find the right characteristics for a suitable SEIRAS substrate.

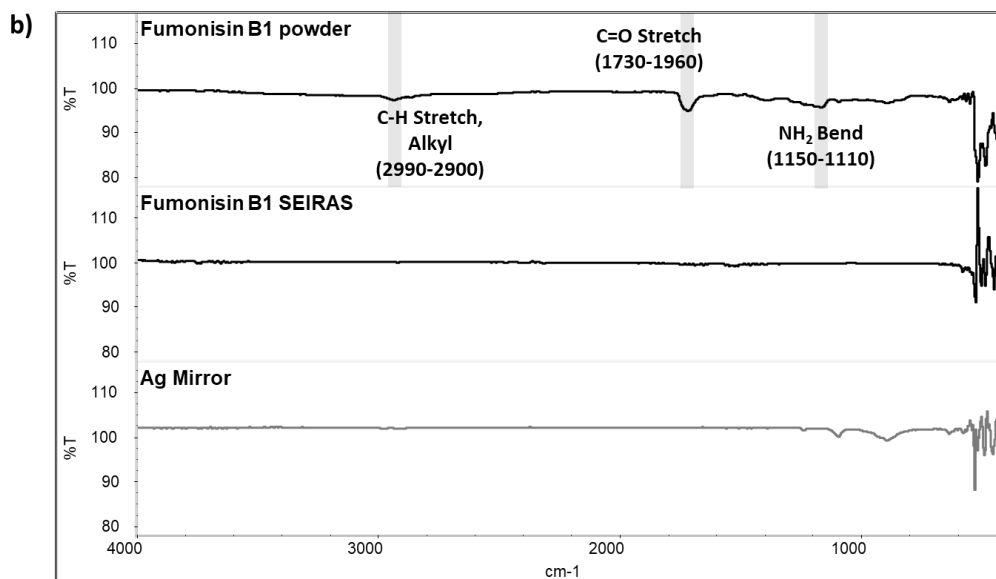
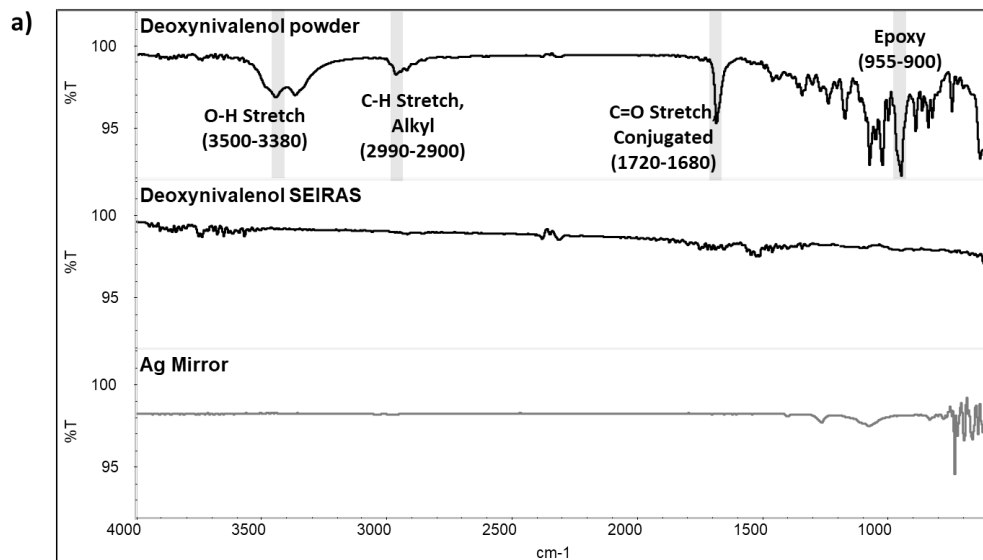


**Figure 29.** ATR-FTIR and SEIRAS spectra of (a) DON and (b) FB1.

Both methods, Raman and IR have advantages and limitations, but when combined, they could become a powerful tool when performing analyte detection. A practical example is the study of the crystallization process, in which the solid crystal forms in a solution and the supersaturation of the solution phase are being studied using Raman and IR, respectively.<sup>266-268</sup> Unlike Raman, IR spectra are typically well understood with respect to band assignments and software such as Panorama Pro analyzer facilitates the identification of peaks by automatic comparison with an spectra library. On the other hand, Raman/SERS spectra still lack a generic public data base, especially for mycotoxins. Nevertheless, the absence of interference of aqueous and organic solvents in the Raman/SERS technique makes it more suitable when detecting mycotoxins in liquid samples.

## **5.5 Conclusion**

SERS enhanced mycotoxin DON signals when compared to Raman. Mycotoxin FB1 did not show satisfactory spectra using Raman or SERS. Both mycotoxins, DON and FB1, revealed strong ATR-FTIR spectra using their powder form, but the signals disappeared when SEIRAS was applied. Infrared spectroscopy has similar advantages to SERS, is a sensitive technique, that uses an instrument that does not require high expertise to handle it and requires minimal sample pretreatment. Future work can expand the studies of IR Spectroscopy, alone or in combination with SERS, as a mycotoxin detection method. Further studies can also focus on the improvement of the SEIRAS substrates.

## CHAPTER 6

### CONCLUDING REMARKS

Mycotoxin contamination in food products compromises human and animal health. In the past few decades, considerable efforts have been dedicated to developing analytical methods for mycotoxin detection. In this dissertation, the potential of Surface-enhanced Raman Spectroscopy (SERS) to detect mycotoxins was evaluated using simple and affordable substrates that can be acquired commercially or synthesized in the laboratory, along with straight-forward sample pretreatments.

Two simple approaches were designed to enhance the detection of mycotoxins produced by the *Aspergillus* and *Penicillium* genera, ochratoxin A and aflatoxin B1. Ochratoxin A was successfully detected in wine samples spiked with the mycotoxin in a range of 0.01 to 1 ppm using a facile solvent-mediated extraction that showed a key role that the food matrix can play on the SERS substrate performance. The detection of aflatoxin B1' SERS signals using bare gold nanoparticles were enhanced with the addition of human serum albumin as a mediating molecule. A rapid SERS method, with on-site potential application, showed that this technique can differentiate between aflatoxigenic and non-aflatoxigenic strains of *Aspergillus*, independent of the culture medium used. SERS showed improved mycotoxin DON Raman fingerprint only at high concentrations, indicating that the technique could be useful for identification but not for quantitative detection. Infrared Spectroscopy (IR) arises as an alternative spectroscopic technique and

preliminary results showed both mycotoxins, deoxynivalenol and fumonisin B1, have their own characteristic IR fingerprints.

Although methods based on the SERS technique successfully detected mycotoxins in several food commodities, challenging issues such as the lack of flexible substrates, effective sample pretreatments, or simplified data processing remain when taking the laboratory research to commercially available analytical tools that can benefit the agri-food industry. In this research, it is proven that these problems can be addressed without increasing the cost or complexity of the technique and future work should continue along this path. Some approaches to take in the future can focus on finding a flexible substrate and a sample pretreatment to allow simultaneous detection of multiple mycotoxins or collecting Raman fingerprint maps of other existing mycotoxins to construct a database to simplify data analysis. Furthermore, SERS can be complemented with other techniques such as IR, TLC, or microfluidic devices that along with the faster development of miniature Raman spectrometers can help SERS become a platform that integrates rapid and accurate on-site mycotoxin detection to prevent food contamination and to avoid economical losses. Ultimately, SERS can be applied to the study of these molecules at a molecular level, and therefore contribute to a better understanding of these mycotoxins considered to be one of the key challenges in the food and beverage industry.

## BIBLIOGRAPHY

- (1) Bhat, R.; Rai, R. V.; Karim, A. A. Mycotoxins in Food and Feed: Present Status and Future Concerns. *Comprehensive Reviews in Food Science and Food Safety* **2010**, *9* (1), 57–81. <https://doi.org/10.1111/j.1541-4337.2009.00094.x>.
- (2) Alshannaq, A.; Yu, J.-H. Occurrence, Toxicity, and Analysis of Major Mycotoxins in Food. *International Journal of Environmental Research and Public Health* **2017**, *14* (6), 632. <https://doi.org/10.3390/ijerph14060632>.
- (3) Palumbo, R.; Crisci, A.; Venâncio, A.; Cortiñas Abrahantes, J.; Dorne, J.-L.; Battilani, P.; Toscano, P. Occurrence and Co-Occurrence of Mycotoxins in Cereal-Based Feed and Food. *Microorganisms* **2020**, *8* (1), 74. <https://doi.org/10.3390/microorganisms8010074>.
- (4) Wan, J.; Chen, B.; Rao, J. Occurrence and Preventive Strategies to Control Mycotoxins in Cereal-Based Food. *Comprehensive Reviews in Food Science and Food Safety* **2020**, *19* (3), 928–953. <https://doi.org/10.1111/1541-4337.12546>.
- (5) Mohamed amine, G.; Aminata, K.; Badreddine, B.; Hiba, G. Mycotoxins Occurrence, Toxicity and Detection Methods; 2020; pp 1–42. [https://doi.org/10.1007/978-3-030-33281-5\\_1](https://doi.org/10.1007/978-3-030-33281-5_1).
- (6) Corominas, A. V. Mycotoxins: presence and stability during processing of cereal based food. <http://purl.org/dc/dcmitype/Text>, Universitat de Lleida, 2017.
- (7) Chilaka, C. A.; De Boevre, M.; Atanda, O. O.; De Saeger, S. Stability of Fumonisin B1, Deoxynivalenol, Zearalenone, and T-2 Toxin during Processing of Traditional Nigerian Beer and Spices. *Mycotoxin Research* **2018**, *34* (4), 229–239. <https://doi.org/10.1007/s12550-018-0318-1>.
- (8) Piacentini, K. C.; Běláková, S.; Benešová, K.; Pernica, M.; Savi, G. D.; Rocha, L. O.; Hartman, I.; Čáslavský, J.; Corrêa, B. Fusarium Mycotoxins Stability during the Malting and Brewing Processes. *Toxins* **2019**, *11* (5), 257. <https://doi.org/10.3390/toxins11050257>.

- (9) Milani, J.; Heidari, S. Stability of Ochratoxin a During Bread Making Process. *Journal of Food Safety* **2017**, *37* (1), e12283. <https://doi.org/10.1111/jfs.12283>.
- (10) Gupta, R. C.; Lasher, M. A.; Mukherjee, I. R. M.; Srivastava, A.; Lall, R. Chapter 48 - Aflatoxins, Ochratoxins, and Citrinin. In *Reproductive and Developmental Toxicology (Second Edition)*; Gupta, R. C., Ed.; Academic Press, 2017; pp 945–962. <https://doi.org/10.1016/B978-0-12-804239-7.00048-2>.
- (11) Jackson, L. S.; DeVries, J. W.; Bullerman, L. B. *Fumonisin in Food*; Springer Science & Business Media, 2013.
- (12) Agents Classified by the IARC Monographs, Volumes 1–127 – IARC Monographs on the Identification of Carcinogenic Hazards to Humans <https://monographs.iarc.fr/agents-classified-by-the-iarc/> (accessed 2020 -09 -28).
- (13) Ji, F.; He, D.; Olaniran, A. O.; Mokoena, M. P.; Xu, J.; Shi, J. Occurrence, Toxicity, Production and Detection of Fusarium Mycotoxin: A Review. *Food Production, Processing and Nutrition* **2019**, *1* (1), 6. <https://doi.org/10.1186/s43014-019-0007-2>.
- (14) Lee, H. J.; Ryu, D. Worldwide Occurrence of Mycotoxins in Cereals and Cereal-Derived Food Products: Public Health Perspectives of Their Co-Occurrence. *Journal of Agricultural and Food Chemistry* **2017**, *65* (33), 7034–7051. <https://doi.org/10.1021/acs.jafc.6b04847>.
- (15) Steinkellner, H.; Binaglia, M.; Dall'Asta, C.; Gutleb, A. C.; Metzler, M.; Oswald, I. P.; Parent-Massin, D.; Alexander, J. Combined Hazard Assessment of Mycotoxins and Their Modified Forms Applying Relative Potency Factors: Zearalenone and T2/HT2 Toxin. *Food and Chemical Toxicology* **2019**, *131*, 110599. <https://doi.org/10.1016/j.fct.2019.110599>.
- (16) Fremy, J.-M.; Alassane-Kpembi, I.; Oswald, I. P.; Cottrill, B.; Van Egmond, H. P. A Review on Combined Effects of Moniliformin and Co-Occurring Fusarium Toxins in Farm Animals. *World Mycotoxin Journal* **2019**, *12* (3), 281–291. <https://doi.org/10.3920/WMJ2018.2405>.

- (17) Smith, M.-C.; Madec, S.; Coton, E.; Hymery, N. Natural Co-Occurrence of Mycotoxins in Foods and Feeds and Their in Vitro Combined Toxicological Effects. *Toxins* **2016**, *8* (4), 94. <https://doi.org/10.3390/toxins8040094>.
- (18) Robens, J.; Cardwell, K. The Costs of Mycotoxin Management to the USA: Management of Aflatoxins in the United States. *Journal of Toxicology: Toxin Reviews* **2003**, *22* (2–3), 139–152. <https://doi.org/10.1081/TXR-120024089>.
- (19) Savary, S.; Ficke, A.; Aubertot, J.-N.; Hollier, C. Crop Losses Due to Diseases and Their Implications for Global Food Production Losses and Food Security. *Food Security* **2012**, *4* (4), 519–537. <https://doi.org/10.1007/s12571-012-0200-5>.
- (20) Kumar, P.; Mahato, D. K.; Kamle, M.; Mohanta, T. K.; Kang, S. G. Aflatoxins: A Global Concern for Food Safety, Human Health and Their Management. *Frontiers in Microbiology* **2017**, *7*, 2170. <https://doi.org/10.3389/fmicb.2016.02170>.
- (21) Ellis, W. O.; Smith, J. P.; Simpson, B. K.; Oldham, J. H.; Scott, P. M. Aflatoxins in Food: Occurrence, Biosynthesis, Effects on Organisms, Detection, and Methods of Control. *Critical Reviews in Food Science and Nutrition* **1991**, *30* (4), 403–439. <https://doi.org/10.1080/10408399109527551>.
- (22) Ngindu, A.; Kenya, PatrickR.; Ocheng, DavidM.; Omondi, ThomasN.; Ngare, W.; Gatei, D.; Johnson, BruceK.; Ngira, JuliusA.; Nandwa, H.; Jansen, AdrianJ.; Kaviti, JasonN.; Arap Siongok, T. OUTBREAK OF ACUTE HEPATITIS CAUSED BY AFLATOXIN POISONING IN KENYA. *The Lancet* **1982**, *319* (8285), 1346–1348. [https://doi.org/10.1016/S0140-6736\(82\)92411-4](https://doi.org/10.1016/S0140-6736(82)92411-4).
- (23) Lye, M. S.; Ghazali, A. A.; Mohan, J.; Alwin, N.; Nair, R. C. An Outbreak of Acute Hepatic Encephalopathy Due to Severe Aflatoxicosis in Malaysia. *The American Journal of Tropical Medicine and Hygiene* **1995**, *53* (1), 68–72.
- (24) Probst, C.; Njapau, H.; Cotty, P. J. Outbreak of an Acute Aflatoxicosis in Kenya in 2004: Identification of the Causal Agent. *Applied and Environmental Microbiology* **2007**, *73* (8), 2762–2764. <https://doi.org/10.1128/AEM.02370-06>.

- (25) de Groene, E. M.; Jahn, A.; Horbach, G. J.; Fink-Gremmels, J. Mutagenicity and Genotoxicity of the Mycotoxin Ochratoxin A. *Environmental Toxicology and Pharmacology* **1996**, *1* (1), 21–26. [https://doi.org/10.1016/1382-6689\(95\)00005-4](https://doi.org/10.1016/1382-6689(95)00005-4).
- (26) Baudrimont, I.; Murn, M.; Betbeder, A. M.; Guilcher, J.; Creppy, E. E. Effect of Piroxicam on the Nephrotoxicity Induced by Ochratoxin A in Rats. *Toxicology* **1995**, *95* (1–3), 147–154. [https://doi.org/10.1016/0300-483x\(94\)02899-6](https://doi.org/10.1016/0300-483x(94)02899-6).
- (27) Dutton, M. F. Fumonisin, Mycotoxins of Increasing Importance: Their Nature and Their Effects. *Pharmacology & Therapeutics* **1996**, *70* (2), 137–161. [https://doi.org/10.1016/0163-7258\(96\)00006-X](https://doi.org/10.1016/0163-7258(96)00006-X).
- (28) Gelderblom, W. C. A.; Marasas, W. F. O.; Vleggaar, R.; Thiel, P. G.; Cawood, M. E. Fumonisin: Isolation, Chemical Characterization and Biological Effects. *Mycopathologia* **1992**, *117* (1), 11–16. <https://doi.org/10.1007/BF00497273>.
- (29) Shephard, G. S.; Thiel, P. G.; Sydenham, E. W. Determination of Fumonisin B1 in Plasma and Urine by High-Performance Liquid Chromatography. *Journal of Chromatography B: Biomedical Sciences and Applications* **1992**, *574* (2), 299–304. [https://doi.org/10.1016/0378-4347\(92\)80043-P](https://doi.org/10.1016/0378-4347(92)80043-P).
- (30) Shephard, G. S.; Thiel, P. G.; Sydenham, E. W.; Alberts, J. F.; Cawood, M. E. Distribution and Excretion of a Single Dose of the Mycotoxin Fumonisin B1 in a Non-Human Primate. *Toxicon* **1994**, *32* (6), 735–741. [https://doi.org/10.1016/0041-0101\(94\)90342-5](https://doi.org/10.1016/0041-0101(94)90342-5).
- (31) Reddy, K. E.; Song, J.; Lee, H.-J.; Kim, M.; Kim, D.-W.; Jung, H. J.; Kim, B.; Lee, Y.; Yu, D.; Kim, D.-W.; Oh, Y. K.; Lee, S. D. Effects of High Levels of Deoxynivalenol and Zearalenone on Growth Performance, and Hematological and Immunological Parameters in Pigs. *Toxins* **2018**, *10* (3), 114. <https://doi.org/10.3390/toxins10030114>.
- (32) Vignal, C.; Djouina, M.; Pichavant, M.; Caboche, S.; Waxin, C.; Beury, D.; Hot, D.; Gower-Rousseau, C.; Body-Malapel, M. Chronic Ingestion of Deoxynivalenol at Human Dietary Levels Impairs Intestinal Homeostasis and Gut Microbiota in Mice. *Archives of Toxicology* **2018**, *92* (7), 2327–2338. <https://doi.org/10.1007/s00204-018-2228-6>.

- (33) Rogowska, A.; Pomastowski, P.; Sagandykova, G.; Buszewski, B. Zearalenone and Its Metabolites: Effect on Human Health, Metabolism and Neutralisation Methods. *Toxicon* **2019**, *162*, 46–56. <https://doi.org/10.1016/j.toxicon.2019.03.004>.
- (34) Warth Benedikt; Preindl Karin; Manser Pius; Wick Peter; Marko Doris; Buerki-Thurnherr Tina. Transfer and Metabolism of the Xenoestrogen Zearalenone in Human Perfused Placenta. *Environmental Health Perspectives* **2019**, *127* (10), 107004. <https://doi.org/10.1289/EHP4860>.
- (35) Rahmani, A.; Jinap, S.; Soleimany, F. Qualitative and Quantitative Analysis of Mycotoxins. *Comprehensive Reviews in Food Science and Food Safety* **2009**, *8* (3), 202–251. <https://doi.org/10.1111/j.1541-4337.2009.00079.x>.
- (36) Turner, N. W.; Subrahmanyam, S.; Piletsky, S. A. Analytical Methods for Determination of Mycotoxins: A Review. *Analytica Chimica Acta* **2009**, *632* (2), 168–180. <https://doi.org/10.1016/j.aca.2008.11.010>.
- (37) Affairs, O. of R. Field Science - Laboratory Manual <https://www.fda.gov/science-research/field-science-and-laboratories/field-science-laboratory-manual> (accessed 2020 -09 -28).
- (38) Zheng, M. Z.; Richard, J. L.; Binder, J. A Review of Rapid Methods for the Analysis of Mycotoxins. *Mycopathologia* **2006**, *161* (5), 261–273. <https://doi.org/10.1007/s11046-006-0215-6>.
- (39) Maragos, C. M.; Busman, M. Rapid and Advanced Tools for Mycotoxin Analysis: A Review. *Food Additives & Contaminants. Part A, Chemistry, Analysis, Control, Exposure & Risk Assessment* **2010**, *27* (5), 688–700. <https://doi.org/10.1080/19440040903515934>.
- (40) Nolan, P.; Auer, S.; Spehar, A.; Elliott, C. T.; Campbell, K. Current Trends in Rapid Tests for Mycotoxins. *Food Additives & Contaminants: Part A* **2019**, *36* (5), 800–814. <https://doi.org/10.1080/19440049.2019.1595171>.
- (41) Kolosova, A. Y.; Sibanda, L.; Dumoulin, F.; Lewis, J.; Duveiller, E.; Van Peteghem, C.; De Saeger, S. Lateral-Flow Colloidal Gold-Based Immunoassay for the Rapid

Detection of Deoxynivalenol with Two Indicator Ranges. *Analytica Chimica Acta* **2008**, *616* (2), 235–244. <https://doi.org/10.1016/j.aca.2008.04.029>.

- (42) Molinelli, A.; Grossalber, K.; Führer, M.; Baumgartner, S.; Sulyok, M.; Krska, R. Development of Qualitative and Semiquantitative Immunoassay-Based Rapid Strip Tests for the Detection of T-2 Toxin in Wheat and Oat. *Journal of Agricultural and Food Chemistry* **2008**, *56* (8), 2589–2594. <https://doi.org/10.1021/jf800393j>.
- (43) Delmulle, B. S.; De Saeger, S. M. D. G.; Sibanda, L.; Barna-Vetro, I.; Van Peteghem, C. H. Development of an Immunoassay-Based Lateral Flow Dipstick for the Rapid Detection of Aflatoxin B1 in Pig Feed. *Journal of Agricultural and Food Chemistry* **2005**, *53* (9), 3364–3368. <https://doi.org/10.1021/jf0404804>.
- (44) Xiulan, S.; Xiaolian, Z.; Jian, T.; Xiaohong, G.; Jun, Z.; Chu, F. S. Development of an Immunochromatographic Assay for Detection of Aflatoxin B1 in Foods. *Food Control* **2006**, *17* (4), 256–262. <https://doi.org/10.1016/j.foodcont.2004.10.007>.
- (45) Wang, S.; Quan, Y.; Lee, N.; Kennedy, I. R. Rapid Determination of Fumonisin B1 in Food Samples by Enzyme-Linked Immunosorbent Assay and Colloidal Gold Immunoassay. *Journal of Agricultural and Food Chemistry* **2006**, *54* (7), 2491–2495. <https://doi.org/10.1021/jf0530401>.
- (46) Cho, Y.-J.; Lee, D.-H.; Kim, D.-O.; Min, W.-K.; Bong, K.-T.; Lee, G.-G.; Seo, J.-H. Production of a Monoclonal Antibody against Ochratoxin A and Its Application to Immunochromatographic Assay. *Journal of Agricultural and Food Chemistry* **2005**, *53* (22), 8447–8451. <https://doi.org/10.1021/jf051681q>.
- (47) Wang, X.-H.; Liu, T.; Xu, N.; Zhang, Y.; Wang, S. Enzyme-Linked Immunosorbent Assay and Colloidal Gold Immunoassay for Ochratoxin A: Investigation of Analytical Conditions and Sample Matrix on Assay Performance. *Analytical and Bioanalytical Chemistry* **2007**, *389* (3), 903–911. <https://doi.org/10.1007/s00216-007-1506-6>.

- (48) Kolosova, A. Y.; De Saeger, S.; Sibanda, L.; Verheijen, R.; Van Peteghem, C. Development of a Colloidal Gold-Based Lateral-Flow Immunoassay for the Rapid Simultaneous Detection of Zearalenone and Deoxynivalenol. *Analytical and Bioanalytical Chemistry* **2007**, 389 (7), 2103–2107. <https://doi.org/10.1007/s00216-007-1642-z>.
- (49) Wang, Z.; Li, H.; Li, C.; Yu, Q.; Shen, J.; De Saeger, S. Development and Application of a Quantitative Fluorescence-Based Immunochromatographic Assay for Fumonisin B1 in Maize. *Journal of Agricultural and Food Chemistry* **2014**, 62 (27), 6294–6298. <https://doi.org/10.1021/jf5017219>.
- (50) Radoi, A.; Targa, M.; Prieto-Simon, B.; Marty, J.-L. Enzyme-Linked Immunosorbent Assay (ELISA) Based on Superparamagnetic Nanoparticles for Aflatoxin M1 Detection. *Talanta* **2008**, 77 (1), 138–143. <https://doi.org/10.1016/j.talanta.2008.05.048>.
- (51) Shim, W.-B.; Kolosova, A. Y.; Kim, Y.-J.; Yang, Z.-Y.; Park, S.-J.; Eremin, S. A.; Lee, I.-S.; Chung, D.-H. Fluorescence Polarization Immunoassay Based on a Monoclonal Antibody for the Detection of Ochratoxin A. *International Journal of Food Science & Technology* **2004**, 39 (8), 829–837. <https://doi.org/10.1111/j.1365-2621.2004.00856.x>.
- (52) Nasir, M. S.; Jolley, M. E. Fluorescence Polarization (FP) Assays for the Determination of Grain Mycotoxins (Fumonisin, DON Vomitoxin and Aflatoxins). *Combinatorial Chemistry & High Throughput Screening* **2003**, 6 (3), 267–273. <https://doi.org/10.2174/138620703106298310>.
- (53) Krska, R.; Molinelli, A. Rapid Test Strips for Analysis of Mycotoxins in Food and Feed. *Analytical and Bioanalytical Chemistry* **2009**, 393 (1), 67–71. <https://doi.org/10.1007/s00216-008-2424-y>.
- (54) Agriopoulou, S.; Stamatelopoulou, E.; Varzakas, T. Advances in Analysis and Detection of Major Mycotoxins in Foods. *Foods* **2020**, 9 (4), 518. <https://doi.org/10.3390/foods9040518>.

- (55) Pohanka, M.; Jun, D.; Kuca, K. Mycotoxin Assays Using Biosensor Technology: A Review. *Drug and Chemical Toxicology* **2007**, *30* (3), 253–261. <https://doi.org/10.1080/01480540701375232>.
- (56) Man, Y.; Liang, G.; Li, A.; Pan, L. Recent Advances in Mycotoxin Determination for Food Monitoring via Microchip. *Toxins* **2017**, *9* (10), 324. <https://doi.org/10.3390/toxins9100324>.
- (57) Guo, L.; Feng, J.; Fang, Z.; Xu, J.; Lu, X. Application of Microfluidic “Lab-on-a-Chip” for the Detection of Mycotoxins in Foods. *Trends in Food Science & Technology* **2015**, *46* (2, Part A), 252–263. <https://doi.org/10.1016/j.tifs.2015.09.005>.
- (58) Almeahadi, L. M.; Curley, S. M.; Tokranova, N. A.; Tenenbaum, S. A.; Lednev, I. K. Surface Enhanced Raman Spectroscopy for Single Molecule Protein Detection. *Scientific Reports* **2019**, *9* (1), 12356. <https://doi.org/10.1038/s41598-019-48650-y>.
- (59) Kneipp, J.; Wittig, B.; Bohr, H.; Kneipp, K. Surface-Enhanced Raman Scattering: A New Optical Probe in Molecular Biophysics and Biomedicine. *Theoretical Chemistry Accounts* **2010**, *125* (3), 319–327. <https://doi.org/10.1007/s00214-009-0665-2>.
- (60) Nie, S.; Emory, S. R. Probing Single Molecules and Single Nanoparticles by Surface-Enhanced Raman Scattering. *Science* **1997**, *275* (5303), 1102–1106. <https://doi.org/10.1126/science.275.5303.1102>.
- (61) Hao, E.; Schatz, G. C. Electromagnetic Fields around Silver Nanoparticles and Dimers. *The Journal of Chemical Physics* **2004**, *120* (1), 357–366. <https://doi.org/10.1063/1.1629280>.
- (62) Le Ru, E. C.; Etchegoin, P. G. Single-Molecule Surface-Enhanced Raman Spectroscopy. *Annual Review of Physical Chemistry* **2012**, *63* (1), 65–87. <https://doi.org/10.1146/annurev-physchem-032511-143757>.
- (63) Pilot, R.; Signorini, R.; Durante, C.; Orian, L.; Bhamidipati, M.; Fabris, L. A Review on Surface-Enhanced Raman Scattering. *Biosensors* **2019**, *9* (2), 57. <https://doi.org/10.3390/bios9020057>.

- (64) Schlücker, S. Surface-Enhanced Raman Spectroscopy: Concepts and Chemical Applications. *Angewandte Chemie International Edition* **2014**, *53* (19), 4756–4795. <https://doi.org/10.1002/anie.201205748>.
- (65) Pang, S.; Yang, T.; He, L. Review of Surface Enhanced Raman Spectroscopic (SERS) Detection of Synthetic Chemical Pesticides. *TrAC Trends in Analytical Chemistry* **2016**, *85*, 73–82. <https://doi.org/10.1016/j.trac.2016.06.017>.
- (66) Gillibert, R.; N. Triba, M.; Chapelle, M. L. de la. Surface Enhanced Raman Scattering Sensor for Highly Sensitive and Selective Detection of Ochratoxin A. *Analyst* **2018**, *143* (1), 339–345. <https://doi.org/10.1039/C7AN01730H>.
- (67) Yaseen, T.; Pu, H.; Sun, D.-W. Functionalization Techniques for Improving SERS Substrates and Their Applications in Food Safety Evaluation: A Review of Recent Research Trends. *Trends in Food Science & Technology* **2018**, *72*, 162–174. <https://doi.org/10.1016/j.tifs.2017.12.012>.
- (68) Craig, A. P.; Franca, A. S.; Irudayaraj, J. Surface-Enhanced Raman Spectroscopy Applied to Food Safety. *Annual Review of Food Science and Technology* **2013**, *4* (1), 369–380. <https://doi.org/10.1146/annurev-food-022811-101227>.
- (69) Xie, X.; Pu, H.; Sun, D.-W. Recent Advances in Nanofabrication Techniques for SERS Substrates and Their Applications in Food Safety Analysis. *Critical Reviews in Food Science and Nutrition* **2018**, *58* (16), 2800–2813. <https://doi.org/10.1080/10408398.2017.1341866>.
- (70) Fini, G. Applications of Raman Spectroscopy to Pharmacy. *Journal of Raman Spectroscopy* **2004**, *35* (5), 335–337. <https://doi.org/10.1002/jrs.1161>.
- (71) DONG, Q.; YANG, Y.; LIANG, P.; LI, X.; WANG, L. Research on the Substrates of Surface Enhanced Raman Scattering (SERS) and Their Applications to Biomedicine and Environmental Analysis. *Spectroscopy and Spectral Analysis* **2013**, *33* (6), 1547–1552. [https://doi.org/10.3964/j.issn.1000-0593\(2013\)06-1547-06](https://doi.org/10.3964/j.issn.1000-0593(2013)06-1547-06).

- (72) Halvorson, R. A.; Vikesland, P. J. Surface-Enhanced Raman Spectroscopy (SERS) for Environmental Analyses. *Environmental Science & Technology* **2010**, *44* (20), 7749–7755. <https://doi.org/10.1021/es101228z>.
- (73) Li, D.-W.; Zhai, W.-L.; Li, Y.-T.; Long, Y.-T. Recent Progress in Surface Enhanced Raman Spectroscopy for the Detection of Environmental Pollutants. *Microchimica Acta* **2014**, *181* (1), 23–43. <https://doi.org/10.1007/s00604-013-1115-3>.
- (74) Muehlethaler, C.; Leona, M.; Lombardi, J. R. Review of Surface Enhanced Raman Scattering Applications in Forensic Science. *Analytical Chemistry* **2016**, *88* (1), 152–169. <https://doi.org/10.1021/acs.analchem.5b04131>.
- (75) Fikiet, M. A.; Khandasammy, S. R.; Mistek, E.; Ahmed, Y.; Halámková, L.; Bueno, J.; Lednev, I. K. Surface Enhanced Raman Spectroscopy: A Review of Recent Applications in Forensic Science. *Spectrochimica Acta Part A: Molecular and Biomolecular Spectroscopy* **2018**, *197*, 255–260. <https://doi.org/10.1016/j.saa.2018.02.046>.
- (76) Bellot-Gurlet, L.; Pagès-Camagna, S.; Coupry, C. Raman spectroscopy in art and archaeology. *Journal of Raman Spectroscopy* **2006**, *37* (10), 962–965. <https://doi.org/10.1002/jrs.1615>.
- (77) Pozzi, F.; Leona, M. Surface-Enhanced Raman Spectroscopy in Art and Archaeology. *Journal of Raman Spectroscopy* **2016**, *47* (1), 67–77. <https://doi.org/10.1002/jrs.4827>.
- (78) Sharma, B.; Frontiera, R. R.; Henry, A.-I.; Ringe, E.; Van Duyne, R. P. SERS: Materials, Applications, and the Future. *Materials Today* **2012**, *15* (1), 16–25. [https://doi.org/10.1016/S1369-7021\(12\)70017-2](https://doi.org/10.1016/S1369-7021(12)70017-2).
- (79) Sun, J.; Gong, L.; Wang, W.; Gong, Z.; Wang, D.; Fan, M. Surface-Enhanced Raman Spectroscopy for on-Site Analysis: A Review of Recent Developments. *Luminescence* **2020**, *35* (6), 808–820. <https://doi.org/10.1002/bio.3796>.

- (80) Hudson, S. D.; Chumanov, G. Bioanalytical Applications of SERS (Surface-Enhanced Raman Spectroscopy). *Analytical and Bioanalytical Chemistry* **2009**, *394* (3), 679–686. <https://doi.org/10.1007/s00216-009-2756-2>.
- (81) Lee, K.-M.; Herrman, T. J.; Bisrat, Y.; Murray, S. C. Feasibility of Surface-Enhanced Raman Spectroscopy for Rapid Detection of Aflatoxins in Maize. *Journal of Agricultural and Food Chemistry* **2014**, *62* (19), 4466–4474. <https://doi.org/10.1021/jf500854u>.
- (82) Lee, K.-M.; Herrman, T. J. Determination and Prediction of Fumonisin Contamination in Maize by Surface-Enhanced Raman Spectroscopy (SERS). *Food and Bioprocess Technology* **2016**, *9* (4), 588–603. <https://doi.org/10.1007/s11947-015-1654-1>.
- (83) Wu, X.; Gao, S.; Wang, J.-S.; Wang, H.; Huang, Y.-W.; Zhao, Y. The Surface-Enhanced Raman Spectra of Aflatoxins: Spectral Analysis, Density Functional Theory Calculation, Detection and Differentiation. *Analyst* **2012**, *137* (18), 4226–4234. <https://doi.org/10.1039/C2AN35378D>.
- (84) Cialla, D.; März, A.; Böhme, R.; Theil, F.; Weber, K.; Schmitt, M.; Popp, J. Surface-Enhanced Raman Spectroscopy (SERS): Progress and Trends. *Analytical and Bioanalytical Chemistry* **2012**, *403* (1), 27–54. <https://doi.org/10.1007/s00216-011-5631-x>.
- (85) Sur, U. K. Surface-Enhanced Raman Scattering (SERS) Spectroscopy: A Versatile Spectroscopic and Analytical Technique Used in Nanoscience and Nanotechnology. *Advances in nano research* **2013**, *1* (2), 111–124. <https://doi.org/10.12989/ANR.2013.1.2.111>.
- (86) Mosier-Boss, P. A. Review of SERS Substrates for Chemical Sensing. *Nanomaterials* **2017**, *7* (6), 142. <https://doi.org/10.3390/nano7060142>.
- (87) Singh, D. K.; Ganbold, E.-O.; Cho, E.-M.; Cho, K.-H.; Kim, D.; Choo, J.; Kim, S.; Lee, C. M.; Yang, S. I.; Joo, S.-W. Detection of the Mycotoxin Citrinin Using Silver Substrates and Raman Spectroscopy. *Journal of Hazardous Materials* **2014**, *265*, 89–95. <https://doi.org/10.1016/j.jhazmat.2013.11.041>.

- (88) Yuan, J.; Sun, C.; Guo, X.; Yang, T.; Wang, H.; Fu, S.; Li, C.; Yang, H. A Rapid Raman Detection of Deoxynivalenol in Agricultural Products. *Food Chemistry* **2017**, *221*, 797–802. <https://doi.org/10.1016/j.foodchem.2016.11.101>.
- (89) Fan, M.; Andrade, G. F. S.; Brolo, A. G. A Review on the Fabrication of Substrates for Surface Enhanced Raman Spectroscopy and Their Applications in Analytical Chemistry. *Analytica Chimica Acta* **2011**, *693* (1), 7–25. <https://doi.org/10.1016/j.aca.2011.03.002>.
- (90) Sun, X.; Li, H. A Review: Nanofabrication of Surface-Enhanced Raman Spectroscopy (SERS) Substrates. *Current Nanoscience* **2016**, *12* (2), 175–183.
- (91) Li, J.; Yan, H.; Tan, X.; Lu, Z.; Han, H. Cauliflower-Inspired 3D SERS Substrate for Multiple Mycotoxins Detection. *Analytical Chemistry* **2019**, *91* (6), 3885–3892. <https://doi.org/10.1021/acs.analchem.8b04622>.
- (92) Zhao, Y.; Yang, Y.; Luo, Y.; Yang, X.; Li, M.; Song, Q. Double Detection of Mycotoxins Based on SERS Labels Embedded Ag@Au Core–Shell Nanoparticles. *ACS Applied Materials & Interfaces* **2015**, *7* (39), 21780–21786. <https://doi.org/10.1021/acsami.5b07804>.
- (93) Fang, C.; Wei, C.; Xu, M.; Yuan, Y.; Gu, R.; Yao, J. Ni@Au Nanoparticles for Surface Enhanced Raman Spectroscopy Based Ultrasensitive Magnetic Immunoassay on Aflatoxin B<sub>1</sub>. *RSC Advances* **2016**, *6* (66), 61325–61333. <https://doi.org/10.1039/C6RA09397C>.
- (94) Zhang, W.; Tang, S.; Jin, Y.; Yang, C.; He, L.; Wang, J.; Chen, Y. Multiplex SERS-Based Lateral Flow Immunosensor for the Detection of Major Mycotoxins in Maize Utilizing Dual Raman Labels and Triple Test Lines. *Journal of Hazardous Materials* **2020**, *393*, 122348. <https://doi.org/10.1016/j.jhazmat.2020.122348>.
- (95) Li, Y.; Chen, Q.; Xu, X.; Jin, Y.; Wang, Y.; Zhang, L.; Yang, W.; He, L.; Feng, X.; Chen, Y. Microarray Surface Enhanced Raman Scattering Based Immunosensor for Multiplexing Detection of Mycotoxin in Foodstuff. *Sensors and Actuators B: Chemical* **2018**, *266*, 115–123. <https://doi.org/10.1016/j.snb.2018.03.040>.

- (96) Lin, B.; Kannan, P.; Qiu, B.; Lin, Z.; Guo, L. On-Spot Surface Enhanced Raman Scattering Detection of Aflatoxin B1 in Peanut Extracts Using Gold Nanobipyramids Evenly Trapped into the AAO Nanoholes. *Food Chemistry* **2020**, *307*, 125528. <https://doi.org/10.1016/j.foodchem.2019.125528>.
- (97) Liu, S.-H.; Wen, B.-Y.; Lin, J.-S.; Yang, Z.-W.; Luo, S.-Y.; Li, J.-F. Rapid and Quantitative Detection of Aflatoxin B1 in Grain by Portable Raman Spectrometer. *Applied Spectroscopy* **2020**, 0003702820951891. <https://doi.org/10.1177/0003702820951891>.
- (98) Kutsanedzie, F. Y. H.; Agyekum, A. A.; Annavaram, V.; Chen, Q. Signal-Enhanced SERS-Sensors of CAR-PLS and GA-PLS Coupled AgNPs for Ochratoxin A and Aflatoxin B1 Detection. *Food Chemistry* **2020**, *315*, 126231. <https://doi.org/10.1016/j.foodchem.2020.126231>.
- (99) Zheng, F.; Ke, W.; Shi, L.; Liu, H.; Zhao, Y. Plasmonic Au–Ag Janus Nanoparticle Engineered Ratiometric Surface-Enhanced Raman Scattering Aptasensor for Ochratoxin A Detection. *Analytical Chemistry* **2019**, *91* (18), 11812–11820. <https://doi.org/10.1021/acs.analchem.9b02469>.
- (100) Jing, X.; Chang, L.; Shi, L.; Liu, X.; Zhao, Y.; Zhang, W. Au Film–Au@Ag Core–Shell Nanoparticle Structured Surface-Enhanced Raman Spectroscopy Aptasensor for Accurate Ochratoxin A Detection. *ACS Applied Bio Materials* **2020**, *3* (4), 2385–2391. <https://doi.org/10.1021/acsabm.0c00120>.
- (101) Rostami, S.; Zór, K.; Zhai, D. S.; Viehrig, M.; Morelli, L.; Mehdinia, A.; Smedsgaard, J.; Rindzevicius, T.; Boisen, A. High-Throughput Label-Free Detection of Ochratoxin A in Wine Using Supported Liquid Membrane Extraction and Ag-Capped Silicon Nanopillar SERS Substrates. *Food Control* **2020**, *113*, 107183. <https://doi.org/10.1016/j.foodcont.2020.107183>.
- (102) Hernández, Y.; Lagos, L. K.; Galarreta, B. C. Development of a Label-Free-SERS Gold Nanoaptasensor for the Accessible Determination of Ochratoxin A. *Sensing and Bio-Sensing Research* **2020**, *28*, 100331. <https://doi.org/10.1016/j.sbsr.2020.100331>.

- (103) He, D.; Wu, Z.; Cui, B.; Xu, E. Aptamer and Gold Nanorod–Based Fumonisin B1 Assay Using Both Fluorometry and SERS. *Microchimica Acta* **2020**, *187* (4), 215. <https://doi.org/10.1007/s00604-020-4192-0>.
- (104) Tegegne, W. A.; Mekonnen, M. L.; Beyene, A. B.; Su, W.-N.; Hwang, B.-J. Sensitive and Reliable Detection of Deoxynivalenol Mycotoxin in Pig Feed by Surface Enhanced Raman Spectroscopy on Silver Nanocubes@polydopamine Substrate. *Spectrochimica Acta Part A: Molecular and Biomolecular Spectroscopy* **2020**, *229*, 117940. <https://doi.org/10.1016/j.saa.2019.117940>.
- (105) Liu, J.; Hu, Y.; Zhu, G.; Zhou, X.; Jia, L.; Zhang, T. Highly Sensitive Detection of Zearalenone in Feed Samples Using Competitive Surface-Enhanced Raman Scattering Immunoassay. *Journal of Agricultural and Food Chemistry* **2014**, *62* (33), 8325–8332. <https://doi.org/10.1021/jf503191e>.
- (106) Kang, Y.; Gu, H.-X.; Zhang, X. A Self-Referenced Method for Determination of Patulin by Surface-Enhanced Raman Scattering Using Gold Nanobipyramids as the Substrate. *Analytical Methods* **2019**, *11* (40), 5142–5149. <https://doi.org/10.1039/C9AY01366K>.
- (107) Wu, L.; Yan, H.; Li, G.; Xu, X.; Zhu, L.; Chen, X.; Wang, J. Surface-Imprinted Gold Nanoparticle-Based Surface-Enhanced Raman Scattering for Sensitive and Specific Detection of Patulin in Food Samples. *Double Detection of Mycotoxins Based on SERS Labels Embedded Ag@Au* **2019**, *12* (7), 1648–1657. <https://doi.org/10.1007/s12161-019-01498-4>.
- (108) Pan, T.; Sun, D.-W.; Pu, H.; Wei, Q. Simple Approach for the Rapid Detection of Alternariol in Pear Fruit by Surface-Enhanced Raman Scattering with Pyridine-Modified Silver Nanoparticles. *Journal of Agricultural and Food Chemistry* **2018**, *66* (9), 2180–2187. <https://doi.org/10.1021/acs.jafc.7b05664>.
- (109) Nutrition, C. for F. S. and A. Natural Toxins and Mycotoxins <https://www.fda.gov/food/chemicals-metals-pesticides-food/natural-toxins-and-mycotoxins> (accessed 2020 -10 -01).

- (110) Anonymous. Mycotoxins  
[https://ec.europa.eu/food/safety/chemical\\_safety/contaminants/catalogue/mycotoxins\\_en](https://ec.europa.eu/food/safety/chemical_safety/contaminants/catalogue/mycotoxins_en) (accessed 2020-10-01).
- (111) Lu, L.-Q.; Zheng, Y.; Qu, W.-G.; Yu, H.-Q.; Xu, A.-W. Hydrophobic Teflon Films as Concentrators for Single-Molecule SERS Detection. *Journal of Materials Chemistry* **2012**, *22* (39), 20986–20990. <https://doi.org/10.1039/C2JM33955B>.
- (112) Rojas, L. M.; Qu, Y.; He, L. A Facile Solvent Extraction Method Facilitating Surface-Enhanced Raman Spectroscopic Detection of Ochratoxin A in Wine and Wheat. *Talanta* **2020**, 121792. <https://doi.org/10.1016/j.talanta.2020.121792>.
- (113) Hahm, E.; Kim, Y.-H.; Pham, X.-H.; Jun, B.-H. Highly Reproducible Surface-Enhanced Raman Scattering Detection of Alternariol Using Silver-Embedded Silica Nanoparticles. *Sensors* **2020**, *20* (12), 3523. <https://doi.org/10.3390/s20123523>.
- (114) Chaney, S. B.; Shanmukh, S.; Dluhy, R. A.; Zhao, Y.-P. Aligned Silver Nanorod Arrays Produce High Sensitivity Surface-Enhanced Raman Spectroscopy Substrates. *Applied Physics Letters* **2005**, *87* (3), 031908. <https://doi.org/10.1063/1.1988980>.
- (115) Chen, Q.; Jiao, T.; Yang, M.; Li, H.; Ahmad, W.; Hassan, M. M.; Guo, Z.; Ali, S. Pre Etched Ag Nanocluster as SERS Substrate for the Rapid Quantification of AFB1 in Peanut Oil via DFT Coupled Multivariate Calibration. *Spectrochimica Acta Part A: Molecular and Biomolecular Spectroscopy* **2020**, *239*, 118411. <https://doi.org/10.1016/j.saa.2020.118411>.
- (116) Liu, Q.; Vanmol, K.; Lycke, S.; Erps, J. V.; Vandenabeele, P.; Thienpont, H.; Ottevaere, H. SERS Using Two-Photon Polymerized Nanostructures for Mycotoxin Detection. *RSC Advances* **2020**, *10* (24), 14274–14282. <https://doi.org/10.1039/D0RA01909G>.
- (117) Diegel, O. 10.02 - Additive Manufacturing: An Overview. In *Comprehensive Materials Processing*; Hashmi, S., Batalha, G. F., Van Tyne, C. J., Yilbas, B., Eds.; Elsevier: Oxford, 2014; pp 3–18. <https://doi.org/10.1016/B978-0-08-096532-1.01000-1>.

- (118) Ko, J.; Lee, C.; Choo, J. Highly Sensitive SERS-Based Immunoassay of Aflatoxin B1 Using Silica-Encapsulated Hollow Gold Nanoparticles. *Journal of Hazardous Materials* **2015**, *285*, 11–17. <https://doi.org/10.1016/j.jhazmat.2014.11.018>.
- (119) Wang, J.; Chen, Q.; Jin, Y.; Zhang, X.; He, L.; Zhang, W.; Chen, Y. Surface Enhanced Raman Scattering-Based Lateral Flow Immunosensor for Sensitive Detection of Aflatoxin M1 in Urine. *Analytica Chimica Acta* **2020**, *1128*, 184–192. <https://doi.org/10.1016/j.aca.2020.06.076>.
- (120) Leslie, J. F.; Bandyopadhyay, R.; Visconti, A. *Mycotoxins: Detection Methods, Management, Public Health and Agricultural Trade*; CABI, 2008.
- (121) Jarvis, B. B. Analysis for Mycotoxins: The Chemist's Perspective. *Archives of Environmental Health: An International Journal* **2003**, *58* (8), 479–483. <https://doi.org/10.3200/AEOH.58.8.479-483>.
- (122) Rushing, B. R.; Selim, M. I. Aflatoxin B1: A Review on Metabolism, Toxicity, Occurrence in Food, Occupational Exposure, and Detoxification Methods. *Food and Chemical Toxicology* **2019**, *124*, 81–100. <https://doi.org/10.1016/j.fct.2018.11.047>.
- (123) Rawal, S.; Kim, J. E.; Coulombe, R. Aflatoxin B1 in Poultry: Toxicology, Metabolism and Prevention. *Research in Veterinary Science* **2010**, *89* (3), 325–331. <https://doi.org/10.1016/j.rvsc.2010.04.011>.
- (124) Aflatoxin B1: Binding to DNA in vitro and Alteration of RNA Metabolism in vivo | Science <https://science.sciencemag.org/content/151/3717/1539.abstract> (accessed 2020 -09 -17).
- (125) Kim, N. H.; Lee, S. J.; Moskovits, M. Reversible Tuning of SERS Hot Spots with Aptamers. *Advanced Materials* **2011**, *23* (36), 4152–4156. <https://doi.org/10.1002/adma.201101847>.
- (126) Ganbold, E.-O.; Lee, C. M.; Cho, E.-M.; Son, S. J.; Kim, S.; Joo, S.-W.; Yang, S. I. Subnanomolar Detection of Ochratoxin A Using Aptamer-Attached Silver Nanoparticles and Surface-Enhanced Raman Scattering. *Anal. Methods* **2014**, *6* (11), 3573. <https://doi.org/10.1039/c4ay00440j>.

- (127) Chen, Q.; Yang, M.; Yang, X.; Li, H.; Guo, Z.; Rahma, M. H. A Large Raman Scattering Cross-Section Molecular Embedded SERS Aptasensor for Ultrasensitive Aflatoxin B1 Detection Using CS-Fe<sub>3</sub>O<sub>4</sub> for Signal Enrichment. *Spectrochimica Acta Part A: Molecular and Biomolecular Spectroscopy* **2018**, *189*, 147–153. <https://doi.org/10.1016/j.saa.2017.08.029>.
- (128) Feng, Y.; He, L.; Wang, L.; Mo, R.; Zhou, C.; Hong, P.; Li, C. Detection of Aflatoxin B1 Based on a Porous Anodized Aluminum Membrane Combined with Surface-Enhanced Raman Scattering Spectroscopy. *Nanomaterials* **2020**, *10* (5), 1000. <https://doi.org/10.3390/nano10051000>.
- (129) Song, D.; Yang, R.; Fang, S.; Liu, Y.; Long, F.; Zhu, A. SERS Based Aptasensor for Ochratoxin A by Combining Fe<sub>3</sub>O<sub>4</sub>@Au Magnetic Nanoparticles and Au-DTNB@Ag Nanoprobes with Multiple Signal Enhancement. *Microchimica Acta* **2018**, *185* (10), 491. <https://doi.org/10.1007/s00604-018-3020-2>.
- (130) Shao, B.; Ma, X.; Zhao, S.; Lv, Y.; Hun, X.; Wang, H.; Wang, Z. Nanogapped Au(Core) @ Au-Ag(Shell) Structures Coupled with Fe<sub>3</sub>O<sub>4</sub> Magnetic Nanoparticles for the Detection of Ochratoxin A. *Analytica Chimica Acta* **2018**, *1033*, 165–172. <https://doi.org/10.1016/j.aca.2018.05.058>.
- (131) Li, Q.; Lu, Z.; Tan, X.; Xiao, X.; Wang, P.; Wu, L.; Shao, K.; Yin, W.; Han, H. Ultrasensitive Detection of Aflatoxin B1 by SERS Aptasensor Based on Exonuclease-Assisted Recycling Amplification. *Biosensors and Bioelectronics* **2017**, *97*, 59–64. <https://doi.org/10.1016/j.bios.2017.05.031>.
- (132) Turiel, E.; Martín-Esteban, A. Molecularly Imprinted Polymers for Sample Preparation: A Review. *Analytica Chimica Acta* **2010**, *668* (2), 87–99. <https://doi.org/10.1016/j.aca.2010.04.019>.
- (133) Haupt, K. Peer Reviewed: Molecularly Imprinted Polymers: The Next Generation. *Anal. Chem.* **2003**, *75* (17), 376 A–383 A. <https://doi.org/10.1021/ac031385h>.
- (134) Zhang, W.; Xiong, H.; Chen, M.; Zhang, X.; Wang, S. Surface-Enhanced Molecularly Imprinted Electrochemiluminescence Sensor Based on Ru@SiO<sub>2</sub> for Ultrasensitive Detection of Fumonisin B1. *Biosensors and Bioelectronics* **2017**, *96*, 55–61. <https://doi.org/10.1016/j.bios.2017.04.035>.

- (135) Gao, X.; Cao, W.; Chen, M.; Xiong, H.; Zhang, X.; Wang, S. A High Sensitivity Electrochemical Sensor Based on Fe<sup>3+</sup>-Ion Molecularly Imprinted Film for the Detection of T-2 Toxin. *Electroanalysis* **2014**, *26* (12), 2739–2746. <https://doi.org/10.1002/elan.201400237>.
- (136) Choi, S.-W.; Chang, H.-J.; Lee, N.; Chun, H. S. A Surface Plasmon Resonance Sensor for the Detection of Deoxynivalenol Using a Molecularly Imprinted Polymer. *Sensors* **2011**, *11* (9), 8654–8664. <https://doi.org/10.3390/s110908654>.
- (137) Baggiani, C.; Giraudi, G.; Vanni, A. A Molecular Imprinted Polymer with Recognition Properties towards the Carcinogenic Mycotoxin Ochratoxin A. *Bioseparation* **2001**, *10* (6), 389–394. <https://doi.org/10.1023/A:1021506223136>.
- (138) Ali, W. H.; Derrien, D.; Alix, F.; Pérollier, C.; Lépine, O.; Bayouhd, S.; Chapuis-Hugon, F.; Pichon, V. Solid-Phase Extraction Using Molecularly Imprinted Polymers for Selective Extraction of a Mycotoxin in Cereals. *Journal of Chromatography A* **2010**, *1217* (43), 6668–6673. <https://doi.org/10.1016/j.chroma.2010.04.071>.
- (139) Weiss, R.; Freudenschuss, M.; Krska, R.; Mizaikoff, B. Improving Methods of Analysis for Mycotoxins: Molecularly Imprinted Polymers for Deoxynivalenol and Zearalenone. *Food Additives & Contaminants* **2003**, *20* (4), 386–395. <https://doi.org/10.1080/0265203031000065827>.
- (140) Shanakhat, H.; Sorrentino, A.; Raiola, A.; Romano, A.; Masi, P.; Cavella, S. Current Methods for Mycotoxins Analysis and Innovative Strategies for Their Reduction in Cereals: An Overview. *Journal of the Science of Food and Agriculture* **2018**, *98* (11), 4003–4013. <https://doi.org/10.1002/jsfa.8933>.
- (141) Koesukwiwat, U.; Sanguankaew, K.; Leepipatpiboon, N. Evaluation of a Modified QuEChERS Method for Analysis of Mycotoxins in Rice. *Food Chemistry* **2014**, *153*, 44–51. <https://doi.org/10.1016/j.foodchem.2013.12.029>.
- (142) Tolosa, J.; Graziani, G.; Gaspari, A.; Chianese, D.; Ferrer, E.; Mañes, J.; Ritieni, A. Multi-Mycotoxin Analysis in Durum Wheat Pasta by Liquid Chromatography Coupled to Quadrupole Orbitrap Mass Spectrometry. *Toxins* **2017**, *9* (2), 59. <https://doi.org/10.3390/toxins9020059>.

- (143) Rejczak, T.; Tuzimski, T. A Review of Recent Developments and Trends in the QuEChERS Sample Preparation Approach. *Open Chemistry* **2015**, *1* (open-issue), 980–1010. <https://doi.org/10.1515/chem-2015-0109>.
- (144) Qian, M.; Yang, H.; Li, Z.; Liu, Y.; Wang, J.; Wu, H.; Ji, X.; Xu, J. Detection of 13 Mycotoxins in Feed Using Modified QuEChERS with Dispersive Magnetic Materials and UHPLC–MS/MS. *Journal of Separation Science* **2018**, *41* (3), 756–764. <https://doi.org/10.1002/jssc.201700882>.
- (145) Xu, X.; Xu, X.; Han, M.; Qiu, S.; Hou, X. Development of a Modified QuEChERS Method Based on Magnetic Multiwalled Carbon Nanotubes for the Simultaneous Determination of Veterinary Drugs, Pesticides and Mycotoxins in Eggs by UPLC–MS/MS. *Food Chemistry* **2019**, *276*, 419–426. <https://doi.org/10.1016/j.foodchem.2018.10.051>.
- (146) Ma, S.; Wang, M.; You, T.; Wang, K. Using Magnetic Multiwalled Carbon Nanotubes as Modified QuEChERS Adsorbent for Simultaneous Determination of Multiple Mycotoxins in Grains by UPLC–MS/MS. *Journal of Agricultural and Food Chemistry* **2019**, *67* (28), 8035–8044. <https://doi.org/10.1021/acs.jafc.9b00090>.
- (147) Moreno, V.; Zougagh, M.; Ríos, Á. Hybrid Nanoparticles Based on Magnetic Multiwalled Carbon Nanotube–NanoC18SiO<sub>2</sub> Composites for Solid Phase Extraction of Mycotoxins Prior to Their Determination by LC–MS. *Microchimica Acta* **2016**, *183* (2), 871–880. <https://doi.org/10.1007/s00604-015-1722-2>.
- (148) Barbera, G. L.; Capriotti, A. L.; Cavaliere, C.; Foglia, P.; Montone, C. M.; Chiozzi, R. Z.; Laganà, A. A Rapid Magnetic Solid Phase Extraction Method Followed by Liquid Chromatography–Tandem Mass Spectrometry Analysis for the Determination of Mycotoxins in Cereals. *Toxins* **2017**, *9* (4), 147. <https://doi.org/10.3390/toxins9040147>.
- (149) González-Sálamo, J.; Socas-Rodríguez, B.; Hernández-Borges, J.; Rodríguez-Delgado, M. Á. Core-Shell Poly(Dopamine) Magnetic Nanoparticles for the Extraction of Estrogenic Mycotoxins from Milk and Yogurt Prior to LC–MS Analysis. *Food Chemistry* **2017**, *215*, 362–368. <https://doi.org/10.1016/j.foodchem.2016.07.154>.

- (150) Wang, X.; Park, S.-G.; Ko, J.; Xiao, X.; Giannini, V.; Maier, S. A.; Kim, D.-H.; Choo, J. Sensitive and Reproducible Immunoassay of Multiple Mycotoxins Using Surface-Enhanced Raman Scattering Mapping on 3D Plasmonic Nanopillar Arrays. *Small* **2018**, *14* (39), 1801623. <https://doi.org/10.1002/sml.201801623>.
- (151) Yang, T.; Zhang, Z.; Zhao, B.; Hou, R.; Kinchla, A.; Clark, J. M.; He, L. Real-Time and in Situ Monitoring of Pesticide Penetration in Edible Leaves by Surface-Enhanced Raman Scattering Mapping. *Analytical Chemistry* **2016**, *88* (10), 5243–5250. <https://doi.org/10.1021/acs.analchem.6b00320>.
- (152) Ma, B.; Li, P.; Yang, L.; Liu, J. Based on Time and Spatial-Resolved SERS Mapping Strategies for Detection of Pesticides. *Talanta* **2015**, *141*, 1–7. <https://doi.org/10.1016/j.talanta.2015.03.053>.
- (153) Pahlow, S.; Weber, K.; Popp, J.; Wood, B. R.; Kochan, K.; R  ther, A.; Perez-Guaita, D.; Heraud, P.; Stone, N.; Dudgeon, A.; Gardner, B.; Reddy, R.; Mayerich, D.; Bhargava, R. Application of Vibrational Spectroscopy and Imaging to Point-of-Care Medicine: A Review. *Applied spectroscopy* **2018**, *72* (1 Suppl), 52–84. <https://doi.org/10.1177/0003702818791939>.
- (154) Zhang, Y.; Zhao, S.; Zheng, J.; He, L. Surface-Enhanced Raman Spectroscopy (SERS) Combined Techniques for High-Performance Detection and Characterization. *TrAC Trends in Analytical Chemistry* **2017**, *90*, 1–13. <https://doi.org/10.1016/j.trac.2017.02.006>.
- (155) Qu, L.-L.; Jia, Q.; Liu, C.; Wang, W.; Duan, L.; Yang, G.; Han, C.-Q.; Li, H. Thin Layer Chromatography Combined with Surface-Enhanced Raman Spectroscopy for Rapid Sensing Aflatoxins. *Journal of Chromatography A* **2018**, *1579*, 115–120. <https://doi.org/10.1016/j.chroma.2018.10.024>.
- (156) Wu, Z.; He, D.; Cui, B.; Jin, Z.; Xu, E.; Yuan, C.; Liu, P.; Fang, Y.; Chai, Q. Trimer-Based Aptasensor for Simultaneous Determination of Multiple Mycotoxins Using SERS and Fluorimetry. *Microchimica Acta* **2020**, *187* (9), 495. <https://doi.org/10.1007/s00604-020-04487-1>.

- (157) Galarreta, B. C.; Tabatabaei, M.; Guieu, V.; Peyrin, E.; Lagugn -Labarthe, F. Microfluidic Channel with Embedded SERS 2D Platform for the Aptamer Detection of Ochratoxin A. *Analytical and Bioanalytical Chemistry* **2013**, *405* (5), 1613–1621. <https://doi.org/10.1007/s00216-012-6557-7>.
- (158) Pu, H.; Xiao, W.; Sun, D.-W. SERS-Microfluidic Systems: A Potential Platform for Rapid Analysis of Food Contaminants. *Trends in Food Science & Technology* **2017**, *70*, 114–126. <https://doi.org/10.1016/j.tifs.2017.10.001>.
- (159) Zeng, F.; Mou, T.; Zhang, C.; Huang, X.; Wang, B.; Ma, X.; Guo, J. Paper-Based SERS Analysis with Smartphones as Raman Spectral Analyzers. *Analyst* **2019**, *144* (1), 137–142. <https://doi.org/10.1039/C8AN01901K>.
- (160) Stadler, D.; Berthiller, F.; Suman, M.; Schuhmacher, R.; Krska, R. Novel Analytical Methods to Study the Fate of Mycotoxins during Thermal Food Processing. *Analytical and Bioanalytical Chemistry* **2020**, *412* (1), 9–16. <https://doi.org/10.1007/s00216-019-02101-9>.
- (161) Yue, S.; Ye, W.; Xu, Z. SERS Monitoring of the Fenton Degradation Reaction Based on Microfluidic Droplets and Alginate Microparticles. *Analyst* **2019**, *144* (19), 5882–5889. <https://doi.org/10.1039/C9AN01077G>.
- (162) Calvet, A.; Ryder, A. G. Monitoring Cell Culture Media Degradation Using Surface Enhanced Raman Scattering (SERS) Spectroscopy. *Analytica Chimica Acta* **2014**, *840*, 58–67. <https://doi.org/10.1016/j.aca.2014.06.021>.
- (163) Cai, Q.; Lu, S.; Liao, F.; Li, Y.; Ma, S.; Shao, M. Catalytic Degradation of Dye Molecules and in Situ SERS Monitoring by Peroxidase-like Au/CuS Composite. *Nanoscale* **2014**, *6* (14), 8117–8123. <https://doi.org/10.1039/C4NR01751J>.
- (164) Lussier, F.; Thibault, V.; Charron, B.; Wallace, G. Q.; Masson, J.-F. Deep Learning and Artificial Intelligence Methods for Raman and Surface-Enhanced Raman Scattering. *TrAC Trends in Analytical Chemistry* **2020**, *124*, 115796. <https://doi.org/10.1016/j.trac.2019.115796>.

- (165) Logrieco, A.; Arrigan, D. W. M.; Brengel-Pesce, K.; Siciliano, P.; Tothill, I. DNA Arrays, Electronic Noses and Tongues, Biosensors and Receptors for Rapid Detection of Toxigenic Fungi and Mycotoxins: A Review. *Food Additives & Contaminants* **2005**, *22* (4), 335–344. <https://doi.org/10.1080/02652030500070176>.
- (166) Leggieri, M. C.; Pont, N. P.; Battilani, P.; Magan, N. Detection and Discrimination between Ochratoxin Producer and Non-Producer Strains of *Penicillium Nordicum* on a Ham-Based Medium Using an Electronic Nose. *Mycotoxin Research* **2011**, *27* (1), 29–35. <https://doi.org/10.1007/s12550-010-0072-5>.
- (167) I. Ellis, D.; Broadhurst, D.; J. Clarke, S.; Goodacre, R. Rapid Identification of Closely Related Muscle Foods by Vibrational Spectroscopy and Machine Learning. *Analyst* **2005**, *130* (12), 1648–1654. <https://doi.org/10.1039/B511484E>.
- (168) Uysal, R. S.; Boyaci, I. H.; Genis, H. E.; Tamer, U. Determination of Butter Adulteration with Margarine Using Raman Spectroscopy. *Food Chemistry* **2013**, *141* (4), 4397–4403. <https://doi.org/10.1016/j.foodchem.2013.06.061>.
- (169) Mohamadi Monavar, H.; Afseth, N. K.; Lozano, J.; Alimardani, R.; Omid, M.; Wold, J. P. Determining Quality of Caviar from Caspian Sea Based on Raman Spectroscopy and Using Artificial Neural Networks. *Talanta* **2013**, *111*, 98–104. <https://doi.org/10.1016/j.talanta.2013.02.046>.
- (170) Cheung, W.; Shadi, I. T.; Xu, Y.; Goodacre, R. Quantitative Analysis of the Banned Food Dye Sudan-1 Using Surface Enhanced Raman Scattering with Multivariate Chemometrics. *The Journal of Physical Chemistry C* **2010**, *114* (16), 7285–7290. <https://doi.org/10.1021/jp908892n>.
- (171) Wu, Y.; Liang, P.; Dong, Q.; Bai, Y.; Yu, Z.; Huang, J.; Zhong, Y.; Dai, Y.-C.; Ni, D.; Shu, H.; Pittman, C. U. Design of a Silver Nanoparticle for Sensitive Surface Enhanced Raman Spectroscopy Detection of Carmine Dye. *Food Chemistry* **2017**, *237*, 974–980. <https://doi.org/10.1016/j.foodchem.2017.06.057>.
- (172) Ai, Y.; Liang, P.; Wu, Y.; Dong, Q.; Li, J.; Bai, Y.; Xu, B.-J.; Yu, Z.; Ni, D. Rapid Qualitative and Quantitative Determination of Food Colorants by Both Raman Spectra and Surface-Enhanced Raman Scattering (SERS). *Food Chemistry* **2018**, *241*, 427–433. <https://doi.org/10.1016/j.foodchem.2017.09.019>.

- (173) Weng, S.; Yu, S.; Dong, R.; Zhao, J.; Liang, D. Detection of Pirimiphos-Methyl in Wheat Using Surface-Enhanced Raman Spectroscopy and Chemometric Methods. *Molecules* **2019**, *24* (9), 1691. <https://doi.org/10.3390/molecules24091691>.
- (174) Weng, S.; Qiu, M.; Dong, R.; Wang, F.; Huang, L.; Zhang, D.; Zhao, J. Fast Detection of Fenthion on Fruit and Vegetable Peel Using Dynamic Surface-Enhanced Raman Spectroscopy and Random Forests with Variable Selection. *Spectrochimica Acta Part A: Molecular and Biomolecular Spectroscopy* **2018**, *200*, 20–25. <https://doi.org/10.1016/j.saa.2018.04.012>.
- (175) Li, J.-L.; Sun, D.-W.; Pu, H.; Jayas, D. S. Determination of Trace Thiophanate-Methyl and Its Metabolite Carbendazim with Teratogenic Risk in Red Bell Pepper (*Capsicum annuum* L.) by Surface-Enhanced Raman Imaging Technique. *Food Chemistry* **2017**, *218*, 543–552. <https://doi.org/10.1016/j.foodchem.2016.09.051>.
- (176) el Khoury, A.; Atoui, A. Ochratoxin A: General Overview and Actual Molecular Status. *Toxins* **2010**, *2* (4), 461–493. <https://doi.org/10.3390/toxins2040461>.
- (177) Petzinger, E.; Ziegler, K. Ochratoxin A from a Toxicological Perspective. *Journal of veterinary pharmacology and therapeutics* **2000**, *23*, 91–98. <https://doi.org/10.1046/j.1365-2885.2000.00244.x>.
- (178) Haynes, C. L.; McFarland, A. D.; Van Duyne, R. P. Surface-Enhanced Raman Spectroscopy. *Surface-Imprinted Gold Nanoparticle-Based Surface-Enhanced Raman Scattering* **2005**, *77* (17), 338 A–346 A. <https://doi.org/10.1021/ac053456d>.
- (179) Andrade, M. A.; Lanças, F. M. Determination of Ochratoxin A in Wine by Packed In-Tube Solid Phase Microextraction Followed by High Performance Liquid Chromatography Coupled to Tandem Mass Spectrometry. *Journal of Chromatography. A* **2017**, *1493*, 41–48. <https://doi.org/10.1016/j.chroma.2017.02.053>.
- (180) Beltrán, E.; Ibáñez, M.; Sancho, J. V.; Hernández, F. Determination of Mycotoxins in Different Food Commodities by Ultra-High-Pressure Liquid Chromatography Coupled to Triple Quadrupole Mass Spectrometry. *Rapid communications in mass spectrometry: RCM* **2009**, *23* (12), 1801–1809. <https://doi.org/10.1002/rcm.4077>.

- (181) Juan, C.; Lino, C. M.; Pena, A.; Moltó, J. C.; Mañes, J.; Silveira, I. Determination of Ochratoxin A in Maize Bread Samples by LC with Fluorescence Detection. *Talanta* **2007**, *73* (2), 246–250. <https://doi.org/10.1016/j.talanta.2007.03.029>.
- (182) Zhao, X.; Yuan, Y.; Zhang, X.; Yue, T. Identification of Ochratoxin A in Chinese Spices Using HPLC Fluorescent Detectors with Immunoaffinity Column Cleanup. *Food Control* **2014**, *46*, 332–337. <https://doi.org/10.1016/j.foodcont.2014.05.052>.
- (183) Monaci, L.; Palmisano, F.; Matrella, R.; Tantillo, G. Determination of Ochratoxin A at Part-per-Trillion Level in Italian Salami by Immunoaffinity Clean-up and High-Performance Liquid Chromatography with Fluorescence Detection. *Journal of Chromatography A* **2005**, *1090* (1), 184–187. <https://doi.org/10.1016/j.chroma.2005.07.020>.
- (184) Meulenbergh, E. P. Immunochemical Methods for Ochratoxin A Detection: A Review. *Toxins* **2012**, *4* (4), 244–266. <https://doi.org/10.3390/toxins4040244>.
- (185) Santos Pereira, C.; C. Cunha, S.; Fernandes, J. O. Prevalent Mycotoxins in Animal Feed: Occurrence and Analytical Methods. *Toxins* **2019**, *11* (5). <https://doi.org/10.3390/toxins11050290>.
- (186) Brown, R. J. C.; Milton, M. J. T. Nanostructures and Nanostructured Substrates for Surface—Enhanced Raman Scattering (SERS). *Journal of Raman Spectroscopy* **2008**, *39* (10), 1313–1326. <https://doi.org/10.1002/jrs.2030>.
- (187) Zimmerli, B.; Dick, R. Determination of Ochratoxin A at the Ppt Level in Human Blood, Serum, Milk and Some Foodstuffs by High-Performance Liquid Chromatography with Enhanced Fluorescence Detection and Immunoaffinity Column Cleanup: Methodology and Swiss Data. *Journal of Chromatography B: Biomedical Sciences and Applications* **1995**, *666* (1), 85–99. [https://doi.org/10.1016/0378-4347\(94\)00569-Q](https://doi.org/10.1016/0378-4347(94)00569-Q).
- (188) Pietri, A.; Bertuzzi, T.; Pallaroni, L.; Piva, G. Occurrence of Ochratoxin A in Italian Wines. *Food Additives and Contaminants* **2001**, *18* (7), 647–654. <https://doi.org/10.1080/02652030119480>.

- (189) Ribeiro, E.; Alves, A. Comparative Study of Screening Methodologies for Ochratoxin A Detection in Winery By-Products. *Analytical and Bioanalytical Chemistry* **2008**, *391* (4), 1443–1450. <https://doi.org/10.1007/s00216-008-1861-y>.
- (190) Haaland, D. M.; Thomas, E. V. Partial Least-Squares Methods for Spectral Analyses. 1. Relation to Other Quantitative Calibration Methods and the Extraction of Qualitative Information. *Analytical Chemistry* **1988**, *60* (11), 1193–1202. <https://doi.org/10.1021/ac00162a020>.
- (191) Huang, H.; Shi, H.; Feng, S.; Lin, J.; Chen, W.; Huang, Z.; Li, Y.; Yu, Y.; Lin, D.; Xu, Q.; Chen, R. Silver Nanoparticle Based Surface Enhanced Raman Scattering Spectroscopy of Diabetic and Normal Rat Pancreatic Tissue under Near-Infrared Laser Excitation. *Surface-enhanced Raman scattering (SERS) revealing chemical variation during biofilm formation* **2013**, *10* (4), 045603. <https://doi.org/10.1088/1612-2011/10/4/045603>.
- (192) Chao, Y.; Zhang, T. Surface-Enhanced Raman Scattering (SERS) Revealing Chemical Variation during Biofilm Formation: From Initial Attachment to Mature Biofilm. *Analytical and Bioanalytical Chemistry* **2012**, *404* (5), 1465–1475. <https://doi.org/10.1007/s00216-012-6225-y>.
- (193) Chen, W.; Lin, J.; Chen, R.; Feng, S.; Yu, Y.; Lin, D.; Huang, M.; Shi, H.; Huang, H. Detection and Identification of Huo–Xue–Hua–Yu Decoction (HXHYD) Using Surface-Enhanced Raman Scattering (SERS) Spectroscopy and Multivariate Analysis. *Laser Physics Letters* **2015**, *12* (4), 045602. <https://doi.org/10.1088/1612-2011/12/4/045602>.
- (194) Aggregation Kinetics and Dissolution of Coated Silver Nanoparticles | Langmuir <https://pubs.acs.org/doi/10.1021/la202328n> (accessed 2020 -10 -06).
- (195) Chaturvedi, D.; Balaji, S. A.; Bn, V. K.; Ariese, F.; Umopathy, S.; Rangarajan, A. Different Phases of Breast Cancer Cells: Raman Study of Immortalized, Transformed, and Invasive Cells. *Biosensors* **2016**, *6* (4), 57. <https://doi.org/10.3390/bios6040057>.

- (196) Huang, H.; Chen, W.; Pan, J.; Chen, Q.; Feng, S.; Yu, Y.; Chen, Y.; Su, Y.; Chen, R. SERS spectra of a single nasopharyngeal carcinoma cell based on intracellularly grown and passive uptake Au nanoparticles <https://www.hindawi.com/journals/jspec/2011/971256/> (accessed 2020 -10 -06). <https://doi.org/10.3233/SPE-2011-0540>.
- (197) Shen, Y.; Liang, L.; Zhang, S.; Huang, D.; Deng, R.; Zhang, J.; Qu, H.; Xu, S.; Liang, C.; Xu, W. Organelle-Targeting Gold Nanorods for Macromolecular Profiling of Subcellular Organelles and Enhanced Cancer Cell Killing. *ACS Applied Materials & Interfaces* **2018**, *10* (9), 7910–7918. <https://doi.org/10.1021/acsami.8b01320>.
- (198) Yu, Y.; Lin, J.; Lin, D.; Feng, S.; Chen, W.; Huang, Z.; Huang, H.; Chen, R. Leukemia Cells Detection Based on Electroporation Assisted Surface-Enhanced Raman Scattering. *Biomedical Optics Express* **2017**, *8* (9), 4108–4121. <https://doi.org/10.1364/BOE.8.004108>.
- (199) Zhao, B.; Yang, T.; Qu, Y.; Mills, A. J.; Zhang, G.; He, L. Rapid Capture and SERS Detection of Triclosan Using a Silver Nanoparticle Core – Protein Satellite Substrate. *Science of The Total Environment* **2020**, *716*, 137097. <https://doi.org/10.1016/j.scitotenv.2020.137097>.
- (200) Pavão, A. C.; Neto, L. A. S.; Neto, J. F.; Leão, M. B. C. Structure and Activity of Aflatoxins B and G. *Journal of Molecular Structure: THEOCHEM* **1995**, *337* (1), 57–60. [https://doi.org/10.1016/0166-1280\(94\)04104-Z](https://doi.org/10.1016/0166-1280(94)04104-Z).
- (201) Worldwide Mycotoxin Regulations <https://www.romerlabs.com/en/knowledge-center/knowledge-library/articles/news/worldwide-mycotoxin-regulations/> (accessed 2021 -03 -18).
- (202) Wacoo, A. P.; Wendi, D.; Vuzi, P. C.; Hawumba, J. F. Methods for Detection of Aflatoxins in Agricultural Food Crops. *Journal of Applied Chemistry* **2014**, *2014*, e706291. <https://doi.org/10.1155/2014/706291>.
- (203) Miklós, G.; Angeli, C.; Ambrus, Á.; Nagy, A.; Kardos, V.; Zentai, A.; Kerekes, K.; Farkas, Z.; Józwiak, Á.; Bartók, T. Detection of Aflatoxins in Different Matrices and Food-Chain Positions. *Front. Microbiol.* **2020**, *11*. <https://doi.org/10.3389/fmicb.2020.01916>.

- (204) Fleischmann, M.; Hendra, P. J.; McQuillan, A. J. Raman Spectra of Pyridine Adsorbed at a Silver Electrode. *Chemical Physics Letters* **1974**, *26* (2), 163–166. [https://doi.org/10.1016/0009-2614\(74\)85388-1](https://doi.org/10.1016/0009-2614(74)85388-1).
- (205) Xu, K.; Zhou, R.; Takei, K.; Hong, M. Toward Flexible Surface-Enhanced Raman Scattering (SERS) Sensors for Point-of-Care Diagnostics. *Advanced Science* **2019**, *6* (16), 1900925. <https://doi.org/10.1002/advs.201900925>.
- (206) Mu, T.; Wang, S.; Li, T.; Wang, B.; Ma, X.; Huang, B.; Zhu, L.; Guo, J. Detection of Pesticide Residues Using Nano-SERS Chip and a Smartphone-Based Raman Sensor. *IEEE Journal of Selected Topics in Quantum Electronics* **2019**, *25* (2), 1–6. <https://doi.org/10.1109/JSTQE.2018.2869638>.
- (207) Pilot, R. SERS Detection of Food Contaminants by Means of Portable Raman Instruments. *Journal of Raman Spectroscopy* **2018**, *49* (6), 954–981. <https://doi.org/10.1002/jrs.5400>.
- (208) Lin, X.-M.; Cui, Y.; Xu, Y.-H.; Ren, B.; Tian, Z.-Q. Surface-Enhanced Raman Spectroscopy: Substrate-Related Issues. *Anal Bioanal Chem* **2009**, *394* (7), 1729–1745. <https://doi.org/10.1007/s00216-009-2761-5>.
- (209) Mosier-Boss, P. A. Review of SERS Substrates for Chemical Sensing. *Nanomaterials* **2017**, *7* (6), 142. <https://doi.org/10.3390/nano7060142>.
- (210) Poór, M.; Lemli, B.; Bálint, M.; Hetényi, C.; Sali, N.; Kőszegi, T.; Kunsági-Máté, S. Interaction of Citrinin with Human Serum Albumin. *Toxins* **2015**, *7* (12), 5155–5166. <https://doi.org/10.3390/toxins7124871>.
- (211) Poór, M.; Kunsági-Máté, S.; Bálint, M.; Hetényi, C.; Gerner, Z.; Lemli, B. Interaction of Mycotoxin Zearalenone with Human Serum Albumin. *Journal of Photochemistry and Photobiology B: Biology* **2017**, *170*, 16–24. <https://doi.org/10.1016/j.jphotobiol.2017.03.016>.

- (212) Faisal, Z.; Vörös, V.; Fliszár-Nyúl, E.; Lemli, B.; Kunsági-Máté, S.; Csepregi, R.; Kőszegi, T.; Zsila, F.; Poór, M. Probing the Interactions of Ochratoxin B, Ochratoxin C, Patulin, Deoxynivalenol, and T-2 Toxin with Human Serum Albumin. *Toxins* **2020**, *12* (6), 392. <https://doi.org/10.3390/toxins12060392>.
- (213) Fliszár-Nyúl, E.; Lemli, B.; Kunsági-Máté, S.; Dellafiora, L.; Dall'Asta, C.; Cruciani, G.; Pethő, G.; Poór, M. Interaction of Mycotoxin Alternariol with Serum Albumin. *International Journal of Molecular Sciences* **2019**, *20* (9), 2352. <https://doi.org/10.3390/ijms20092352>.
- (214) Bagheri, M.; Fatemi, M. H. Fluorescence Spectroscopy, Molecular Docking and Molecular Dynamic Simulation Studies of HSA-Aflatoxin B1 and G1 Interactions. *Journal of Luminescence* **2018**, *202*, 345–353. <https://doi.org/10.1016/j.jlum.2018.05.066>.
- (215) Tan, H.; Chen, L.; Ma, L.; Liu, S.; Zhou, H.; Zhang, Y.; Guo, T.; Liu, W.; Dai, H.; Yu, Y. Fluorescence Spectroscopic Investigation of Competitive Interactions between Quercetin and Aflatoxin B1 for Binding to Human Serum Albumin. *Toxins* **2019**, *11* (4), 214. <https://doi.org/10.3390/toxins11040214>.
- (216) Bolaños, K.; Kogan, M. J.; Araya, E. Capping Gold Nanoparticles with Albumin to Improve Their Biomedical Properties. *Int J Nanomedicine* **2019**, *14*, 6387–6406. <https://doi.org/10.2147/IJN.S210992>.
- (217) Zhai, W.; You, T.; Ouyang, X.; Wang, M. Recent Progress in Mycotoxins Detection Based on Surface-Enhanced Raman Spectroscopy. *Comprehensive Reviews in Food Science and Food Safety* **2021**, *20* (2), 1887–1909. <https://doi.org/10.1111/1541-4337.12686>.
- (218) Brulé, T. Spectral and Temporal Distribution of Biomolecules by Dynamic SERS, 2014.
- (219) Kahraman, M.; Mullen, E. R.; Korkmaz, A.; Wachsmann-Hogiu, S. Fundamentals and Applications of SERS-Based Bioanalytical Sensing. *Nanophotonics* **2017**, *6* (5), 831–852. <https://doi.org/10.1515/nanoph-2016-0174>.

- (220) Lakshmi, P.; Mondal, M.; Ramadas, K.; Natarajan, S. Molecular Interaction of 2,4-Diacetylphloroglucinol (DAPG) with Human Serum Albumin (HSA): The Spectroscopic, Calorimetric and Computational Investigation. **2017**.
- (221) Foo, Y. Y.; Kabir, Md. Z.; Periasamy, V.; Malek, S. N. A.; Tayyab, S. Spectroscopic Studies on the Interaction of Green Synthesized-Gold Nanoparticles with Human Serum Albumin. *Journal of Molecular Liquids* **2018**, *265*, 105–113. <https://doi.org/10.1016/j.molliq.2018.05.115>.
- (222) Lee, N.; Hummer, D.; Sverjensky, D.; Rajh, T.; Hazen, R.; Steele, A.; Cody, G. D. Speciation of L-DOPA on Nanorutile as a Function of PH and Surface Coverage Using Surface-Enhanced Raman Spectroscopy (SERS). *Langmuir : the ACS journal of surfaces and colloids* **2012**. <https://doi.org/10.1021/la303607a>.
- (223) Rout, C. S.; Kumar, A.; Fisher, T. Carbon Nanowalls Amplify the Surface-Enhanced Raman Scattering from Ag Nanoparticles. *Nanotechnology* **2011**. <https://doi.org/10.1088/0957-4484/22/39/395704>.
- (224) Perry, J. L.; Il'ichev, Y. V.; Kempf, V. R.; McClendon, J.; Park, G.; Manderville, R. A.; Rüker, F.; Dockal, M.; Simon, J. D. Binding of Ochratoxin A Derivatives to Human Serum Albumin. *J. Phys. Chem. B* **2003**, *107* (27), 6644–6647. <https://doi.org/10.1021/jp034284w>.
- (225) Il'ichev, Y. V.; Perry, J. L.; Simon, J. D. Interaction of Ochratoxin A with Human Serum Albumin. A Common Binding Site of Ochratoxin A and Warfarin in Subdomain IIA. *J. Phys. Chem. B* **2002**, *106* (2), 460–465. <https://doi.org/10.1021/jp012315m>.
- (226) Il'ichev, Y. V.; Perry, J. L.; Simon, J. D. Interaction of Ochratoxin A with Human Serum Albumin. Preferential Binding of the Dianion and PH Effects. *J. Phys. Chem. B* **2002**, *106* (2), 452–459. <https://doi.org/10.1021/jp012314u>.
- (227) Beattie, J.; Caraher, M. C.; Cummins, N.; O'driscoll, O.; Eastell, R.; Ralston, S.; Towler, M. Raman Spectral Variation for Human Fingernails of Postmenopausal Women Is Dependent on Fracture Risk and Osteoporosis Status. **2017**. <https://doi.org/10.1002/JRS.5123>.

- (228) Xu, C.; Karan, K.; Yao, X.; Wang, Y. Molecular Structural Analysis of Noncarious Cervical Sclerotic Dentin Using Raman Spectroscopy. **2009**. <https://doi.org/10.1002/JRS.2320>.
- (229) Aksoy, C.; Severcan, F. Role of Vibrational Spectroscopy in Stem Cell Research. *Spectroscopy: An International Journal* **2012**, *27* (3), 167–184. <https://doi.org/10.1155/2012/513286>.
- (230) Ashton, L.; Brewster, V. L.; Correa, E.; Goodacre, R. Detection of Glycosylation and Iron-Binding Protein Modifications Using Raman Spectroscopy. *Analyst* **2017**, *142* (5), 808–814. <https://doi.org/10.1039/C6AN02516A>.
- (231) Hedayati, M. T.; Pasqualotto, A. C.; Warn, P. A.; Bowyer, P.; Denning, D. W. *Aspergillus Flavus: Human Pathogen, Allergen and Mycotoxin Producer. Microbiology (Reading)* **2007**, *153* (Pt 6), 1677–1692. <https://doi.org/10.1099/mic.0.2007/007641-0>.
- (232) *The Aspergilli: Genomics, Medical Aspects, Biotechnology, and Research Methods*; Goldman, G. H., Osmani, S. A., Eds.; CRC Press: Boca Raton, 2007. <https://doi.org/10.1201/9781420008517>.
- (233) Chang, P.-K.; Ehrlich, K. C. What Does Genetic Diversity of *Aspergillus Flavus* Tell Us about *Aspergillus Oryzae*? *International Journal of Food Microbiology* **2010**, *138* (3), 189–199. <https://doi.org/10.1016/j.ijfoodmicro.2010.01.033>.
- (234) Barbesgaard, P.; Heldt-Hansen, H. P.; Diderichsen, B. On the Safety of *Aspergillus Oryzae*: A Review. *Appl Microbiol Biotechnol* **1992**, *36* (5), 569–572. <https://doi.org/10.1007/BF00183230>.
- (235) Abarca, M. L.; Bragulat, M. R.; Bruguera, M. T.; Cabañes, F. J. Comparison of Some Screening Methods for Aflatoxigenic Moulds. *Mycopathologia* **1988**, *104* (2), 75–79. <https://doi.org/10.1007/BF00436930>.

- (236) Filtenborg, O.; Frisvad, J. C.; Svendsen, J. A. Simple Screening Method for Molds Producing Intracellular Mycotoxins in Pure Cultures. *Applied and Environmental Microbiology* **1983**, *45* (2), 581–585. <https://doi.org/10.1128/aem.45.2.581-585.1983>.
- (237) Wicklow, D. T.; Shotwell, O. L.; Adams, G. L. Use of Aflatoxin-Producing Ability Medium to Distinguish Aflatoxin-Producing Strains of *Aspergillus Flavus*. *Appl Environ Microbiol* **1981**, *41* (3), 697–699.
- (238) Rodríguez, A.; Rodríguez, M.; Luque, M. I.; Martín, A.; Córdoba, J. J. Real-Time PCR Assays for Detection and Quantification of Aflatoxin-Producing Molds in Foods. *Food Microbiology* **2012**, *31* (1), 89–99. <https://doi.org/10.1016/j.fm.2012.02.009>.
- (239) Levin, R. E. PCR Detection of Aflatoxin Producing Fungi and Its Limitations. *International Journal of Food Microbiology* **2012**, *156* (1), 1–6. <https://doi.org/10.1016/j.ijfoodmicro.2012.03.001>.
- (240) Mayer, Z.; Bagnara, A.; Färber, P.; Geisen, R. Quantification of the Copy Number of Nor-1, a Gene of the Aflatoxin Biosynthetic Pathway by Real-Time PCR, and Its Correlation to the Cfu of *Aspergillus Flavus* in Foods. *International Journal of Food Microbiology* **2003**, *82* (2), 143–151. [https://doi.org/10.1016/S0168-1605\(02\)00250-7](https://doi.org/10.1016/S0168-1605(02)00250-7).
- (241) Passone, M. A.; Rosso, L. C.; Ciancio, A.; Etcheverry, M. Detection and Quantification of *Aspergillus Section Flavi* Spp. in Stored Peanuts by Real-Time PCR of nor-1 Gene, and Effects of Storage Conditions on Aflatoxin Production. *International Journal of Food Microbiology* **2010**, *138* (3), 276–281. <https://doi.org/10.1016/j.ijfoodmicro.2010.01.003>.
- (242) Pearson, B.; Mills, A.; Tucker, M.; Gao, S.; McLandsborough, L.; He, L. Rationalizing and Advancing the 3-MPBA SERS Sandwich Assay for Rapid Detection of Bacteria in Environmental and Food Matrices. *Food Microbiology* **2018**, *72*, 89–97. <https://doi.org/10.1016/j.fm.2017.11.007>.

- (243) Gao, S.; Pearson, B.; He, L. Mapping Bacteria on Filter Membranes, an Innovative SERS Approach. *Journal of Microbiological Methods* **2018**, *147*, 69–75. <https://doi.org/10.1016/j.mimet.2018.03.005>.
- (244) Sayin, I.; Kahraman, M.; Sahin, F.; Yurdakul, D.; Culha, M. Characterization of Yeast Species Using Surface-Enhanced Raman Scattering. *Appl. Spectrosc., AS* **2009**, *63* (11), 1276–1282.
- (245) Jolliffe, I. T.; Cadima, J. Principal Component Analysis: A Review and Recent Developments. *Philos Trans A Math Phys Eng Sci* **2016**, *374* (2065), 20150202. <https://doi.org/10.1098/rsta.2015.0202>.
- (246) Antonissen, G.; Martel, A.; Pasmans, F.; Ducatelle, R.; Verbrugghe, E.; Vandebroucke, V.; Li, S.; Haesebrouck, F.; Van Immerseel, F.; Croubels, S. The Impact of Fusarium Mycotoxins on Human and Animal Host Susceptibility to Infectious Diseases. *Toxins (Basel)* **2014**, *6* (2), 430–452. <https://doi.org/10.3390/toxins6020430>.
- (247) *Mycotoxigenic Fungi: Methods and Protocols*; Moretti, A., Susca, A., Eds.; Methods in Molecular Biology; Humana Press, 2017. <https://doi.org/10.1007/978-1-4939-6707-0>.
- (248) Kamle, M.; Mahato, D. K.; Devi, S.; Lee, K. E.; Kang, S. G.; Kumar, P. Fumonisin: Impact on Agriculture, Food, and Human Health and Their Management Strategies. *Toxins (Basel)* **2019**, *11* (6). <https://doi.org/10.3390/toxins11060328>.
- (249) Guselnikova, O.; Postnikov, P.; Elashnikov, R.; Miliutina, E.; Svorcik, V.; Lyutakov, O. Metal-Organic Framework (MOF-5) Coated SERS Active Gold Gratings: A Platform for the Selective Detection of Organic Contaminants in Soil. *Analytica Chimica Acta* **2019**, *1068*, 70–79. <https://doi.org/10.1016/j.aca.2019.03.058>.
- (250) Ong, C. C.; Siva Sangu, S.; Illias, N. M.; Chandra Bose Gopinath, S.; Saheed, M. S. M. Iron Nanoflorets on 3D-Graphene-Nickel: A ‘Dandelion’ Nanostructure for Selective Deoxynivalenol Detection. *Biosensors and Bioelectronics* **2020**, *154*, 112088. <https://doi.org/10.1016/j.bios.2020.112088>.

- (251) Sackmann, M.; Materny, A. Surface Enhanced Raman Scattering (SERS)—a Quantitative Analytical Tool? *Journal of Raman Spectroscopy* **2006**, *37* (1–3), 305–310. <https://doi.org/10.1002/jrs.1443>.
- (252) Pasquini, C. Near Infrared Spectroscopy: A Mature Analytical Technique with New Perspectives – A Review. *Analytica Chimica Acta* **2018**, *1026*, 8–36. <https://doi.org/10.1016/j.aca.2018.04.004>.
- (253) OsawaMasatoshi. Dynamic Processes in Electrochemical Reactions Studied by Surface-Enhanced Infrared Absorption Spectroscopy (SEIRAS). *Bulletin of the Chemical Society of Japan* **2006**. <https://doi.org/10.1246/bcsj.70.2861>.
- (254) Gaspardo, B.; Del Zotto, S.; Torelli, E.; Cividino, S. R.; Firrao, G.; Della Riccia, G.; Stefanon, B. A Rapid Method for Detection of Fumonisin B1 and B2 in Corn Meal Using Fourier Transform near Infrared (FT-NIR) Spectroscopy Implemented with Integrating Sphere. *Food Chemistry* **2012**, *135* (3), 1608–1612. <https://doi.org/10.1016/j.foodchem.2012.06.078>.
- (255) Acuña-Gutiérrez, C.; Schock, S.; Jiménez, V. M.; Müller, J. Detecting Fumonisin B1 in Black Beans (*Phaseolus Vulgaris* L.) by near-Infrared Spectroscopy (NIRS). *Food Control* **2021**, *130*, 108335. <https://doi.org/10.1016/j.foodcont.2021.108335>.
- (256) Ruan, R.; Li, Y.; Lin, X.; Chen, P. Non-Destructive Determination of Deoxynivalenol Levels in Barley Using near-Infrared Spectroscopy. *Applied Engineering in Agriculture* **2002**, *18* (5), 549–553.
- (257) De Girolamo, A.; Cervellieri, S.; Cortese, M.; Porricelli, A. C. R.; Pascale, M.; Longobardi, F.; von Holst, C.; Ciaccheri, L.; Lippolis, V. Fourier Transform Near-Infrared and Mid-Infrared Spectroscopy as Efficient Tools for Rapid Screening of Deoxynivalenol Contamination in Wheat Bran. *Journal of the Science of Food and Agriculture* **2019**, *99* (4), 1946–1953. <https://doi.org/10.1002/jsfa.9392>.
- (258) Peiris, K. H. S.; Pumphrey, M. O.; Dong, Y.; Maghirang, E. B.; Berzonsky, W.; Dowell, F. E. Near-Infrared Spectroscopic Method for Identification of Fusarium Head Blight Damage and Prediction of Deoxynivalenol in Single Wheat Kernels. *Cereal Chemistry* **2010**, *87* (6), 511–517. <https://doi.org/10.1094/CCHEM-01-10-0006>.

- (259) De Girolamo, A.; Lippolis, V.; Nordkvist, E.; Visconti, A. Rapid and Non-Invasive Analysis of Deoxynivalenol in Durum and Common Wheat by Fourier-Transform Near Infrared (FT-NIR) Spectroscopy. *Food Additives & Contaminants: Part A* **2009**, *26* (6), 907–917. <https://doi.org/10.1080/02652030902788946>.
- (260) Abramovi, B.; Jaji, I.; Abramovi, B. Detection of Deoxynivalenol in Wheat by Fourier Transform Infrared Spectroscopy. *Acta Chim. Slov.* **2007**, *9*.
- (261) Comparison of Raman and IR Spectroscopy  
<http://www.chemvista.org/ramanir4.html> (accessed 2021-10-08).
- (262) Levasseur-Garcia, C.; Bailly, S.; Kleiber, D.; Bailly, J.-D. Assessing Risk of Fumonisin Contamination in Maize Using Near-Infrared Spectroscopy. *Journal of Chemistry* **2015**, *2015*, e485864. <https://doi.org/10.1155/2015/485864>.
- (263) Berardo, N.; Pisacane, V.; Battilani, P.; Scandolara, A.; Pietri, A.; Marocco, A. Rapid Detection of Kernel Rots and Mycotoxins in Maize by Near-Infrared Reflectance Spectroscopy. *J. Agric. Food Chem.* **2005**, *53* (21), 8128–8134. <https://doi.org/10.1021/jf0512297>.
- (264) Piergies, N.; Oćwieja, M.; Paluszkiwicz, C.; Kwiatek, W. M. Nanoparticle Stabilizer as a Determining Factor of the Drug/Gold Surface Interaction: SERS and AFM-SEIRA Studies. *Applied Surface Science* **2021**, *537*, 147897. <https://doi.org/10.1016/j.apsusc.2020.147897>.
- (265) Bibikova, O.; Haas, J.; I. López-Lorente, A.; Popov, A.; Kinnunen, M.; Meglinski, I.; Mizaikoff, B. Towards Enhanced Optical Sensor Performance: SEIRA and SERS with Plasmonic Nanostars. *Analyst* **2017**, *142* (6), 951–958. <https://doi.org/10.1039/C6AN02596J>.
- (266) Cornel, J.; Lindenberg, C.; Mazzotti, M. Quantitative Application of in Situ ATR-FTIR and Raman Spectroscopy in Crystallization Processes. *Ind. Eng. Chem. Res.* **2008**, *47* (14), 4870–4882. <https://doi.org/10.1021/ie800236v>.

- (267) Pataki, H.; Markovits, I.; Vajna, B.; Nagy, Z. K.; Marosi, G. In-Line Monitoring of Carvedilol Crystallization Using Raman Spectroscopy. *Crystal Growth & Design* **2012**, *12* (11), 5621–5628. <https://doi.org/10.1021/cg301135z>.
- (268) Keramidas, V. G.; White, W. B. Raman Scattering Study of the Crystallization and Phase Transformations of ZrO<sub>2</sub>. *Journal of the American Ceramic Society* **1974**, *57* (1), 22–24. <https://doi.org/10.1111/j.1151-2916.1974.tb11355.x>.
- (269) Knutsen, H. K. Risks to Human and Animal Health Related to the Presence of Deoxynivalenol and Its Acetylated and Modified Forms in Food and Feed. *EFSA Journal* **2017**, *15* (9), e04718. <https://doi.org/10.2903/j.efsa.2017.4718>.